FGF Regulated Cadherin Expression in Cranial Nucleogenesis

Marc R. Astick

Thesis submitted for the degree of Doctor of Philosophy

University College London

March 2012

Declaration

I, Marc R. Astick, confirm that the work presented in this thesis is my own. Where information has been derived from other sources, I confirm that this has been indicated in the thesis.

Signed

Date

Abstract

A recurrent and evolutionarily ancient mode of neuronal organisation juxtaposes functionally related neurons in to so called neuronal nuclei. Neuronal nuclei are the predominant mode of organisation of motor neurons in the vertebrate hindbrain. The coalescence of nuclei during development, a process known as nucleogenesis, is a crucial step in the construction of neural circuits. However, the signals and molecules which govern nucleogenesis are currently not understood. This study demonstrates that members of the classical (Type II) sub family of cadherin cell-cell adhesion molecules are differentially expressed in cranial motor nuclei of rhombomere (r) 5 and 8 as well as the auditory nuclei of r5 in the chicken hindbrain. The dynamic and differential expression of type II cadherins drives the segregation of motor neurons into spatially distinct nuclei. Normalising the type II cadherin expression profile between two motor nuclei; the dorsal Facial Motor Nucleus and Accessory Abducens Nucleus leads to nucleus desegregation, as indicated by aberrant intermixing of neuronal populations. Refinement of the dynamic cadherin expression in r5 is modulated by Fibroblast Growth Factors (Fgf); specifically Fgf8 which is expressed within r5 itself and mediates its action through the MAPK/ERK signalling pathway. Both up and down regulation of this signalling pathway results in the disruption of nucleogenesis, with associated alterations in cadherin expression. Taken together this suggests a model whereby Fgf signalling modulates the dynamic expression of cadherins, which in turn drives cranial nucleogenesis.

Acknowledgements

I would like to thank Dr. Stephen Price for allowing me the opportunity to work in his laboratory and for his unending patience, guidance, teaching and support over the past five years. Also Professors David McAlpine and Steve Hunt; for critical evaluation and advice, which has aided the development of the project and this thesis.

Present and former members of the Price lab who have provided such a friendly, supportive and creative environment in which to work; Dr. Rosanna Smith, Dr. Sanusi Bello, Kristina Tubby, Mark Hintze, Dr. Waleed Mubarak, Zahra Samji and Samanta Kviklyte.

I would also like to thank my friends and family who have helped me throughout this process specifically, Lucy Carty, James Lawrence, Liam Burnham, Gemma Bridge, Dr. Alec Smith, Dr. Claire De-May, Robert Crawford, Timothy Heal, Dr. Timothy O'Neill, Dr. John Kelly, Dr. Stephen Freeman, Dr. Robert Salter and my brother, Paul Astick as well as the many others who have shown an interest in this work. Also I would like to thank The Medical Research Council for funding my work.

Above all I wish to thank my parents for providing me with the chance to pursue my studies over the past ten years. Without their continued support and encouragement this would not have been possible.

Dedicated to Uncle John, for all that he taught me.

Contents

List of Figures

List of Tables

1. Introduction

1.1 Neuronal Nuclei

In his work “Texture of the nervous system of Man and Vertebrates” Ramon y Cajal discusses the basic principle of a nervous system:

“Teleologically the nervous system appears as an apparatus of improvement, destined to collect a greater number of excitations from the external world, classify and distinguish them into separate species, as well as impart greater speed, extent and energies to the motor energies” (Cajal, 1909).

In essence the basic vertebrate nervous system consists of two major aspects; a sensory and a motor component. The purpose of the sensory component is to receive input from external stimuli and then process this into a network which is able to mediate an appropriate response using the motor component.

The most basic form of such a system is found, according to Cajal, in coelenterates (known now as the Ctenophora and Cnidaria phyla of jellies and coral organisms). In these organisms a nervous system exists which consists purely of the sensory neuron; “it exhibits a bipolar shape, with a thick peripheral process ending in a cilium, and a finer central extrusion that branches to the subjacent mesoderm”. The second aspect of this system is the motor neuron, which “adopts a stellate shape and gives off several processes”. (Cajal, 1909)

In comparison the vertebrate nervous system is highly complex; the human nervous system for example consists of hundreds of billions of neurons and glia. However, broadly speaking the nervous system of humans, and indeed all vertebrate species, retains the same basic principle as discussed by Cajal; consisting of sensory pathways and motor pathways, which relay signals via the central nervous system (Figure 1.1).

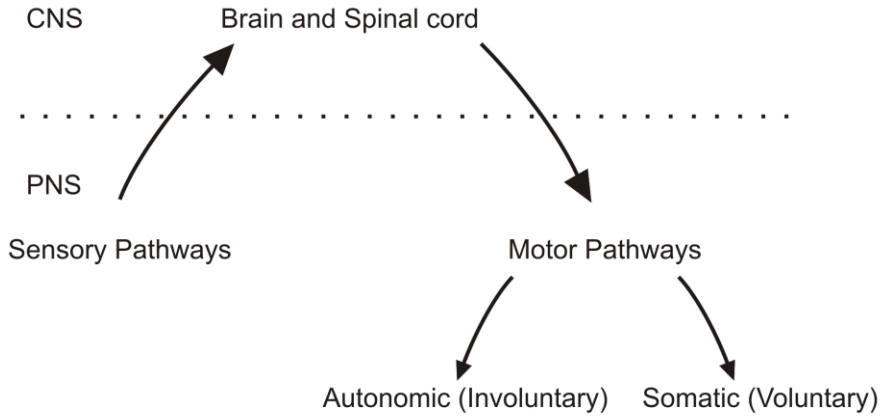

Figure 1.1: The nervous system can be divided in to peripheral (PNS) and central (CNS) aspects. Sensory and Motor pathways relay signals via the CNS.

How the nervous system is able to perform this task is dependent upon the organisation of individual neurons into precise anatomical circuits which are able to mediate behaviour. The nervous system is divided into two parts; the peripheral (PNS) and central (CNS) nervous systems. The CNS consists of the brain and spinal cord each of which can be subdivided into specific regions which are functionally related. Within the CNS there are two major forms of neuronal organisation; the stratified layers of the **cortices**, for example in the cerebral or cerebellar cortex and clusters of functionally related neurons called **nuclei.**

The cerebellum provides an example of both types of neuronal organisation (Figure 1.2). The cerebellar cortex consists of 3 distinct layers, which are defined by the subtype of neuron they each contain and receives input from the motor cortex, spinal cord, vestibular and auditory circuits. Output from the cerebellar cortex is relayed via the three deep cerebellar nuclei, each of which contains one neuronal subtype, to either the premotor/motor cortex or motor neurons which mediate behavioural responses. In this way individual neurons are connected in a functional anatomical unit, which mediates behavioural responses (Eccles, 1973).

*Image Removed

Figure 1.2: Illustration of neuronal organisation found in the cerebellum. Cerebellar cortex is organised into 3 stratified layers each containing different cell types; Pc, Purkinje cell; Gc, Ganglion cell; pf, parallel fibre; bc, basket cell; gr, granule cell. Output from the cerebellar cortex is relayed via the cerebellar nuclei (cn). Figure from Eccles, 1973.

The major advantage of organising neurons in this way is that of allowing intercellular communication and integration of multiple neuronal subtypes. Using an example taken from Cajal it is possible to illustrate the growing need for high level organisation in a complex nervous system. Figure 1.3 A, shows a basic nervous system consisting only of Cutaneous sensory neurons and the muscle fibre. Each neuron sends three projections, one to each target muscle which will mediate movement in response to cutaneous stimuli. In the second scenario (Figure 1.3 B) a motor neuron is introduced, this extra layer of complexity allows the organism to integrate input from all three sensory neurons at one point before eliciting a response. Behaviourally this is significant as it allows a greater flexibility in response to multiple cutaneous inputs. However, this is not the most efficient conformation of neuronal organisation as each sensory neuron must still send three projections and each motor neuron is isolated. Concentrating motor neurons into a central ganglion, as seen in figure 1.3, C, reduces the amount of projections each cutaneous sensory neuron is required to make and allows communication between each of the motor neurons directly. This acts to integrate all of the sensory inputs prior to eliciting a behavioural response.

*Image removed

Figure 1.3: Organisation of neurons into central nuclei is advantageous. **A:** A basic circuit consisting of a single neuron innervating muscle fibres. **B:** Addition of a motor neuron to the system allows greater integration of sensory input. **C:** Organisation of the motor neurons into a central ganglion increases the efficiency of the system and facilitates their direct interaction. Modified after Cajal, 1909.

If we look at, for example, vertebrate spinal motor circuits it is possible to see how this principle is maintained (Figure 1.4). Motor neurons (MNs) within the ventral horn of the spinal cord are organised into discrete groups which reflect their axonal projections to the periphery (Landmesser et al.,, 1978). This can be considered in three major divisions, firstly motor neurons are organised into distinct motor columns which occupy stereotyped positions along the rostrocaudal axis reflecting their common target, for example the lateral motor column, which projects axons to target muscles in the limb is generated at the axial level of the limb itself (Romanes, 1951). Within the motor columns MNs are segregated into a medial division, which projects axons to ventral limb muscle targets and a lateral division which projects axons to the dorsal limb muscles. Finally within each motor column division MNs are clustered into motor pools (Romanes, 1942), each of which extends axons towards one specific muscle. In turn each motor pool is innervated by afferent input from the same muscle target. Significantly, within each motor pool each of the MNs is electrically coupled (Brenowitz et al., 1983), allowing coordinated firing in response to sensory input. This basic circuitry provides the basis for the stretch reflex arc within the spinal cord.

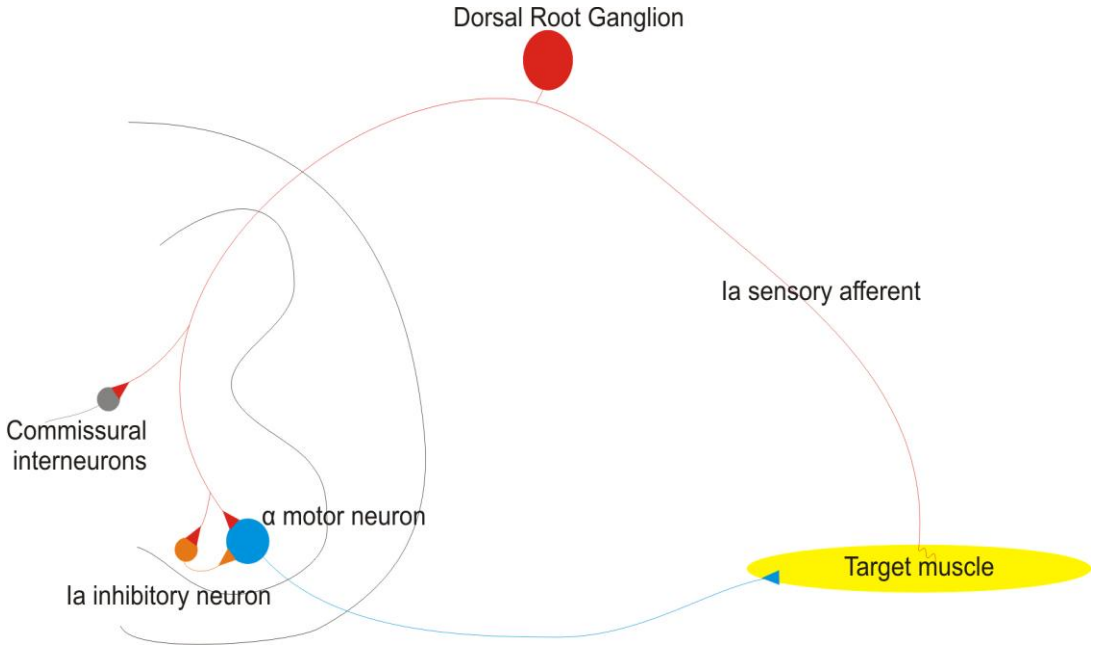

Figure 1.4: The spinal reflex arc; α motor neurons are coalesced into distinct pools within the ventral horn of the spinal cord. A circuit is constructed such that each motor pool projects to a target muscle and receives sensory input form that muscle via the Ia afferent fibre. Projections are also made for example to commissural neurons which are important in mediating locomotion and the Ia inhibitory neuron which acts after a delay to inhibit motor neuron firing. These are not the only inputs to the α-motor neurons, which also receive inputs from interneurons and the corticospinal tract (in higher vertebrates).

Whilst much has been elucidated as to the development of cortices and, to lesser extent spinal motor pools, little is known as to the mechanisms which drive nucleus development in other regions of the CNS. The focus of this research is the development of sensory and motor neuronal nuclei in the embryonic chicken hindbrain and the molecules and signalling pathways which mediate this process.

1.2 Development of the chicken embryonic hindbrain.

The focus of this study is the mechanisms which drive nucleus formation in terms of coalescence and segregation; specifically the motor nuclei of r5 and r8 and the sensory nuclei of r5. It is important therefore to understand the function, positioning, origin and peripheral targets of these nuclei in wild type embryos.

1.2.1 Rhombomeres; transient cell lineage restriction compartments

Neuronal nuclei within the chicken hindbrain occupy spatially distinct positions along the rostrocaudal, dorsoventral and mediolateral axes (Reviewed in Guthrie, 2007). The correct axial positioning of neurons in this manner is, in part, defined during early neural development. The mechanisms which impart this regional specificity have to some extent been elucidated and we now know that the correct patterning of the nervous system is dependent upon the development of transient structures known as neuromeres. The development of the chicken embryo was extensively characterised in 1951 by Hamburger and Hamilton; embryonic days are not a suitable measure of chick development due to the rapid and inconsistent rate of growth. Hamburger and Hamilton instead described a series of 46 chicken embryonic development stages, which I shall refer to as HH1-46 (Hamburger and Hamilton, 1951).

Early in development (around HH9) the neural tube begins to acquire a series of swellings along its rostrocaudal axis which are precursory to each of the major CNS brain regions; Prosencephalon (Forebrain), Mesencephalon (Midbrain) and Rhombencephalon (Hindbrain). The boundaries between each division are visible as slight furrows in the neural tube. Looking specifically at the developing rhombencephalon, immediately following neural tube closure (HH9) there are 7 clearly distinct rhombomeres (Vaage, 1969) which persist until HH24. There is an 8^{th}, most caudal, rhombomere which is intermediate in character as it does not have a clearly defined boundary with the developing spinal cord (Cambronero & Puelles, 2000; Lumsden, 2004).

Rhombomeres are cell lineage restriction regions, each giving rise to specific cell types which will occupy nearby axial positions (Fraser et al., 1990; Guthrie et al., 1991). Neurogenesis begins at HH11-12 with different neuronal subtypes found to differentiate in spatially segregated regions within each rhombomere. The alar

(lateral) neural plate giving rise to second order sensory interneurons and relay neurons, whilst the basal (medial) neural plate gives rise to interneurons and motor neurons (Reviewed in Lumsden 2004; Guthrie 2007). The specific development of motor and sensory neurons within the hindbrain is discussed later (Introduction 1.3, 1.4).

It has been demonstrated by Fraser et al., 1990, that each rhombomere is essentially a compartment which acts to segregate groups of cells with the similar properties. Lineage tracing by injecting dye into single progenitors at HH11 demonstrated that the daughter cells are restricted to a single rhombomere. However,, subsequent investigation by the same group demonstrated that later in development around HH25, a small proportion of cells migrate to neighbouring rhombomeres (Birgbauer & Fraser, 1994). What is the significance of the lineage restriction provided by rhombomeres and how is it established?

1.2.2 The positional identity of rhombomeres is determined by *Hox* gene expression

The development of regional patterning within the hindbrain is controlled by *Hox* gene expression (Wilkinson et al., 1989). First identified in *Drosophila melanogaster*; where they act to control regional patterning and segment identity along the embryonic body axis (Reviewed in Lewis, 1978), *Hox* genes are a large family of chromosomally clustered genes which encode helix-turn-helix transcription factors. *Hox* genes are highly conserved across species and interestingly the 3' to 5' directionality of gene clustering on the chromosome reflects their anterior-posterior expression patterns (McGinnis et al., 1984a, 1984b; Dressler & Gross, 1989) Unlike *Drosophila melanogaster*, which has eight *Hox* genes organised on one chromosome, vertebrate species have 39 separate *Hox* genes clustered on 4 chromosomes (Reviewed in Lemons & McGinnis, 2006). This presents the possibility that a combinatorial *Hox* gene expression drives regional patterning involving overlapping expression of *Hox* genes across several gene loci.

Each rhombomere is found to express a combination of *Hox* genes (Reviewed in Tümpel et al., 2009), the expression of which precedes rhombomere formation and is induced by diffusible signals in rostral and caudal hindbrain regions. In the rostral hindbrain FGF8, which is expressed in the midbrain hindbrain boundary, establishes

the rostral extent of *Hoxa2* expression at the r1-2 boundary leaving r1 as the only rhombomere not to express any *Hox* genes (Irving & Mason, 2000). Whilst caudally, Retinoic Acid (RA) expressed in the spinal cord and paraxial mesoderm induces *Hox* gene expression in a dose dependant manner (Glover et al., 2006) (Figure 1.5). The combination of *Hox* gene expression defines the identity of each rhombomere. For example r4 expresses a combination of *Hoxa2, Hoxb2, Hoxa1* and, uniquely *Hoxb1*; targeted mutation of *Hoxb1* in mice leads to the loss of rhombomere 4 identities and adoption of a rhombomere 2 phenotype (Studer et al., 1996). This is due to the similarity in *Hox* gene expression between r2 and r4, which also expresses *Hoxa2* and *Hoxb2*, and r4. A great deal of research relating to the role of *Hox* genes in determining regional patterning has been performed based upon the stereotyped and highly conserved pattern of cranial motor nucleus and cranial nerve development within rhombomeres.

*Image removed

Figure 1.5: *Hox* gene expression boundaries in the rhombomeres are determined by the Fgf and RA signalling. The anterior limit of activation is limited by Fgf8 from the midbrain hindbrain boundary, whilst RA signalling induces the expression of different hos genes in a dose dependant manner. Figure from Irving & Mason 2000.

1.3 Cranial motor nuclei

1.3.1 Motor neuron organisation is highly conserved across vertebrate species

Cranial motor neurons comprise three subsets each of which projects axons to different muscle targets; Branchiomotor (BM), Visceral Motor (VM) and Somatic Motor (SM). In the hindbrain these neurons are organised into distinct motor nuclei, each of which may contain one or more motor neuron subtype (Lumsden et al., 1989). These motor nuclei occupy specific, spatially segregated positions along the rostrocaudal, dorsoventral and mediolateral axes. The positioning of motor nuclei is highly stereotyped and conserved across vertebrate species, for example between the mouse and chick hindbrain (Gilland & Baker, 2005. Also Figure 1.6).

BM and VM neurons extend their axons towards large common exit points in the lateral neuroepithelium, whereas SM neurons extend their axons through small ventral exit points (with the exception of the Trochlear SM axons which project dorsally from the hindbrain), where they will form constituent parts of nine of the cranial nerves. BM neurons contribute motor components to five of the cranial nerves which innervate muscle targets in the branchial arches and tongue. Specifically the muscles of mastication, Trigeminal (V); the muscles of facial expression, the diagastric muscle of the jaw and the stapedius muscle of the inner ear, Facial (VII). As well as the Glossopharyngeal (IX) nerve which innervates the stylopharyngeus muscle and both the Vagus (X) and cranial accessory (XI) nerves, which provide innervation to the pharyngeal and laryngeal muscle groups (Review see Guthrie, 2007).

VM neuron axons form part of the Oculomotor (III) and Facial (VII) nerves, innervating the parasympathetic ganglia of the head; the ciliary body of the inner eye (III) and the pterygopalatine, sphenopalatine and submandibular ganglia (VII). VM neurons also contribute axons to the Vagus (X) nerve, specifically projecting to the thoracic viscera.

The Oculomotor (III) nerve also contains axons of SM neurons which constitute the oculomotor nucleus; they project their axons to the superior, inferior and medial recti muscles as well as the levator palpebrae superioris and inferior oblique muscles. These extraocular muscles control most eye movements except lateral motion away from the midline, which is controlled by the lateral rectus muscle, and internal

rotation of the eye which is provided by the superior oblique muscle. The lateral rectus receives innervation from, and is the sole target of, the SM axons of the Abducens (VI) nerve. Similarly the Trochlear (IV) nerve which innervates the superior oblique muscle is formed entirely of axons of SM neurons. Finally, the Hypoglossal (XII) nerve, consisting of SM axons projects to the muscles of the tongue.

The position of many cranial motor nuclei is retained between mouse and chick embryonic hindbrain with subtle differences in positioning of others (Figure 1.6). The Trochlear (IV) and Oculomotor (III) nuclei are located in r1 and the caudal midbrain respectively. The trigeminal nucleus (V) occupies r2 and 3 in chick, but extends into r1 in mice. The facial (VII) and vestibuloacoustic (which is not a motor nucleus, but innervates the sensory epithelia of the inner ear, Simon & Lumsden, 1993) (VIII) nuclei are found in r4, 5 and 6 in the mouse, but only in r4 and 5 in chick. In chick hindbrain we find the abducens (VI) nucleus in r5 and 6 with the smaller accessory abducens restricted to r5; in mouse abducens is found only in r5. Rhombomere 6 also contains the glossopharyngeal nucleus (IX) in mouse, which extends into r7 in chick hindbrain. In the more caudal region of the hindbrain the vagus (X) and cranial accessory (XI) are found in r7 and 8. Finally in r8 of both mouse and chick we find the hypoglossal nucleus (XII) (Guthrie 2007).

*Image removed

Figure 1.6: The position of motor nuclei and ganglia in chick (left) and mouse (right) hindbrain. III, Oculomotor; IV, Trochlear; V Trigeminal; VI, Abducens; aVI, accessory Abducens; VII; Facial; VIII, vestibuloacoustic; IX, glossopharyngeal; X, Vagus; XI, cranial accessory; XII, hypoglossal. Figure from Guthrie, 2007.

1.3.2 *Hox* genes regulate cranial motor nuclei differentiation and positioning

The distribution of the cranial motor nuclei can therefore help to inform the role of *Hox* genes in controlling the regional patterning and neuronal specification in the hindbrain. For example, r4 has been the focus of much study due to its unique expression of *Hoxb1.* Within r4 the BM neurons of the facial nucleus (FBM) differentiate and in mice, but not chick, subsequently migrate to r6. Following *Hoxb1* mutation, as mentioned previously, r4 takes on an r2 phenotype .That is, FBM fail to migrate and eventually are lost. The remaining motor neurons extend their axons aberrantly to the first branchial arch as opposed to the second. Thus it appears that the remaining MNs take on a trigeminal identity. Misexpression of *Hoxb1* in r2 results in, as would be predicted, trigeminal MNs adopting a FBM neuronal fate; here MNs project their axons to the second branchial arch (Goddard et al., 1996; Studer et al., 1996; Bell et al., 1999) (Figure 1.7).

Importantly, following *Hoxb1* disruption the structural formation of the rhombomeres is not altered, indicating that *Hoxb1* plays a role in specification of FBM identity within r4. Further to this, it is known that *Hoxb1* expression in the neural crest cells

is required for correct guidance of the facial nerve in the periphery and survival of the FBM neurons in r4. Conditional knock out of *Hoxb1* expression in these cells leads to failure of the facial nerve to develop and eventual death of FBM neurons (Arenkiel et al., 2004).

*Image removed

Figure 1.7: Following *Hox*b1 double knockout in mouse hindbrain (left) Facial Motor Neurons (green) fail to migrate caudally or across the floorplate as observed in *Hox*b1$^{+/-}$ or WT conditions. In the *Hox*b1$^{-/-}$ Facial Motor Neurons migrate laterally in a similar manner to trigeminal motor neurons (red) in r2. In Chick hindbrain, misexpression of *Hox*b1 in r2 results in aberrant path finding of trigeminal motor axons to the second branchial arch (Green). Figure from Lumsden, 2004.

Similarly the expression of the *Hox3* genes is thought to regulate the differentiation of SM motor neurons in r5 and 6. The *Hox3* genes, *Hoxa3*, *Hoxb3* and *Hoxd3* are expressed in r5-8 in chick, with highest expression of *Hoxa3* in r5&6. Knock down of any of these three *Hox* genes leads to defects in rhombomere identity, specifically *Hox3* genes act to inhibit expression of *Hoxb1*, thus suppressing BM neuron development. Double knock out of *Hoxa3* and *Hox*b3 in r5 and 6 is sufficient to inhibit differentiation of SM motor neurons which constitute the abducens motor nucleus (Gaufo et al., 2003).

Hox gene expression is refined in the rhombomeres by specific upstream signalling factors for example, the transcription factor *Krox20* which is expressed in r3&5 (Wilkinson et al., 1989) and acts to initiate the transcription of *Hoxa2, Hoxb2* and *EphA4*. In the absence of *Krox20* neuronal populations of r3&5 are found to intermingle with those from neighbouring rhombomeres (Schneider-Maunoury et al., 1997). In *Krox20*$^{-/-}$ mice motor neurons populations are depleted (Schneider-Maunoury et al., 1997). Similarly the upstream *Hox* regulator *MafB* is expressed in r5&6 and regulates their development. In *MafB*$^{-/-}$ mice these rhombomeres fail to develop causing loss of SM and VM nuclei in these regions (McKay et al., 1997).

Hox genes are also thought to control MN differentiation in the dorsoventral axis of the hindbrain from progenitor populations in the basal plate of the developing hindbrain. The process of MN differentiation in this axis has been extensively studied in spinal MNs which are specified in distinct progenitor domains along the dorso ventral axis under the control of Sonic Hedgehog (Shh) secreted from the floor plate and notochord, which in turn modulates the expression of homeodomain transcription factors (Briscoe & Ericson, 1999; Briscoe et al., 2000). Molecularly distinct ventral neuronal subtypes are generated in five distinct domains in the developing spinal cord. The generation of these neuronal subtypes can be induced in vitro by selective two to three fold increases in Shh concentration. Importantly the position of each progenitor domain from the floorplate and the distinct neuronal subtypes generated there can be predicted in vivo by the concentration of Shh required for different subtype induction in vitro (Ericson et al., 1997).

Each progenitor domain can be specified by its expression of homeodomain transcription factors under the control of the zinc finger-containing *Gli* transcription factors; Stamataki et al., 2005 demonstrated that incremental changes in Gli TF activity can mimic the action of Shh concentration changes in the neural tube (Stamataki et al., 2005). Indeed, in *Gli2*$^{-/-}$ mice the floor plate is not specified diminishing the Shh signal (Ding et al., 1998). Gli3 is thought to act as a transcriptional repressor; in the absence of SHH *Gli3* is proteolytically processed to produce a *Gli* repressor, which acts to down regulate gene transcription. Derepression of *Gli3* is required to specifiy the more dorsal SHH dependant cell types in the neural tube (Persson et al., 2002).

Thus Shh signalling is transduced into a gradient of *Gli* activity which acts to specify the gene expression response in each progenitor domain. Two classes of homeodomain TFs are expressed in ventral spinal neurons designated as either class I; *Pax7, Dbx1, Dbx2, Irx3* and *Pax6* or class II; *Nkx6.1* and *Nkx 2.2* (Briscoe et al., 2000). Class I protein expression is repressed at distinct Shh threshold concentrations, whilst Class II proteins require Shh for induction as a result the boundaries of expression of these proteins delineate the progenitor domain boundaries. The paired cross repression of these transcription factors acts to define the neuronal subtype found in each boundary and relieves the requirement for continued SHH signalling (Jessell 2000). Spinal motor neurons originate in the *Olig2*$^{+}$ pMN domain. *Olig2* is a bHLH class transcription factor which primes neurons to a MN state and is required for the development of motor neurons and

oligodendrocytes sequentially (Lu et al., 2002). Within the pMN domain the combinatorial action of *Nkx 6.1, Nkx 2.2* and *Irx3* lead to a restricted expression of the homeodomain protein, *MNR2*. *MNR2* is a specific determinant of motor neuron identity which is expressed prior to the last mitotic division of MNs in the pMN domain, ectopic *MNR2* expression is sufficient to direct ventral neurons of interneuron subtypes to a motor neuron fate (Tanabe et al., 1998).

Similarly in the hindbrain Shh secreted from the floor plate and notochord produces specific populations of motor neurons in different progenitor domains (Stamataki et al., 2005). In terms of SM, VM and BM populations, BM and VM neurons are generated in the p3 domain, directly adjacent to the floor plate (Pattyn et al., 2003), whereas SM neurons are generated in the more lateral pMN domain (Ericson et al., 2003) (Figure 1.8).

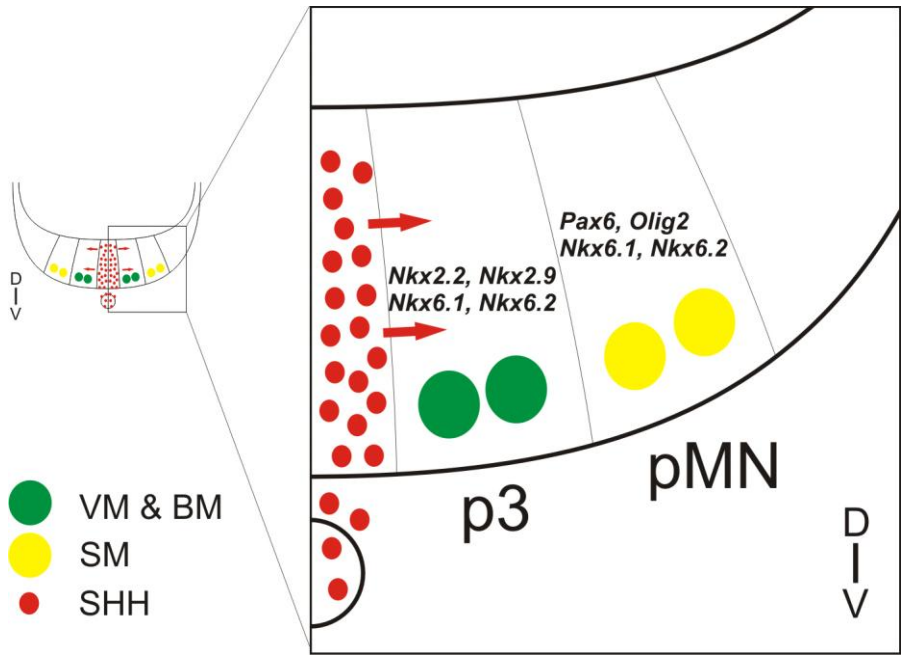

Figure 1.8: Motor neurons in the hindbrain differentiate in different progenitor domains under the control of secreted Shh signalling from the notochord and floorplate.

factors which act to specify neuronal subtype. Both domains express *Nkx 6.1* and *6.2*, which act as repressors of interneuron fate. Loss of function of either or both *Nkx 6.1* and *6.2* leads to aberrant migration of VM and BM neurons and complete loss of the SM neurons which constitute the abducens nucleus. The p3 domain is also found to express *Nkx 2.2* and *2.9* (Figure 1.8) which are believed to specify VM and BM neuron fate in the spinal cord (Briscoe et al., 1999) and hindbrain respectively; Pabst et al., (2003) demonstrated that in *Nkx2.9* deficient mice there

are marked defects in Spinal Accessory (SA) nerve development, which appears reduced in size, concomitant with a reduction of BM neurons which normally migrate to the dorsolateral aspect of the hindbrain. The vagus and glossopharyngeal nerves were also reduced in size in 50% of *Nkx2.9* deficient mice indicating a role in BM neuron development (Pabst et al., 2003). In the pMN domain expression of the homeobox gene *Olig2* induces the expression of *MNR2*, which is a key regulator of motor neuron fate (Tanabe et al., 1998). *Olig2* is crucial for the development of SM neurons in r5 and 6; Zannino & Appel (2009) performed a morpholino knock down of *Olig2* function in r5 and 6 of zebrafish embryos which resulted in the failure of Abducens motor nucleus to develop (Zannino & Appel., 2009).

Following these early specification events both SM and BM/VM neurons are found to express a different repertoire of transcription factors. All cranial MNs express *Islet-1* after exiting the cell cycle (Ericson et al., 1992); a member of the LIM homeobox gene family. LIM genes have been shown shown to control neuronal identity and axon pathfinding in vertebrates; Tsuchida et al., 1994, demonstrated that in the spinal cord, combinatorial expression of LIM genes distinguish subclasses of motor neurons in the spinal cord which topographically extend their axons to the periphery (Tsuchida et al, 1994; also discussed later in terms of motor pool development and identity, Introduction 1.6.2). However, only SM neurons express *Hb9* (Arber et al., 1999); *Hb9* is closely related to *MNR2* however is expressed only in post mitotic motor neurons and is believed to be involved in the consolidation of MN neuron fate. In mice lacking *Hb9* function, MNs develop as normal; however will acquire the molecular identity of interneurons, whilst ectopic expression of *Hb9* or *MNR2* is sufficient to induce MN identity (Arber et al., 1999; Tanabe et al., 1998). This is useful when analysing cranial motor neuron positioning as it allows easy identification of different motor neuron subtypes. Studies in chapters 3.1 and 3.2 of this thesis rely upon this as a method of identifying different motor nuclei.

1.3.3 Peripheral targets of the r5 and r8 cranial motor nuclei

Within r5 of the chicken hindbrain there is a complex of 4 major cranial motor nuclei; abducens, accessory abducens and facial motor nucleus, which consists of dorsal and ventral divisions. The abducens (Ab) is a SM nucleus, its axons project ventrally from the hindbrain to the lateral rectus muscle of the eye, as a major part of the VIth

cranial nerve. The abducens consists of two spatially separated aspects, the abducens which is found in the medial dorsal aspect of the hindbrain and the accessory abducens (AccAb) which is located laterally to the facial motor nucleus. AccAb projects to the retractor bulbi muscle which controls retraction of the eye associated with extension of the nictitating membrane (Disterhoft et al., 1985, Labandeira-Garcia et al., 1989, Wahl et al., 1994). Positioned ventrally to the abducens and medial of the accessory is the facial motor nucleus (FMN). The FMN consists of two divisions (ventral and dorsal) of BM neurons, which extends their axons towards a large dorsal hindbrain exit point. Upon exit into the periphery the axons of the FMN form part of the VIIth cranial nerve which innervates the second branchial arch muscles and the parasympathetic ganglia. (Jacob et al., 2000).

In rhombomere 8 there are also 4 distinct cranial motor nuclei; the glossopharyngeal, vagus dorsal hypoglossal and ventral hypoglossal nuclei. The hypoglossal nuclei consist of SM neurons and are divided into dorsal and ventral aspects close to the midline (Figure 1.9), they project their axons ventrally as the XIIth cranial nerve to the muscles of the tongue (Youngren & Philips 1983). The glossopharyngeal nucleus consists of SM neurons which innervate the pharyngeal muscles and salivary glands as part of the IXth cranial nerve. The vagus motor nucleus, which is made up of BM neurons innervates multiple targets in the thoracic region and the abdominal viscera (Kuratani & Tanaka, 1990).

BM and SM neurons can be distinguished by their respective expression of *Hb9* and *Islet-1*; Figure 1.9, showing transverse sections through rhombomeres 5 and 8 of the chick embryonic hindbrain illustrates this expression difference and demonstrates the positioning of the cranial motor nuclei discussed here.

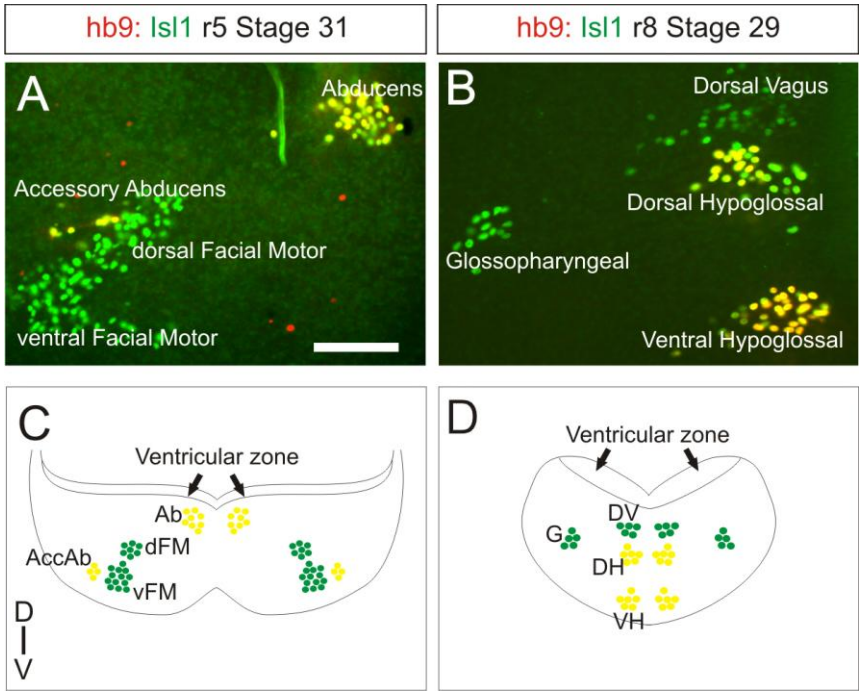

Figure 1.9: Somatic motor and Branchiomotor neurons can be differentiated by their expression of *Hb9*. Somatic MNs (yellow) express *Hb9* and Islet1, whilst Branchiomotor express only *Islet-1* (green). **A:** The motor nuclei of r5 in the chick hindbrain at HH31. **B:** The motor nuclei of r8 at HH29. Scale bar 100µm. **C,D:** Diagrammatic representations of r5 and 8 respectively showing the bilaterally repeated patterns of cranial nucleus organisation.

1.4 Cranial auditory (sensory) nuclei

As well as focusing on the development of cranial motor nuclei, this study will also seek to address potential mechanisms which may control auditory nucleus development. Within r5 and 6 there are 3 distinct sensory nuclei; nucleus Angularis (nA), nucleus Laminaris (nL) and nucleus Magnocellularis (nM), which constitute the auditory hindbrain. The neurons which will constitute these nuclei originate in spatially discrete domains from MNs, however given their close proximity to the motor nuclei; it is likely that the development of these two neuronal populations may be linked. The role of the auditory hindbrain nuclei is that of a second order sensory nucleus which integrates sound input from both ears before passing signals to higher centres. In order to investigate the development of these nuclei it is necessary first to understand the unique structures that are found here and how tightly controlled nucleogenesis is critical for their function.

1.4.1 Structure of the auditory hindbrain

Unlike the motor nuclei of the chick hindbrain, which coalesce into spherical like clusters, the function of the auditory hindbrain requires an unusual anatomical specialisation. One of the three r5 nuclei, the nL is a single cell thick lamina which extends broadly along the rostro caudal axis of the hindbrain. This type of lamination is unusual as it does not exist within the framework of a stratified structure, such as the cerebral cortex, but is isolated. First described by Ramon Y Cajal; the nucleus sits ventral to the nM and consists of approximately 750 individual neurons, each with a bipolar dendritic architecture extending dorsally and ventrally (Cajal 1909; Parks & Rubel., 1975; Smith 1981).

*Image removed

Figure 1.10: Nissl staining of nucleus Laminaris (NL) and nucleus Magnocellularis (NM). NL is a single cell thick neuronal structure, which sits ventral to the NM. NM can be seen as a tight cluster of neurons which extends for approximately half the length of the NL. There is a visible cell sparse region surrounding NL, which is occupied by the bipolar dendrites of NL neurons. Image from Rubel et al., 1985.

The nM forms a bilateral circuit with nL which facilitates processing of Interaural Time Differences (ITD's); the time difference between sound reaching one ear compared to the other. This, in the case of the chicken, is approximately 0-180µs (Overholt et al., 1992; Hyson, 2005) By calculating the ITD a bird can establish from which direction a sound originated and can accurately distinguish between sound sources separated by less than 1-2º along the horizontal plane (Review see Hyson 2005) . It is this nL-nM complex which will provide the model for nucleogenesis which will be investigated in chapters 3.3 and 3.4.

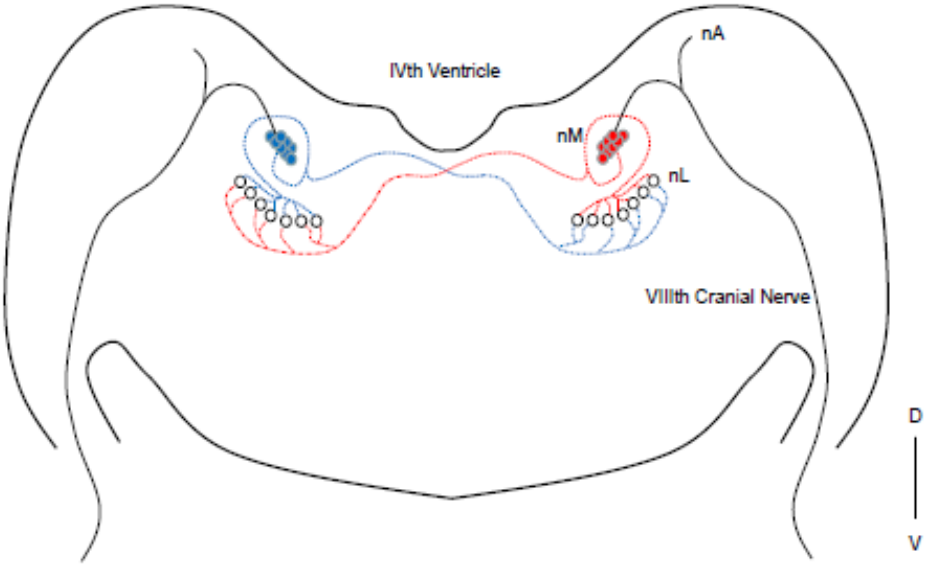

Figure 1.11: Schematic showing the organisation of avian auditory hindbrain circuitry. The VIIth cranial nerve projects to both the nM and nL. The nM then projects in turn to both contralateral and ipsilateral nL (indicated by red/blue dotted lines). In this manner a bilateral circuit is established enabling the processing of ITD's.

Sound waves impinging on the tympanic membrane of the middle ear cause frequency specific oscillation of the columella bone. This in turn vibrates the oval window of the fluid filled cochlea; movement of this fluid induces wave like movement along the basilar papilla membrane. Each region of the basilar papilla responds maximally to oscillations at specific frequencies. Movement of the membrane is registered by the specialised 'hair cells' within the basilla papilla which convert mechanical stimulation by the tectorial membrane of their apical stereocilia or 'hair bundles' into a change in electrical potential within the cell. This change in

membrane potential leads to action potential generation in the spiral ganglion cells which project their axons to the nM within the hindbrain as the VIIIth cranial nerve. The axonal projections of nM extend bilaterally to both ipsilateral and contralateral nL. Ipsilateral nM-nL connections are found exclusively on dorsal nL dendrites, whilst contralateral nM axons synapse with ventral nL dendrites (Young & Rubel, 1983). In this manner auditory information from either ear is spatially segregated onto dorsal or ventral dendrites of nL neurons (Figure 1.11).

Ipsilateral action potential nM input occurs simultaneously across the entire nL, whist contralateral input occurs sequentially across the laminar moving medially to laterally. It is traditionally held the contralateral input is delayed by a series of 'delay lines' established by very fine control of axonal growth and targeting (Jeffress, 1948; Gorlich, 2010). The time taken for action potentials to travel across the array of delay lines will at one point offset the ITD. When simultaneous input from both ipsilateral and contralateral nM occurs, this increases the probability of action potentials being produced by the nL neuron. In this manner, nL neurons are said to act as 'coincidence detectors' (Figure 1.12).

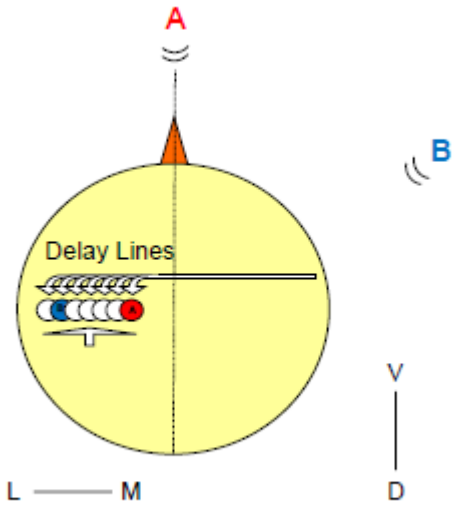

Figure 1.12: nL neurons act as coincidence detectors, representing a place map relating to the origin of a sound source in the horizontal plane. Ipsilateral input occurs simultaneously across the entire nL, whilst contralateral input travels along a series of delay lines. At one point the time taken for a sound to travel from one ear to the other (the ITD) is offset by the time taken for action potentials to reach a certain point on the nL and coincident input occurs. For example, a sound originating at point A will cause coincident input at point A in the medial nL. Where as a sound originating at point B will cause coincident input at point B on the nL. This model was first proposed by Jeffress (1948).

Thus across the medial to lateral extent of nL there exists an ITD axis, which corresponds to a place map; each neuron can be said to fire maximally when a

sound originates at a specific angle from the midline (Overholt, 1992). The nL can also be divided into three broad regions which are specialised to process input from different characteristic frequency (CF) ranges; High 2.5-3.3KHz, Middle 1-2.5KHz and low 0.4-1KHz (Smith & Rubel., 1979; Smith, 1981) (Figure 1.13). Across the frequency axis of nL there exists a gradient in the length of dendritic projections, high CF cells have short highly branched dendrites in comparison to middle and low frequency CF neurons, which have longer relatively unbranched dendrites. The anatomical specialisations of nL neurons have been shown to be important in enhancing the acuity of ITD detection (Agmon-Snir et al., 1998; Grau-Serrat, 2003) across the entire frequency range (Figure 1.12).

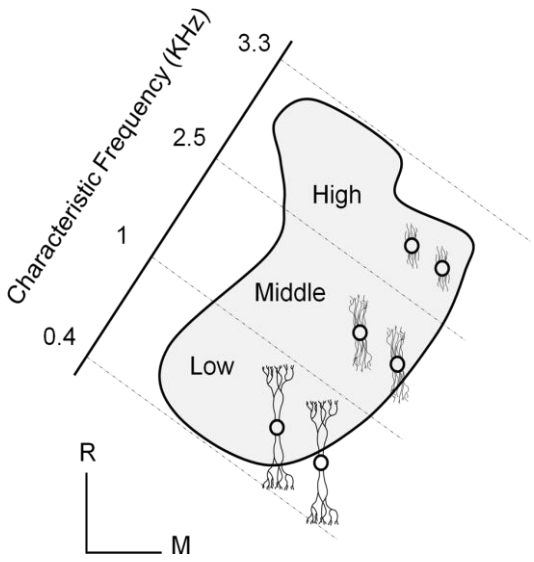

Figure 1.13: The nL is tonotopically organised such that neurons which receive input at high, middle or low frequencies are found in different regions along the rostromedial to dorsolateral axis. In the chick, the audible frequency range of 0.4 to 3.3 KHz is represented here. Specialisations of nL neurons include the differing length of the bipolar dendrites. Illustrated here, high frequency neurons have highly branched, relatively short dendrites, whilst low frequency neurons exhibit long sparsely branched dendrites. This is a graded change, such that the change occurs gradually across the array, not in a few spatially distinct populations.

Another anatomical specialisation of nL neurons is found to be when looking at the site of action potential initiation (the Axon initial Segment, AIS) along the tonotopic axis. The proximal aspect of neuronal axons is found to be myelinated, but only for neurons in the middle and high CF regions of nL, this myelination is absent on low CF neurons (Kuba et al., 2006) suggesting an adaptation for processing higher frequency sounds. Indeed Kuba et al., 2006 demonstrated that in nL neurons there are clusters of the sodium channel Nav1.6 along the axon but it is largely absent from the soma. Structurally these clusters are found at increasing distance from the soma as CF increases, and vary in length. In low CF neurons the AIS is approximately 25µm in length and located 5µm from the soma, in high CF neurons the AIS is approximately 10µm in length and located up to 50µm from the soma.

High CF neurons receive multiple high frequency inputs onto dendritic sites located close to the soma. Modelling this scenario, Kuba demonstrated that these inputs temporally summate and cause a plateau depolarisation of the soma. This depolarisation inactivates sodium channels and acts to inhibit action potential generation. By increasingly isolating the site of action potential initiation from the soma with increasing CF, nL neurons bypass this problem.

Physiologically nL is adapted to enable accurate coincidence detection. This is mediated by two main strategies; a rapid Excitatory Postsynaptic potential (EPSP) time course combined with an active inhibitory input. Neurons in nL are found to express fast activating AMPA receptors (Ravindranathan et al., 2000; Kuba et al., 2002) which act to accelerate EPSP time course. These neurons also have a very low input resistance due to an activated potassium current at rest. This effect is a result of the expression of a low voltage-activated Potassium channel, Kv1.2, which is abundant in nL and is upregulated immediately prior to hatching (Kuba et al., 2005). A rapid EPSP time course significantly reduces the possibility of temporal summation, whereby the depolarisation of the membrane is of sufficient amplitude that subsequent depolarising input occurs whilst the membrane is still depolarised. Under high frequency stimulation this results in summation of the two inputs, pushing the membrane closer to the depolarisation threshold required to initiate action potential generation. Temporal summation can therefore lead to aberrant action potential generation which inputs to nL neurons are not coincident, but sufficiently close to one another to reach the depolarisation threshold. As a result of the rapid EPSP time course the possibility of temporal summation is significantly reduced, preventing accidental action potential generation and thus improving the acuity of coincidence detection. The entire nL also receives a broad inhibitory input across the entire frequency range from the ipsilateral Superior Olivary Nucleus (SON) (Burger et al., 2005) mediated by $GABA_A$ receptors this inhibitory pathway acts as a gain control, inhibiting non specific nL neuronal firing. (Lu et al., 2009)

1.4.2 Development of the auditory hindbrain

The motor neurons of the chick embryonic hindbrain originate in distinct domains adjacent to the floor plate under the control of Gli transcription factors which act to suppress interneuron cell fate. The exact mechanisms which control sensory neuron differentiation in the hindbrain are not currently known, however, experiments using chick-quail chimeras have shown that the neurons which constitute the nL and nM

originate in the alar plate of the hindbrain, in a region lateral to that of motor neuron development (Tan & La Douarin, 1991). The neurons which will constitute nL differentiate at around embryonic day (E) 3.5-4 (HH21-23), those neurons which constitute nM differentiate slightly earlier around E2.5-3 (HH17-20) .The two neuronal populations are spatially distinct and are found initially to be spread across several rhombomeres; nL neurons are found in R5 and 6, whilst nM neurons are located in R5,6 and 7. This suggests that these neurons are specified prior to migration and is indicative of an earlier lineage link (Cramer et al 2000).

Both populations share a common migratory route, moving towards the dorsal aspect of the hindbrain to coalesce in an area known as the Auditory Anlage (AA) (Book & Morest, 1990) by E5-6 (HH28-29). This is the first recognisable manifestation of the auditory hindbrain and is characterised as a ball of neurons surrounded by a cell sparse region. The development of the nL-nM bilateral circuit begins as nM neurons extend their contralateral projections to the ventral aspect of nL, this occurs at E6 and, importantly, prior to nM innervation by cochlea nerve afferents (Hendricks et al., 2006; Molea et al., 2003) (Figure 1.14); suggesting that the preliminary organisation of the circuit is not activity dependent. This is supported by lineage tracing which indicates that in the tonotopically organised nM, neurons originating in R5 will contribute to the higher end of the frequency axis whilst those originating in R7 will contribute to lower end (Cramer et al.,2000)

Subsequently from HH29-34, there is a period of growth in the hindbrain which leads to a medial displacement of the AA. Throughout this period the AA begins to segregate into distinct nM and nL populations; a process which is completed by HH35 (Figure 1.14). At HH35 nL-nM synapses begin to form (Hendricks et al., 2006) and the dendritic trees of nL neurons across the frequency axis begin alteration towards their adult morphologies (Smith 1981). The mapping of nM input on to nL is potentially controlled by Eph protein expression (Cramer et al., 2002); at HH36 there is an expression gradient of EphA4 which is highest on the dorsal neuropil of the rostral nL neurons and lowest on the dorsal neuropil of the caudal nL neurons (Person et al., 2004). Synapses from nM-nL are functional at approximately HH37, and chicks are responsive to sound *in ovo* at HH38, after which the graded expression of EphA4 is lost; indicating that this mapping is not initially dependent upon sensory stimulation.

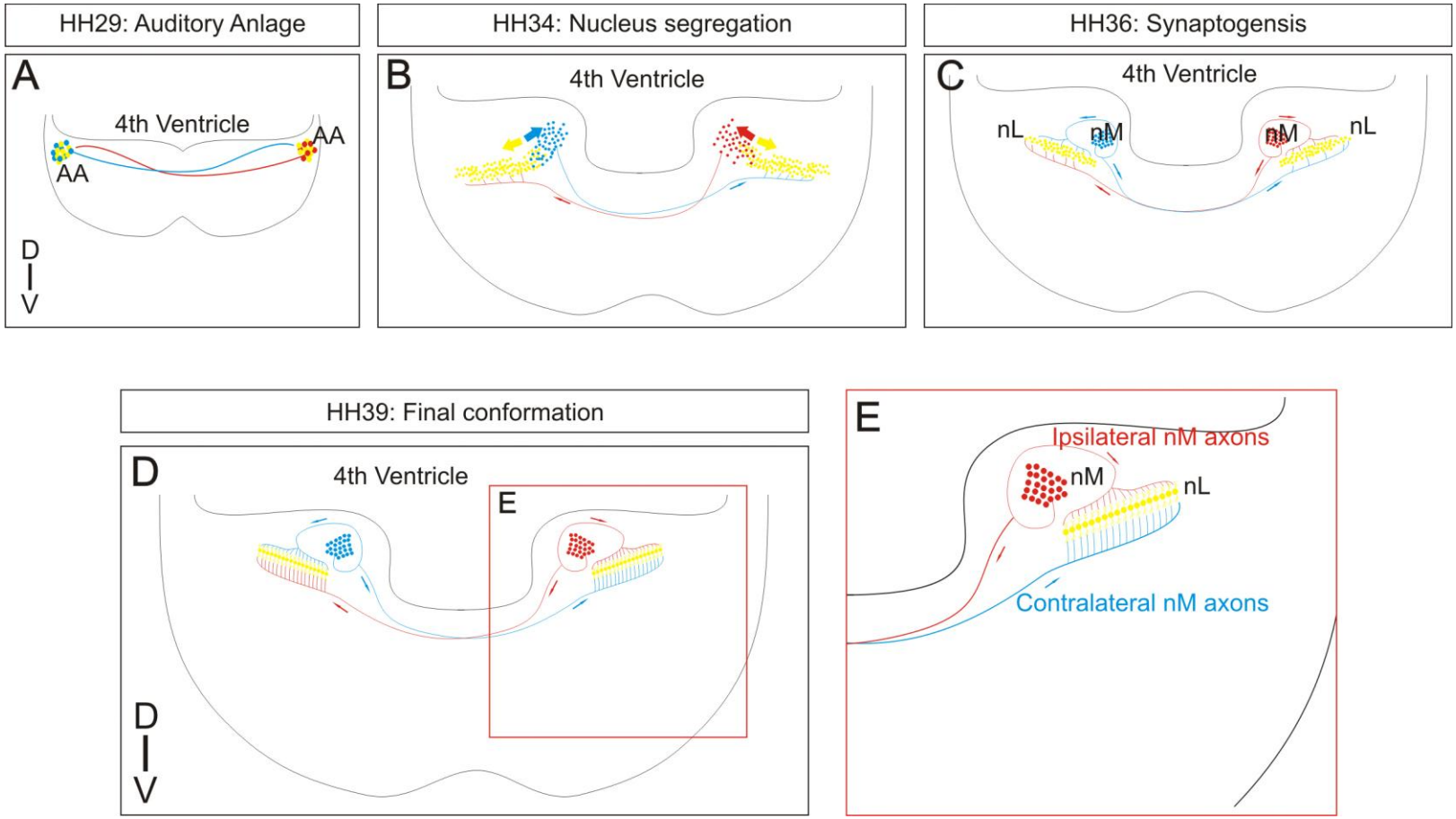

Figure 1.14: Developmental time course of auditory hindbrain nucleogenesis**. A:** At HH29 the Auditory Anlage (AA) is visible in the dorsal hindbrain; nM axons extend across the midline towards the contralateral AA. **B:** The nM and nL are segregating into two distinct population at HH34. (Large arrows indicate cell movements). **C:** By HH36 segregation is complete and synaptogenesis between nM axons and nL neurons begins.**D:** By HH39 the nL has taken its mature form, is one cell thick and is innervated by bilateral nM input. **E:** Magnification of the image in 'D' to illustrate the segregated nM axonal input to the mature nL.

The nL neurons do not achieve their mature architecture until Post hatch day 25 (Saunders et al., 1973). Following segregation, nL appears as a long thick group of cells, ventral to nM. This conformation is altered gradually as the nL appears to 'thin' into a single cell thick sheet of neurons by approximately HH40. Developmentally this process appears to occur first in rostral nL and occurs slightly later in caudal regions (Smith, 2011).It is possible therefore to consider the development of nL in two distinct stages, the first from HH17 to HH40 is a period of intense neuronal migration and organisation which occurs largely in the absence of sound cues. The second from HH41 onwards is a period of late development where auditory function is specialised and refined, a process which is likely driven by auditory input (Review see Gao & Lu., 2008).

To summarise, nuclei occupy specific spatially discrete positions within the hindbrain and are crucial to the formation of functioning neuronal circuits. In the specific case of the nL, the structure of the nucleus itself is also critical to its function in sound source localisation. Positioning of neuronal nuclei appears to be closely linked to regional patterning in both the rostrocaudal and dorsoventral axes of the developing hindbrain. However,, the mechanisms which drive coalescence and organisation of these neuronal nuclei in the hindbrain are yet to be elucidated. The question therefore is how are these cells which are functionally related able to identify and adhere to each other, forming distinct neuronal nuclei?

1.5 Cell adhesion

The development of any multicellular organism requires dynamic and properly regulated intercellular adhesion. Adhesion between cells provides a physical anchor which maintains structural integrity across tissues and facilitates intercellular communication. In the vertebrate nervous system we now know that adhesion between neurons is mediated by several families of cell surface adhesion proteins, the expression of which are highly temporally and spatially controlled throughout development (For reviews see Shapiro et al, 2007. Cavey & Lecuit, 2009). However,, the principle that cells are held together by an intercellular substance has been a topic of interest for over a century.

Early studies on cellular cohesion, for example by H. V. Wilson in 1907, demonstrated that cells from living tissues are able to coalesce with one another following dissociation. Wilson took dissociated cells from living sea sponges and found that they would form aggregates similar in structure and identity to the parent sponge when incubated in sea water (Wilson, 1907); thus demonstrating an inherent ability, and preference, of individual cells to adhere to one another forming organised structures. In vertebrate species observations by Schiefferdecker (1886) indicated that cells which constitute the tissues of vertebrate species were also held together; demonstrated by the separation of dermal layers from pancreatic extracts (Reviewed by Steinberg, 1996). It was proposed by J. Gray (1926) that this binding of cells was mediated by “intercellular cement” “The stability of the epithelium depends upon the presence of this intercellular complex, since if it be removed adjacent cells separate easily from their neighbours” (Gray, 1926). Working with *Mytilus* (a genus of saltwater mussels) Gray demonstrated that cells taken from the gill epithelia were prone to dispersal, which could be accelerated by altering the ion content of water (Figure 1.15) (calcium was identified as a potential factor in cell adhesion as early as 1900 by Herbst) (Gray, 1926).

This concept of a binding intracellular substance was maintained through subsequent studies on vertebrate tissues. Moscona & Moscona (1952) investigated the ability of chick limb bud cells to reconstitute in vitro following complete or partial disintegration; finding that these structures were able to reorganise in a manner reflective of normal development when cultured as mixed aggregates. Isolated populations of myogenic cells were unable to develop in this manner, leading to the

conclusion that this “might also have been due to an impairment of their capacity to secrete in vitro the normal combination of intercellular materials” (Moscona & Moscona, 1952).

*Image removed

Figure 1.15: The degree of cell dispersal from a cohesive tissue in water is increased by reducing calcium concentrations. Figure from Gray, 1926.

Moscona (1960) identified what he believed to be the intercellular substance using crude pancreatic preparations and suggested that this substance “combining the functions of a cell bonding framework and an information network” was crucial to theories of developmental biology. However, this substance was later identified to be DNA which had escaped damaged cells (Moscona, 1960. Steinberg, 1996).

In principle however, this theory of the role of an extracellular substance is true; it is now accepted that proteins on the surface of cells are crucial for cell adhesion, but also perform an instructional role in terms of cell recognition and circuit development. Both of these studies discussed used different methods to dissociate cells; protease treatment (trypsin) or alterations in ionic concentration. Several mechanisms of action for calcium mediated cell adhesion were proposed following the work of Gray (1926), for example Schmitt (1941) who proposed that the Ca^{2+} may act to reduce the negative charge between cell surfaces allowing contact, leading Steinberg et al., to investigate the effect of Ca^{2+} removal versus protease treatment in cell dissociation (Steinberg et al., 1973).

Steinberg et al., found that when dissociated by removal of Ca^{2+} and Mg^{2+} ions, retinal cells would form aggregates immediately when resuspended in culture medium. Conversely, those cells treated with trypsin required a lag period before aggregation would begin following resuspension. Steinberg et al., concluded that trypsinisation “alters the composition of the cell surface” and that the lag time was a consequence of the cells requirement to replace lost or damaged cell surface

components (Steinberg et al., 1973). Interestingly, in the presence of small concentrations of Ca^{2+} during trypsinisation, cells were able to aggregate immediately following resuspension, without a delay period.

This observation was crucially repeated by Takeichi (1977) who described two distinct mechanisms of cell adhesion; Ca^{2+} dependent system (termed CADS) and Ca^{2+} independent system (termed CIDS). The Ca^{2+}-dependent mechanism is sensitive to trypsin, but can be protected by addition of Ca^{2+} from proteolysis. Experimenting with different concentrations of Ca^{2+} and trypsin, Takeichi demonstrated that treatment with high concentrations of trypsin in the absence of Ca^{2+} disables both mechanisms, leaving cells unable to adhere to one another. Low concentrations of trypsin were sufficient to disable Ca^{2+} dependent adhesion, but not Ca^{2+}-independent adhesion. Addition of Ca^{2+} to the trypsin medium is sufficient to protect the CADS alone (Takeichi et al., 1977). It was discovered further to this that cells treated with trypsin and Ca^{2+} were found to express a cell surface protein of approximately 150000MW, which was absent from cells treated with trypsin alone.

Subsequent study focussed, naturally, upon identifying the proteins which mediated these types of cellular adhesion. Utilising the trypsin and Ca^{2+} combination system it was possible to isolate the cell surface protein which was mediating CADS adhesion. Takeichi (1981) and Yoshida & Takeichi used Fab preparations of antibodies raised in rabbit against teratocarcinoma (F9) cells to achieve this. Firstly demonstrating that these Fab fragments were able to inhibit aggregation of T9 cells (Takeichi, 1981) following combined trypsin and Ca^{2+} treatment, thus targeting CADS specifically. This inhibitory effect was neutralised using extracts from cells which had been treated only with trypsin; thus removing the cell surface protein, which acts to sequester the anti-F9 fragments in vitro. Fractionation of this supernatant revealed the presence of a 34K molecule which was bound to the antibody. Subsequent analysis revealed that a 124K protein isolated from trypsin and Ca^{2+} treated cells shared this fragment. It was this protein which mediated calcium dependent cell adhesion; Yoshida & Takeichi termed this molecule ‘cadherin’.

1.6 Cadherins

Following the identification of the teratocarcinoma cadherin it was demonstrated that this cadherin was found in epithelial cells (Oguo et al., 1983) leading to re-classification as E-cadherin. Other cell types which did not express E-cadherin were also demonstrated to be subject to calcium dependent cell adhesion, but did not express E-cadherin specifically. Instead it was revealed that different tissues expressed cadherins which were similar to E-cadherin in molecular weight and protease cleavage activity (Reviewed in Takeichi, 1988), for example N-cadherin (neural cadherin) which was isolated in early embryonic mouse tissues and expressed differentially to E-cadherin, marking boundaries between distinct cellular layers (Hatta et al., 1986).

Since this initial discovery the cadherin family of cell adhesion molecules has grown to include over 100 individual identified cadherins, which are classified into several subfamilies dependent upon their structure; classical cadherins, desmosomal cadherins, protocadherins, Flamingos/CELSRS and FAT cadherins. (For reviews see Shapiro et al., 2007; Suzuki & Takeichi, 2008; and Nollet, Kools & van Roy, 2000). The classical cadherins and desmosomal cadherins are well defined as adhesion molecules, whilst the other subfamilies often have differing roles in vertebrate development. As such the classical cadherins represent a good candidate to drive neuronal coalescence in these regions.

In vertebrates the classical cadherins are single pass transmembrane proteins that can be subdivided into two groups; Type I or two. Type I/II cadherins possess five repeated 110 amino acid extracellular cadherin (EC 1-5) domains, whilst atypical cadherins have a variable number of EC domains (Tanabe et al., 2004). Each domain contains three calcium binding points; calcium binding to these domains causes the extracellular region to rigidify and is essential for cadherin-based cell adhesion (Nagar et al., 1996).

The EC1 domain is the N-terminus of the protein and contains the region which determines the specificity of cadherin binding although each of the domains is potentially involved in the process of dimerisation (Tsuiji et al., 2007). Both *cis* and *trans* dimerisation of cadherins is known to occur, and this is thought to be important for the cell adhesive function of the cadherins. Stabilised cadherins project out from the cell membrane surface and interdigitate with those projected on the opposite cell membrane surface, in what has been described as the ‘adhesion zipper’ (Shapiro et

al., 1994). The alignment of these bound cadherins at the cell surface reflects that of the intracellular actin filaments to which the cadherins associate. These intracellular filaments are stabilised and facilitate the formation of strong adhesive contacts between cells (For review see Pokutta & Weis, 2007). Binding is preferentially homophilic between identical cadherins on the surface of opposed cells, this differential binding is shown to mediate cell sorting both *in vitro* and *in vivo* (Introduction 1.6.1). However, studies have demonstrated that classic cadherins are able to bind heterophilically (Shi et al., 2008).

Cadherins have a highly conserved intracellular region, which has two separate catenin binding domains; the juxtamembrane domain binds p-120 catenin whilst the catenin binding domain can bind either ɣ or β catenin (Nollet et al., 2000). It is through this catenin binding domain that cadherins are able to mediate intercellular adhesion; cadherins bind to ɣ or β catenin which in turn is able to bind cytoplasmic α catenin, subsequently α catenin is coupled to F-actin of the cytoskeleton via an intermediate factor known as EPLIN (epithelial protein lost in neoplasm). This cadherin-catenin-EPLIN-actin complex forms the adherens junction which is the basis of intercellular adhesion. It has been demonstrated that in the absence of either α catenin or EPLIN this complex is unable to form and cadherin-mediated intercellular adhesion is inhibited (Abe & Takechi 2008).

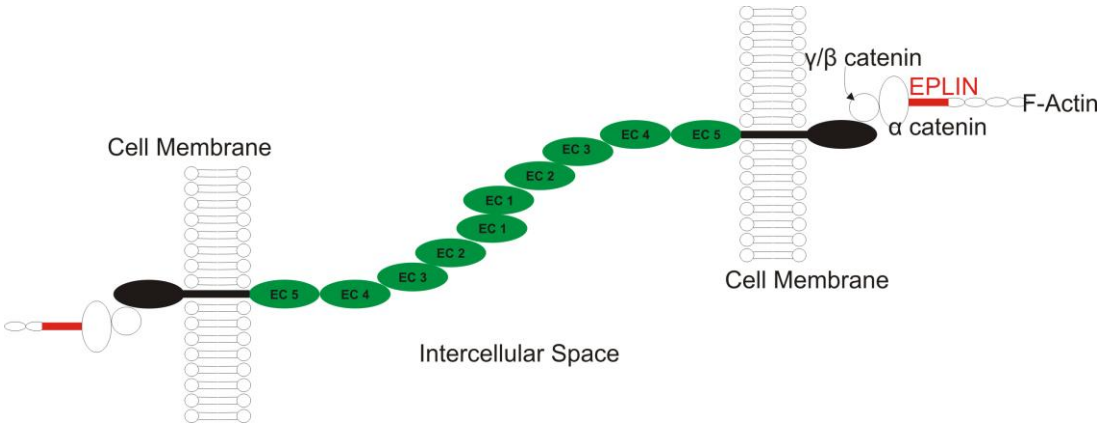

Figure 1.16: Schematic illustrating classical (Type I/II) cadherin structure. Consisting of 5 EC domains, the intracellular aspect of the protein binds ɣ or β catenin which in turn is able to bind to α catenin. This complex binds to the actin cytoskeleton via the intermediary EPLIN, mediating the structural basis of the adherens junction based cell adhesion.

Following the initial discovery of classic cadherins, attention focussed on a possible role for cadherins in morphogenesis. Several studies identified that the expression of different cadherin subtypes was both regionally specific and dynamic as development occurred. Describing this phenomenon, Takeichi (1988) summarises, “when a population of cells is to be separated from a parent layer, those acquire a new type of cadherin and/or lose the originally expressed cadherin type”. This analysis was based on a few examples of cadherin expression in the developing embryo, for example prior to gastrulation the chick epiblast expresses L-CAM (the chick homologue of E-cadherin), as gastrulation proceeds the cells which separate from the epiblast to form the mesoderm begin to express N-cadherin and simultaneously down regulate L-CAM expression. Following neural induction the cells of the neural plate also express N cadherin during and after separation from the surrounding ectoderm in the formation of the neural tube, whilst the ectoderm itself maintains L-CAM expression (Hatta et al., 1987).

Thus cadherins appear to mediate the organisation of cells into distinct epithelia during early embryogenesis. How do cadherins mediate this action? Nagafuchi (1987) investigated the adhesive properties of cadherins, by transfecting mouse fibroblast (L-cells) which have little endogenous cadherin activity, with E cadherin coupled to a virus promoter sequence. It was observed that following transfection these cells acquired a Ca^{2+} dependent aggregating activity and were morphologically altered to reflect an epithelial phenotype, indicating that epithelial adhesion could be a result of Ca^{2+} mediated cadherin adhesion (Nagafuchi et al., 1987).Significantly the level of cadherin expression determines the extent of adhesion in these cells; cells expressing a high level of cadherin will aggregate with those expressing similarly high levels even if all of the cells are expressing the same cadherin.

Subsequently, Nose (1988) sought to investigate the nature of binding specificity of the cadherins, reasoning that differential expression of cadherins in early embryogenesis is linked with organisation of different epithelial layers. This study demonstrated that cells expressing different classic cadherins *in vitro* will aggregate separately, providing the first direct evidence that differential cadherin expression can sort mixed cell populations into homogenous aggregates (Nose et al., 1988). Recently, Katsamba et al (2009) demonstrated that cells expressing different cadherins of the same type will form mixed aggregates of groups of cells, using in vitro assays of CHO cells expressing either N or E cadherin (Type I). These cells in

turn formed separate aggregates when incubated with cells expressing the type II cadherin, 6b, indicating a preferential binding specificity with cadherins of the same class. Type II cadherins appear to show no specific binding specificity *in vitro*, but have been demonstrated to drive cell sorting *in vivo* (Katsamba et al., 2009, Price et al., 2002). This binding specificity was demonstrated to be mediated by the EC1 domain in the classical cadherins. Using chimeric cDNA constructs of E and P cadherin, Nose et al., (1990) demonstrated that swapping the EC1 domain of P cadherin with that of E cadherin alters the binding specificity. Cells expressing the chimeric cadherin formed aggregates with cells expressing wild type E cadherin (Nose et al., 1990). Thus providing evidence, *in vitro,* that differential cadherin expression can drive cell sorting and aggregation that is required for morphogenesis of tissues.

1.6.1 Cadherins in CNS tissue patterning

The restricted and differential expression profiles of cadherins in the CNS combined with their binding specificity in cell adhesion led to the idea that cadherins potentially play a role in the development of specific brain regions and functional neuronal circuits. I have briefly discussed the expression of N cadherin in the developing neural plate; the differential expression of N cadherin in this region is crucial for the tissue separation from the adjacent ectoderm (Hatta et al., 1986). Such examples of spatially restricted cadherin expression are common in early neural development (Reviewed in Redies. 2000), for example in the neuromeres of the CNS cadherin 6 is transiently expressed in rhombomere 6 of the mouse embryonic hindbrain, delineating it from the adjacent rhombomeres. Cadherin 6 positive cells from rhombomere 6 are found to form homogenous aggregates when dissociated and cultured in a calcium-rich environment whilst altering the *Hox* gene expression in r6 leads to rostral shift in cadherin 6 expression associated with altered rhombomeric identity. Exogenously transplanted cadherin 6 positive cells will sort to r6 preferentially, whilst cells expressing a different cadherin will not (Inoue, YH et al., 1997, Inoue, T et al., 2009). Thus cadherin 6 appears to play a crucial role in the compartmentalisation of the developing neural tube.

Further to this, Kimura et al., (1996) investigated the expression patterns of cadherin 11 in the developing mouse CNS, finding that cadherin 11 delineates several different boundaries and compartments, including expression in several central neuronal nuclei. Importantly Kimura et al., noted that cadherin 11 was

expressed in both the developing nuclei and cortical plate of the cerebellum, reasoning that the associated expression of cadherin 11 may be important in functional circuit development (Kimura et al., 1996). In fact, the restricted expression of cadherins and their relation to the compartmentalisation of functional circuits has been extensively studied in the developing cerebellum (Reviewed in Redies et al., 2010).

As discussed the cerebellum exhibits two modes of neuronal organisation; the stratified laminae of the cerebellar cortex and the deep cerebellar nuclei. The neurons which constitute the cerebellar cortex are classified into granular, stellate, basket, golgi and Purkinje cells. These cells are organised into three distinct layers; the outermost molecular layer, the middle Purkinje cell layer and the granular layer. Each of the surface regions of the cerebellar cortex is compartmentalised, representing a specific part of the body, within each compartment the climbing fibre input from the inferior olivary nucleus innervate a specific group of Purkinje cells. In turn the Purkinje cells of the cerebellar cortex project to the deep cerebellar nuclei in a topographic manner.

This highly stereotyped topography of projections is thought, in part, to be mediated by cadherin expression. Throughout cerebellar development cadherins are expressed in Purkinje cell clusters representing the parasagittal domains. For example Arndt & Redies (1996) investigated the expression of the classical cadherins 6b and 7 in the developing cerebellum, finding that both cadherins are expressed in different transverse domains in early development (HH29) which partially overlap. As development proceeds the expression patterns of each cadherin are altered, appearing as patches along the rostrocaudal axis into distinct parasaggital stripes (HH35). This expression pattern was attributed to differential cadherin expression in the Purkinje cells of each separate compartment. Further analysis of cadherin expression in chicken cerebellum has revealed that at least five other classic cadherins and five members of the protocadherin subfamily are expressed in parasagittal domains, appearing to suggest an adhesive code for Purkinje cell compartments in the cerebellar cortex.

In order to assess the role of cadherin expression in cerebellum development, Luo et al., (2003) overexpressed cadherin 6b or 7 in the Purkinje cell progenitors, finding that misexpression led to Purkinje cells invading a cortical territory which expresses that specific cadherin endogenously. The mechanism of this action is proposed to be one of altering the migratory path of Purkinje cells from the ventricular zone. During development radial glia, found in the ventricular zone, give rise to and provide a migratory scaffold for Purkinje cells (Zhang et al., 2010). Luo et al., (2003) found that after the initial migratory step from the ventricular zone to the mantle layer, cadherin 7-positive Purkinje cells would orientate themselves along a nurite fibre tract which expressed cadherin 7. These fascicles led migrating cells to cortical regions expressing cadherin 7 endogenously. A model is suggested such that cadherins guide tangential migration of Purkinje cells to discrete regions of the cerebellar cortex along neurites that express the same cadherin.

In terms of functional connectivity, as noted by Kimura et al., (1996), specific regions of the cerebellar cortex which are connected to the deep cerebellar nuclei are also found to express specific cadherins. Neudert & Redies (2008) examined the functional connectivity of specific Purkinje cell domains, demonstrating that protocadherin 10 positive cortical domains are connected to regions of the deep nuclei which also express protocadherin 10. This data indicates that cadherins, potentially, have a role in cerebellar circuit formation and topographic mapping.

1.6.2 Cadherins in spinal motor pool formation

Cadherins appear therefore to play a role in patterning of the CNS throughout development, by mediating cell sorting and compartmentalisation of functionally related groups of neurons as shown by examples in early neural epithelia formation and the functional mapping of the cerebellar cortex. In terms of the role of cadherins in CNS nucleus development, one model system which has been investigated is that of motor neuron pool formation in the spinal cord.

Motor neurons in the ventral horn of the spinal cord are spatially segregated into distinct groups, the hierarchy of which was briefly discussed earlier (Introduction 1.1). Firstly motor columns which extend longitudinally along the spinal cord and can be divided into several groups; the lateral motor column (LMC) which is found only at the level of, and innervates, the limb mesenchyme and the median motor

column (MMC) part of which extends throughout all rostrocaudal levels (MMCm) and a second division which is found only at thoracic levels (MMCl). The establishment of motor columnar identity at the correct axial level is controlled by *Hox* gene expression and is critical for the topographic mapping of motor neurons to correct muscle targets. Specification of MN columnar identity is dependent upon sequential phases of Hox expression in both progenitors and post mitotic MNs; Dasen et al., 2003, demonstrated that initially the positional identity of progenitor domains along the rostrocaudal axis is reflected in by *Hoxc9* expression. Progenitors at thoracic levels express *Hoxc9* under control of Fgf whilst the brachial progenitor domain lacks *Hoxc9* expression. Absence of *Hoxc9* expression in brachial progenitors permits the expression of *Hoxc6* proteins in post mitotic brachial MNs which will eventually form the LMC. At the thoracic level, *Hoxc9* proteins are continued to be expressed and act in a cross repressive manner with *Hoxc6* to specify the distinct identities and boundaries between the LMC and Column of Terni (CT) neurons (Dasen et al., 2003).

The motor columns can be differentiated by their LIM homeodomain transcription factor expression. Initially it was demonstrated that the combination of *Islet-1, Islet-2, Lim-1 and Lim-3* identifies specific motor columns. These genes are temporally expressed in early post mitotic neurons, for example all MNs express *Islet-1* initially, but this lost in the LMCl by HH25 in chick. LMCl is found to express *Islet-2* and *Lim-1*, whilst MMCm expresses *Islet-1, Islet-2 and Lim3* (Tsuchida et al., 1994). Specifically it has been shown that expression of *Lhx3* and *Lhx4* is a determinant of MMC motor neuron fate; misexpression of *Lhx3* is sufficient to alter the fate of LMC neurons to MMC like identity, with an accompanying change in axonal trajectory (Sharma et al., 1998).

Subsequently the motor columns can be divided into medial and lateral divisions based upon their axonal projection targets. For example the LMCl MNs project axons to the dorsal limb muscles, whereas the LMCm projects axons to the ventral limb muscles (Landmesser, 1978).

The organisation of the motor columns is dependent upon *Hox* gene expression and extrinsic signals from the paraxial mesoderm. For example Retinoic acid (RA), which is synthesised by the enzyme Retinaldehyde dehydrogenase 2 (RALDH2) is initially expressed at all levels in the paraxial mesoderm and is required for multiple steps in the process of spinal motor neuron organisation. RA signalling is important

in the specification of LMC motor neuron identity in the spinal cord, acting initially in combination with Shh to induce Olig2 expression in the pMN domain which in turn mediates the expression of motor neuron specific proteins such as *Hb9* and Islet1/2. Later in development, RALDH2 is expressed in post mitotic LMC neurons themselves. The MNs of the LMCm differentiate earlier in development than those of the LMCl, thus requiring LMCl neurons to migrate through the LMCm to reach their final position. Sockanathan & Jessell (1998) demonstrated that the early born LMC neurons express RALDH2 and are able to induce the expression in a non cell autonomous manner of the LMCl specific marker *Lim-1* (Sockanathan & Jessell. 1998).

This selective expression of LIM homeodomain proteins determines the settling position of cell bodies in the motor column and the topographic axonal guidance of MN afferents to the limb; motor neuron settling position is sensitive to *Islet-1* expression which promotes a medial settling position. *Lim-1* misexpression is sufficient also to alter the axonal trajectory of medial LMC neurons from ventral to dorsal mesenchyme, whilst loss of *Lim-1* function results in random targeting of LMC axons. This action is mediated through the control of downstream EphA receptors; EphA4 is expressed in LMCl neurons and its cognate ephrin A protein is expressed in the ventral limb mesenchyme. *Islet-1* expression reduces whilst *Lim-1* expression increases EphA4 expression in LMC neurons. Interestingly the aberrant expression of EphA4 does not alter the central segregation of motor neuron pools, indicating that the Eph-ephrin signalling pathway does not participate in this process (Kania & Jessell, 2003). Whilst it has also been shown that multiple pathways of Eph-ephrin signalling as well as the Semaphorin family of cell adhesion molecules also participate in this process (Reviewed by Kao et al., 2012; also see discussion).

Following specification of motor columnar and division organisation the next order of complexity is the formation of the specific motor pools. The motor neurons in each motor pool extend their axons to a specific muscle target and receive input from sensory afferents of the same muscle. Sensory afferent input can be mediated via interneurons or in some cases can be a direct monosynaptic connection (Mears & Frank, 1997). Previously it has been demonstrated that functionally-related sensory afferents and motor pools have similar ETS transcription factor expression profiles, for example the expression of PEA3 and Er81 (Lin et al., 1998). This transcription factor profile is potentially important for correct targeting of sensory afferents to the motor pool during the development of spinal circuits (Arber et al., 2000; Vriesling &

Arber, 2002). The factors which drive discrete pool segregation however, were unknown until a study by Price and colleagues (2002). Cell adhesion molecules and specifically cadherins are likely candidates to instigate the coalescence of motor pools due to their known roles in early neural patterning and tissue development.

Price et al., (2002) investigated the potential role of cadherins in the development of motor pools of the LMC in the chick embryonic spinal cord. It was found that several members of the Classical type II family of cadherins were expressed within the motor pools of the LMC at lumbosacral segments 1-3. The expression patterns of theses cadherins was spatially restricted so as to reflect a pool-specific expression mirroring that of the ETS/LIM homeodomain proteins at HH35, when pool organisation approximates its mature conformation. Each pool expressed a unique combination of type II cadherins, for example; the adductor (A) pool expresses cadherins 6b, 8, 13 and 20, the external Femorotibialis (eF) pool expresses only cadherins 6b, 8 and 13, whilst the Anterior Iliotibilalis (ITR) pool expresses cadherins 6b, 7 and 8. This led to the prediction that this differential expression may play a role in the segregation of LMC neurons in to pools.

To test this Price et al., focused upon the two specific motor pools: the A pool and the eF pool, whose cadherin expression profile differs only in the expression of *cadherin 20*. During development eF MNs must migrate past A MNs to reach their final position, this is accompanied by a down regulation of *cadherin 20* expression by eF neurons at HH24. Misexpression of *cadherin 20* via in ovo electroporation, resulted in loss of segregation between the two pools as indicated by an increase in neuronal mixing (Figure 1.17). There is no effect on the ITR pool, which remains segregated following *cadherin 20* misexpression. Significantly, misexpression of either E cadherin which is not endogenously expressed in the LMC neurons or cadherin 6b which is found in both eF and A motor pools had no effect on pool segregation.

*Image removed

Figure 1.17: Misexpression of *cadherin 20* (MN-cad) in the external Femorotibialis motor pool (red) results in aberrant mixing with Adductor motor neurons (yellow), degrading motor pool specificity. From Price et al., 2002

This data demonstrated that the differential cadherin expression between eF and A motor pools of just one cadherin; *cadherin 20*, is sufficient to mediate motor neuron pool sorting. In addition to this study, Patel et al., (2006) demonstrated that the specificity of motor pool sorting by type II cadherins is mediated by the EC1 domain. Using a chimeric cadherin construct combining *cadherin 20* with the EC1 domain of cadherin 6b, Patel et al., were able to mimic the effect of normal cadherin 6b expression, resulting in no alterations in A and eF pool segregation (Patel et al., 2006).

Cadherins have also been demonstrated to place a functional role in the divisional segregation of spinal motor neurons, prior to pool segregation. Recent work by Bello et al., (2012), demonstrated that catenin-dependent cadherin function is required for the migration of motor neurons if the LMC. Specifically, disruptions in either cadherin function via uncoupling of cadherins to their intracellular binding partners using a dominant negative ɣ catenin or specific downregulation of cadherin 7, which is usually expressed during migration of these motor neurons, results in perturbation of motor neuron migration and divisional segregation (Bello et al., 2012).

Interestingly, Luo et al., 2008, demonstrated that *cadherin 20* is induced by SHH signalling in spinal and hindbrain motor neurons as HH12, However,, maintenance of *cadherin 20* expression beyond HH24 (when motor pool sorting begins) is SHH independent (Luo et al., 2008).

If cadherin expression is sufficient to drive neuronal coalescence and specify segregation in the spinal cord, the question remains as to which factors could act to modulate cadherin expression. As discussed previously, certain exogenous factors such as RA can play crucial roles in CNS development. The expression of ETS

transcription factors coincides with the arrival of motor axons to the base of the limb bud (Lin et al., 1998); ablation of the limb bud at HH18 leads to downregulation of Er81 in the LMC and an accompanying loss of the downstream targets *cadherin 20* and T cadherin expression assayed at HH29 (Price et al., 2002). Thus there may be an exogenous signal which drives ETS/LIM homeodomain protein expression, which is crucial for the central topography of motor neurons in the spinal cord.

Livet et. al (2002) sought to address the role of ETS transcription factors on spinal MN organisation; focusing on the expression of PEA3 in mouse spinal cord. A mutant mouse was generated which lacks functional PEA3 activity by insertion of a IRES-NLS-LacZ cassette into the exon encoding the DNA binding domain (PEA3-/). Analysis of MN positioning in the PEA3-/- mouse revealed that the cell bodies of these motor neurons were mispositioned in the ventral horn, in a similar manner to that observed following cadherin deregulation (Price et al., 2002). This phenotype was concomitant with an alteration in the expression profiles of cadherin 7 and 8 (Livet et al., 2002).

Parallel to this a separate study identified a potential exogenous factor which acts to induce PEA3 expression in the spinal cord. Haase et al., (2002) demonstrated that Glial cell line derived neurotrophic factor (GDNF) synthesised in the plexus of the developing forelimb was sufficient to induce PEA3 expression in a subset of spinal motor neurons. Later in development GDNF expression is restricted to two specific muscle targets in the limb; the motor neurons which innervate these muscle targets normally express PEA3. However, in GDNF mutant mice, PEA3 is not induced in these MN populations and their positioning within the spinal cord is subsequently altered.

Taken together these studies present a potential model whereby exogenous signals from the periphery act to induce the expression of ETS transcription factors in spinal motor neurons, which in turn act to modulate cadherin expression. This differential and dynamic cadherin expression drives neuronal coalescence and segregation into distinct motor pools.

1.7 Fibroblast Growth Factors

GDNF expressed in the limb region is sufficient to alter ETS/LIM homeodomain protein expression, which in turn regulates cadherin expression; driving motor pool formation in the spinal cord. The spatially and temporally regulated expression of such exogenous cues, appear to be crucial for correct CNS organisation. Therefore it is reasonable to suggest that such molecular cues may also be involved in patterning and nucleogenesis in other regions of the CNS. On candidate molecule which could play a potential role in hindbrain patterning of the chick embryo is Fibroblast Growth Factor 8 (Fgf8).

First isolated from bovine brain extract, where it was shown to stimulate cell division and accompanying DNA synthesis in fibroblasts (3T3) (Gospodarowiscz. 1974), the Fgf protein family of ligands is now known to consist of at least 22 different members. Of these 22 ligands, 18 are secreted, whilst 4 are non secreted; Fgf 11-14, also known as Fibroblast Growth Factor Homologous Factors (FHF's 1-4) (for reviews see Ornitz and Itoh. 2001 and Goldfarb. 2005) . Secreted Fgfs mediate their actions via 4 cognate Fgf Receptors (FGFR's), receptor tyrosine kinases (RTK's) which activate several downstream signalling pathways. Fgfs can be divided into sub families based upon their sequence homology and binding affinity with each of the respective FGFR's (Ornitz et al., 1996).

1.7.1 Fibroblast Growth Factor Signalling

The FGFRs like all RTKs consist of an extracellular domain, a transmembrane domain and an intracellular domain which contains the catalytic protein tyrosine kinase region. The extracellular domain of the FGFRs is constructed of 3 immunoglobulin (Ig) repeat sequences, which are usually designated D1 - D3, alternative splicing of the D3 sequence in FGFRs 1-3 is responsible for alterations in Fgf binding affinity. There is no alternate splicing in the D3 domain of FGFR4. Alternative splicing of the D3 domains is believed to allow differential responses to Fgfs in juxtaposed tissue during development as the D2-D3 regions are the primary binding point for Fgf ligands. The D1 domain is thought to act in an auto inhibitory

manner; studies have demonstrated that the binding affinity of Fgf ligand and the accessory protein heparin (which binds a positively charged pocket in the D2 repeat) can be enhanced when a cell expressed an FGFR deletion mutant lacking the D1 domain. There is a region between D1 and D2 which contains the heparin sulphate proteoglycan (HSPG) binding domain and a conserved amino acid sequence (the 'Acid Box') which are integral to Fgf signalling. Binding of HSPGs is required to mediate binding of Fgf to the receptor as well as FGFR dimerisation itself, in the absence of bound HSPG the acid box is able to mimic it's negative charge and draw the D1 region closer to the D2-D3 domains by binding the HSPG domain and folding the extracellular domain as whole in on itself. The D1 domain then blocks the D2-D3 specific binding to Fgf ligand, thus acting in an autoinhibitory manner to prevent inappropriate Fgf signalling from being initiated (Eswarakumar et al., 2005).

Upon ligand binding FGFRs dimerise leading to autophosphorylation of the intracellular tyrosine kinase domains. This in turn leads to the establishment of a complex of accessory signalling proteins associated with three distinct intracellular signalling pathways. PLCɣ can be recruited to the phosphorylated tyrosine of the RTK, activating the PLCɣ/Ca2+ signalling pathway associated with cytoskeletal reorganisation. Two other signalling pathways can also be initiated by the FGFR in combination with the docking proteins FRS2α/β. Initially following FGFR dimerisation and autophosphorylation, FRS2α/β binds at the juxtamembrane domain, and subsequently recruits the adaptor protein Grb2. Grb2 is able to bind Gab1 activating the MI3K signalling pathway associated with cell survival through anti-apoptosis. Another protein which binds FRS2α/β is Son of Sevenless (Sos) which mediates another divergent signalling pathway; the MAPK/ERK signalling pathway. The FRS2α/β-Grb2-Sos complex through the guanine nucleotide exchange actions of Sos, activates Ras. Once activated, Ras binds to Raf, which is able to phosphorylate Mek leading to sequential phosphorylation and activation of Erk1/2 as part of the MAPK/ERK signalling pathway (Figure 1.18). Fgf signalling via the MAPK/ERK signalling pathway mediates a variety of cellular responses, dependent upon the strength, pattern and duration of signalling (discussed in the next section). As such the precise control of this signalling pathway in terms of promotion and attenuation is crucial during development.

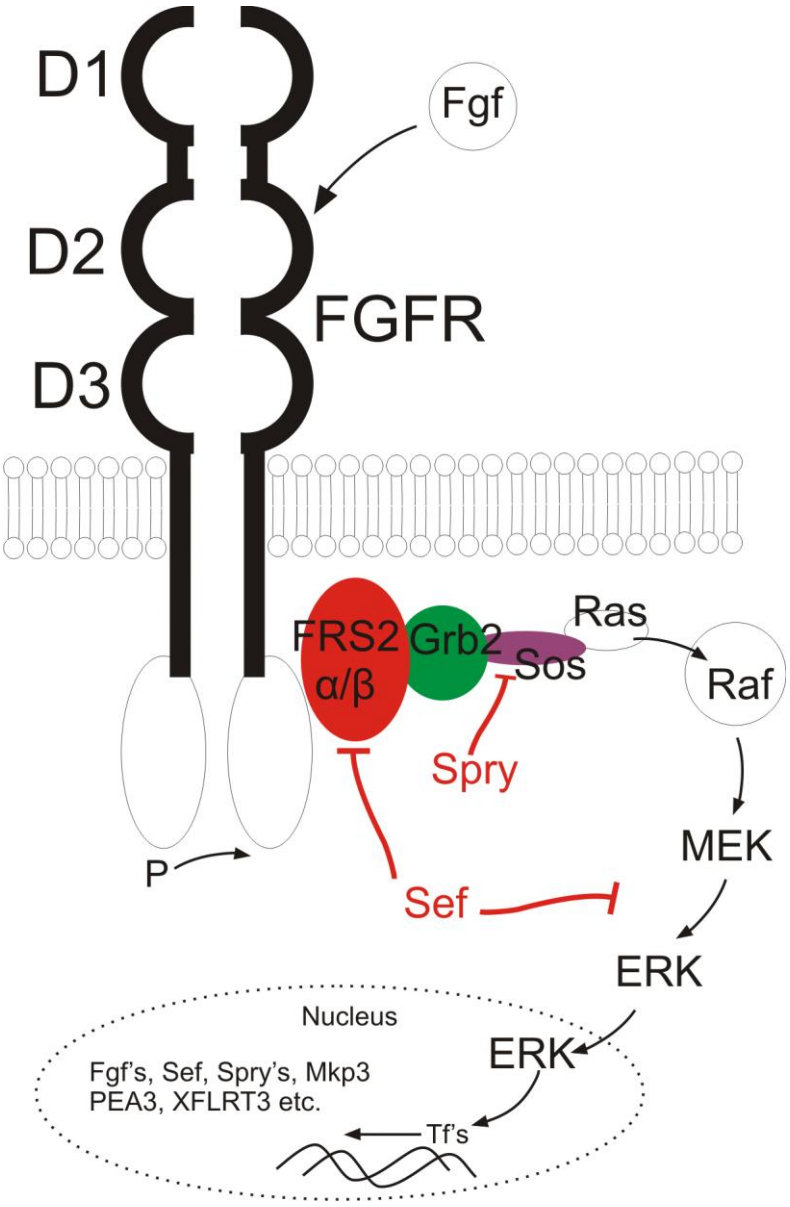

Figure 1.18: Summary of the FGFR MAPK/ERK signalling pathway. Fgf ligand binding leads to the dimerisation of FGFR's resulting in the autophosphorylation of the receptor tyrosine kinase intracellular domains. This promotes the binding of the adaptor molecule FRS2, which in turn recruits Grb2 and Sos. This complex facilitates the activation of Ras, which modulates the activity of Raf and begins the chain of MEK/ERK phosphorylation which ultimately leads to transcription of the Fgf syn-expression group in the nucleus. Spry and Sef are endogenous inhibitors of Fgf signalling, their sites of action are indicated.

Modulation of the MAPK/ERK signalling pathway is mediated via several intracellular proteins including Sprouty, Sef and MKP3 which act as negative feedback inhibitors. Positive regulation of MAPK/ERK signalling is mediated by proteins such as XFLRT3, which has been demonstrated during Xenopus development. The expression of these proteins is induced under the control of ETS transcription factors activated by MAPK/ERK signalling, as part of the Fgf syn-expression group.(Niehrs & Meinhardt. 2002). This study will seek to both up and down regulate the MAPK/ERK signalling pathway, therefore understanding the endogenous mechanisms controlling this pathway is important in the context of any analysis.

Sprouty (Spry) was first identified in *Drosophila melanogaster* as a protein which is involved in Fgf mediated lung growth; mutations in Spry led to ectopic lung growth due to an excess of Fgf signalling (Hacohen et al., 1998). Subsequent studies in both zebrafish and mouse models demonstrated that Spry is a conserved protein in vertebrate species which acts as an intracellular MAPK/Ras pathway antagonist following activation by Fgf signalling. There are 4 identified Spry proteins which contain a conserved 110 amino acid sequence that is thought to direct Spry proteins to the protein complex at the plasma membrane, here activated Spry binds Grb2 thus preventing Sos activation and inhibiting the MAPK/ERK signalling pathway. Sef, another member of the Fgf syn-expression group, is a transmembrane protein unlike Spry's which are found in the cytoplasm and are recruited to the plasma membrane. The mechanism by which Sef acts as a Fgf signalling antagonist is not fully understood, However, it has been demonstrated that Sef misexpression inhibits the phosphorylation of FRS2α/β thus inhibiting MAPK/ERK signalling. Sef is believed to act directly at the level of the FGFR, requiring its intracellular domain to do so, as it also down regulates the other two pathways also activated by Fgf signalling; the PLCɣ and PI3K signalling pathways respectively. The activity of these negative feedback loops ensures that Fgf signalling can be very tightly regulated during development in a cell autonomous manner.

1.7.2 Fibroblast Growth Factors in development

Fibroblast Growth Factors mediate a vast array of diverse functions during neural development; from early neural induction and patterning to neuronal proliferation, axonal guidance and synaptogenesis to name just a few. How one family of secreted extracellular proteins is able to perform a role in such a divergent repertoire of cell behaviours has been the topic of extensive study since the isolation of the first Fgf proteins in 1974 (Reviewed in Guillemot & Zimmer, 2011; Mason, 2007).

Fgfs have been established as a classic morphogen; a term first described by Turing (1952), during embryonic development and organogenesis. Lewis Wolpert proposed the 'French Flag Model' of morphogen action whereby positional information and polarity is imparted upon cells in a field by exposure to different concentrations of a morphogen. High concentrations of a morphogen induce expression of certain genes (Blue), lower concentration exposure instructs the expression of a different molecular identity (White), whilst low concentrations are insufficient to induce certain gene expression and these cells retain a default state (red) (Figure 1.19) (Wolpert, 1969).

*Image removed

Figure 1.19: Diagram to illustrate the interpretation of a morphogen gradient as such to represent a French flag. At increasing distance along the α-axis the concentration of a morphogen induces differential responses from a population of cells. Blue (B) at high concentration, White (W) at an intermediate concentration and Red (R) at low concentration. Figure from Wolpert, 1969.

How exactly these morphogen gradients are established has been a topic of some debate, however, in the case of Fgfs it appears that the gradient is established via a source sink mechanism. First proposed by Crick (1970), a stable gradient of a molecule can be established where one point in a field acts a source secreting a

morphogen into the extracellular region, another point in the field actively removes the molecule from the extracellular region, acting as a sink. The movement of the molecule is dictated by Brownian motion, the random thermal movement of molecules (Crick, 1970). Yu et al (2009) took up this theory and demonstrated; using a GFP tagged Fgf8 protein in zebrafish embryos, that the establishment of a stable Fgf8 extracellular gradient was dependent upon target cell endocytosis. They showed that the spread of Fgf8-GFP in vivo was comparable to that in water, thus ruling out passage of the morphogen through neighbouring cells, and that the distance over which Fgf8-GFP could spread was increased by blocking endocytosis (Yu et al., 2009; Schier & Needleman, 2009).

In neural development Fgfs are known to act as morphogens, being expressed repetitively at different time points and from transient signalling centres throughout embryogenesis. Beginning with neural induction, the first source of Fgf is the hypoblast in the chick embryo which provides a source of Fgf8 which transiently induces the expression of *Sox3* and ERNI (Early response to neural induction) in the overlying epiblast, driving cells into a 'pre-neural' state (Alberzerchi & Stern, 2007). Fgf signalling at this point also acts to inhibit BMP signalling; BMP signalling acts to drive cells in to an epidermal, non-neural fate. Following gastrulation and establishment of the neural plate, Hensen's node provides a source of Fgfs which is thought to be intimately involved in re-enforcing neural induction and the A-P patterning of the developing neural tube. Hensen's node has long been established as a signalling centre in chick neural development, and transplanting the node or an Fgf4 coated bead to ectopic positions of the epiblast is sufficient to induce the expression of posterior neural markers (Storey et al., 1998; Wilson et al., 2000; also reviewed in, Wittler & Kessler, 2004).

Further to this a study by Liu et al., 2001 demonstrated that graded Fgf8 signalling is important in the positional-dependent profile of *Hox*-c expression. Fgf8 expression at Hensen's node was found to coincide with the expression of certain *Hox*-c proteins in spinal MNs. Importantly Fgfs act in vitro in a graded manner whereby higher concentrations of Fgf induce a more caudal neural *Hox*-c expression profile, equally in vivo activation of the FGFR led to a rostral to caudal shift in gene expression profile. The establishment of the *Hox* gene expression profile is crucial

for specifying motor column identity along the rostro caudal axis, as in the hindbrain, where rhombomere specific expression of *Hox* gene repertoire drives neuronal subtype differentiation. For example *Hox* 9, induced by exposure to high Fgf8 concentrations, and is found at the lumbar region of the developing spinal cord. Cross repression by *Hox*6, whose expression is governed by combined Fgf and RA signalling at more rostral regions delineates the boundary between these two regions. *Hox* 9 expression directs the downstream expression of BMP5 and reinforces Column of Terni autonomic MN specification, whilst *Hox* 6 directs the expression of RALDH2, which is involved in the specification of LMC MN fate. In this manner the expression gradient of Fgf8 secreted from Hensen's node, in combination with other factors expressed in the paraxial mesoderm, acts to pattern the spinal cord by directing the molecular identity of neuronal subtypes at different positions from the source (Dasen et al., 2003; Liu et al., 2001).

As neural development proceeds discrete regions of Fgf expression are found along the length of the neural tube, as well as in the periphery. One such example of restricted Fgf expression forming a signalling centre is the Isthmic organiser or midbrain-hindbrain boundary (MHB). The MHB abuts the posterior midbrain and the first rhombomere (r1) of the hindbrain; these neurons express Wnt-1 and at least three members of the Fgf super family; Fgf8, Fgf17 and Fgf18 (Reviewed in Liu & Joyner, 2001). The MHB has been shown to act as an organiser in this region; grafting of the MHB to posterior hindbrain induces cerebellum development, whilst grafting anterior midbrain induces a posterior midbrain phenotype. These effects can be mimicked using the ectopic implantation of Fgf8 coated beads, indicating that Fgf8 is a crucial morphogen mediating organisation of the MHB region (Echevarria et al., 2003; Zervas et al., 2005).

One crucial role for Fgf signalling at the MHB is the control of cellular proliferation and differentiation. Fgf signalling mediated in this region by FGFR1, 2 and 3 is required for the maintenance of a slowly proliferative neuron pool in the ventricular zone. This slowly proliferating pool is maintained by downstream signalling through the MAPK/ERK pathway which induces the expression of Hes1. Knockdown of Fgf signalling results in the loss of Hes1 and increased expression of p57 (which is normally repressed by Hes1) increasing the rate of cell cycle exit, thus increasing

the rate of neurogenesis (Georgia et al., 2006) . In mice models exhibiting a compound knockdown of all FGFRs in this region there is a resultant increase in terminal neuronal differentiation and a concomitant loss of the proliferative progenitor pool. This results in a reduction in the number of Dopaminergic neurons found in the midbrain, as well as alterations in gene expression and patterning defects. The MHB is delineated by the expression of Otx2 in the midbrain and Gbx2 in r1; following FGFR1 knockdown the boundary of this expression is disrupted. Importantly the loss of Fgf signalling also leads to a loss of cadherin 13 expression in r1, indicating potential defects in cell adhesion which may act to segregate the lineage restriction boundary between the midbrain and r1 (Trokovic et al., 2003; Jukkola et al., 2006; Lahti et al., 2010; Saarimaki-Vire et al., 2007).

So Fgf signalling is important for regional specification and patterning in the early development of the neural tube, but it is also closely associated with other important processes such as axonal guidance in cell circuit formation. It has been shown, for example that motor axons from the MMCm extend their axons towards Fgf8 which is expressed in the dermomyotome. Knockdown of FGFR expression in mMMC neurons in vivo results in axonal guidance defects, whilst neurons driven towards mMMC identity using the LIM transcription factor Lhx3 show an increased preference for axonal outgrowth towards Fgf8 in vitro. Downstream Fgf signalling via the MAPK/ERK pathway drives this axonal guidance; transplantation of mMMC neurons in which MAPK/ERK pathway is up regulated results in axonal pathfinding defects in vivo, whereas alterations in other Fgf-mediated signalling pathways do not (although this has only been tested in vitro) (Soundararajan et al., 2010; Shirasaki et al., 2006).

Similarly, Irving et al., (2002) demonstrated that Fgf8 expressed at the MHB acts as a chemo attractive signal for axons of the trochlear cranial motor nerve. The MNs of the trochlear or IVth cranial nerve differentiate in the rostral region of r1, within the MHB. In combination with repulsive signals such as Netrin at the midline and semaphorin 3F which are expressed in the midline and dorsal r1 respectively, Fgf8 acts as a guidance cue, driving trochlear MNs towards a rostral ventral exit point from r1. Alterations in the Fgf8 signalling source, via implantation of Fgf8 coated beads in vivo, or knockdown using the pharmacological FGFR inhibitor, SU5402, in

cultured explants, leads to defects in axonal trajectory and pathfinding (Irving et al., 2002).

One further example of the varied roles that Fgfs can perform is that of the Fibroblast Growth Factor Homologous Factors (FHFs). As mentioned previously this subfamily of the Fgfs is non secreted and is unable to functionally stimulate the FGFR in vitro (Olsen et al., 2003). There are four different FHF variants found in the developing chick embryo and their expression is maintained throughout development and continues to adulthood (Munoz-Sajan et al., 1999). Each FHF has two splice variants, dependant upon the presence or absence of a 60 amino region at the N-terminus, whilst both retain a common Fgf residue which contains a β trefoil loop. It had been previously suggested that this 60 amino acid sequence dictated the sub cellular location of each FHF (Wang et al., 2000), with 'a' isoforms localised to the nucleus, whilst 'b' isoforms are found in the cytoplasm. However,, more recent studies into the roles of FHFs and sodium channel interactions, suggest that both isoforms can be located in the cytoplasm as the 'a' isoforms of each FHF are known to interact with the C terminus region of these ion channels (Schoorlemmer & Goldfarb, 2002; Goldfarb, 2011).

The role of the FHFs in neurons appears to be that of regulating ion channel excitability by mediating long term inactivation; the β trefoil region of the FHF's bind to the C-terminus membrane proximal region of sodium channels acting to raise the voltage dependence of channel fast inactivation, thus slowing the rate of inactivation at specific voltages (Dover et al., 2010; Goldfarb, 2011). Similarly previous studies have demonstrated the FHF2b when misexpressed in vitro localizes with Nav1.6 channels mediates a two fold increase in the whole cell maximum sodium channel current and positively shifts the voltage dependant inactivation of sodium channels (Wittmack et al., 2004). This facilitates the requirement for greater input driving sodium channel activation, allowing repetitive action potential firing by neurons at specific voltage thresholds. Recording from mice cerebellar slices, Golfarb et al., (2007) demonstrated that mice lacking FHF2 and FHF4 gene expression were unable to mantain repetitive action potential firing; they inactivated at a more negative membrane potential, inactivated more rapidly and were slower to recover from the inactive state compared with WT (Golfarb et al., 2007).

1.8 Summary

Both cranial motor and sensory nuclei occupy specific stereotyped positions within the hindbrain. The factors which drive nucleogenesis in this region are not currently understood. Two candidate molecules which could potentially play a role in this process are the cadherins and Fgfs respectively. Cadherins are known to drive motor neuron pool formation in the spinal cord, under the control of ETS transcription factors induced by exogenous signals from the paraxial mesoderm. Fgfs have been extensively characterised as secreted morphogens which play multiple roles in neural development, including specifying neuronal molecular identity, regulating neuronal proliferation and differentiation and acting as axonal guidance cues. Significantly cadherin 11 has been shown to be expressed in cranial motor neurons previously, suggesting that cadherin function could be important in their development. Whilst Fgf8 is expressed at multiple stage throughout embryogenesis in the hindbrain, as well as being expressed in the otic vesicle directly adjacent to r5; providing a potential exogenous source of Fgf8 which may influence regional patterning. The role of FHF's in modulating neuronal excitability is also intriguing and the specific expression of these molecules in hindbrain nuclei has not previously been investigated. FHF expression in either motor or sensory nuclei could be critical to the overall function of the circuits to which they belong.

This study seeks to identify potential mechanisms which may contribute to cranial nucleogenesis in the developing chick embryonic hindbrain by targeted manipulation of the Fgf signalling pathway and cadherin expression.

2. Materials and Methods

2.1 Materials Used

Laboratory reagents used during this study are as follows:

Anhydrous di-sodium hydrogen phosphate (Na_2HPO_4), sodium di-hydrogen phosphate 1-hydrate ($NaH_2PO_4H_2O$), Sodium Chloride (NaCl), Sucrose, Triton-X detergent, Tween detergent and Trizma ™ Base, Hydrochloric acid (HCl), Acetic Anhydride $(CH_3CO)_2O$, and Triethanolomine, agar, LB broth, ampicillin, kanamycin and 50X Denhardts solution were all purchased from Sigma Aldrich, UK.

Sodium citrate, magnesium chloride ($MgCl_2$), potassium chloride (KCl), paraformaldehyde, chloroform and agarose were purchased from Fisher Scientific, UK.

Sodium hydroxide (NaOH) and phenol were purchased from Fluka Chemie, Switzerland.

Formamide, baker's yeast tRNA, salmon sperm DNA and DIG labelled nucleotides were purchased from Roche, UK.

Molecular biology grade water was purchased from Eppendorf, UK.

Glycerol mounting medium was purchased from Dako, UK.

Vectorshield mounting medium and vectorshield mounting medium with DAPI was purchased from Vector laboratories, USA.

2.2 Solutions used

Solutions used for this study are detailed, where applicable, in the text of the methods.

2.3 Experimental Animals

White Leghorn Chicken eggs (Henry Stewart & Co., UK and Winter egg farm, UK) were incubated at 38°C in a forced draught incubator (LYON Technologies Inc., USA). Embryos were allowed to develop until required and staged according to

Hamburger and Hamilton 1951. Prior to incubation egg shells were sterilised with 70% ethanol.

2.4 *In ovo* electroporation

2.4.1 Plasmid Preparation

DNA plasmids used for in ovo electroporation were prepared as follows:

1µg of required plasmid was mixed with 100µl of XL-10 Gold® Ultracompetent cells (Stratagene, USA) and incubated on ice for 30 minutes. The cells were heat shocked for 40 seconds at 42°C in a water bath (Grant Sub, Grant Instruments, UK) then immediately placed on ice for 2 minutes. This mixture was then placed in a shaker (C25 incubator shaker, New Brunswick Scientific Co. Inc., USA) at 37°C with 0.5ml LB broth for 45 minutes. Following incubation 100µl of the mixture was plated on to Agar plates containing 100µg/ml of ampicillin or 50µg/ml kanamycin, dependent upon the plasmid, and incubated overnight at 37°C.

An individual colony was selected and incubated in a shaker at 37°C for 2-3 hours in 10ml of LB broth containing 100µg/ml of the specified antibiotic. This culture was then added to 150mls of LB broth containing 500µg/ml of the specified antibiotic.

DNA was harvested using the Qiafilter™ Plasmid Maxi Kit (25) (Qiagen, UK) as per manufacturer's instructions. DNA was dissolved in 300µl of MB water and the concentration determined using a spectrophotometer (ND-1000, Nanodrop technologies, Thermo Scientific, UK).

2.4.2 Ethanol Precipitation

DNA for use in electroporation was precipitated, either individually or in combination dependent upon the experiment and construct used, to a total final concentration of 10µg/µl using ethanol precipitation. A complete list of plasmids used can be found in section 2.4.4.

A total of 50µg of plasmid DNA was mixed with 2 ½ volumes of absolute ethanol and 1/10th volume of 5M NaCl, and then spun at 13,000rpm at 4°C in a centrifuge for 30 minutes (Eppendorf 5810R, Eppendorf, UK). The supernatant was decanted, replaced with 0.5ml 70% ethanol, and spun at 13,000rpm at 4°C for a further 15 minutes. Following centrifugation the 70% ethanol was removed and the DNA pellet dissolved in 5µl of MB water.

2.4.3 Electroporation

A sterile syringe was used to penetrate the shell and remove 5ml of albumin. Subsequently a small window is cut in the top of the shell, exposing the embryo. Embryos were staged as defined by Hamburger and Hamilton 1951 (HH stage). All experiments were performed at HH stage 17-19.

To enable visualisation of the solution during micro injections, 0.5µl of 1% fast green diluted in water was added. DNA plasmid was injected into the rostral hindbrain immediately adjacent to the otic vesicle, which is visible at this stage, using a drawn glass micropipette (Harvard Apparatus, UK).

Electroporation was performed using an Electro Square Porator (BTX, USA). Electrodes were carefully positioned on either side of the hindbrain and a series of 5, 30 volt pulses delivered for 50ms at 1s intervals.

In order to reduce the risk of infection a 0.2ml dose of Penicillin Streptomycin (5000 units' ml^{-1}) was administered to each embryo using a sterile pipette. The eggs were sealed using Parafilm® (Pechiney Plastic Packaging Company, USA) and replaced in the incubator.

2.4.4 Plasmids used for *in ovo* electroporation

Plasmids used for electroporation consisted of a cDNA coding sequence inserted into a plasmid vector. The Fgf8 misexpression plasmid contains a full murine Fgf8 cDNA sequence inserted into a pBluescript II SK(-) backbone (developed by Stratagene) as described by Mahmood et al. 1995. Cadherin *20, cadherin 6b, dn-cadherin 20, N-cadherin* and NΔ390 constructs were generated by S.R. Price, by cloning full length cDNA into a pCAGGS vector. The dominant negative *cadherin 20* construct contains a truncated cDNA sequence missing aa 684-798, as described in Price et al. 2002. NΔ390 contains a cDNA encoding a truncated, non-binding N-cadherin (Kawakami et al. 2004). The sFGFR3 plasmid consist of a truncated FGFR3 cDNA, lacking the D3 and transmembrane domains inserted into a pEFX vector, it was developed by T.Fukuchi (2001). RafER is a fusion protein containing an oncogenic form of human Raf1 fused to the hormone binding domain of human estrogen receptor (Samuels & McMahon, 1994). The dnFGFR1 is a truncated FGFR1 sequence which lacks its intracellular tyrosine kinase domain (Amaya et al. 1991).

2.5 Tissue Preparation

All procedures were performed in accordance with the Animals (Scientific Procedures) Act 1986.

2.5.1 Dissection and Fixation

Each embryo was allowed to develop until the specified H&H stage required for analysis. Embryos were removed from their eggs and decapitated immediately in iced PBS. The hindbrain was dissected, by removal of the eyes and facial tissue, and placed in fixative (4% Paraformaldehyde (PFA), 0.1M PB) for 1 hour on ice.

2.5.2 Cryoprotection and Sectioning

Following fixation hindbrain tissue was washed 3 times in PBS (3 X 15 minutes each) at room temperature (RT) and then cryoprotected overnight in 30% sucrose, 0.1% PB at 4°C. Tissue was mounted in O.C.T™ compound on dry ice until completely frozen and stored at -80°C.

Sections were taken in the transverse plane on a cryosta at 15µm intervals. Sections were collected in series using positively charged slides (Superfrost® plus, VWR International, UK) and stored until required at -80°C.

2.6 Immunohistochemistry

Slides were washed in 2 ml PBS for 5 minutes to remove excess O.C.T™ compound, then incubated for 30 minutes in 1ml of blocking solution (1% BSA or FCS, 0.1% Triton X in PBS) at RT. Slides were then incubated overnight at 4°C with each primary antibody diluted in 0.5ml of blocking solution in a humidified chamber.

Primary antibody was removed and the slides washed 3 times with 2 ml PBS (3 X 5 minutes each) at RT. Following washing each slide was incubated with the required secondary antibody diluted in 0.5ml of blocking solution for 30 minutes at RT in a darkened humidified chamber. To remove the secondary antibody slides were again washed 3 times with 2ml PBS (3 X 5 minutes each). Excess PBS was removed from each slide by gently tapping on to tissue paper and then each slide mounted with cover slips. To maintain fluorescence and stability of the tissue, two drops of Vectashield (Vector Laboratories Inc., USA) were used under each cover slip. Slides were stored away from light at 4°C.

2.6.1 Antibodies Used

Primary Antibody	**Dilution**	**Manufacturer**
Rabbit anti Green Fluorescent Protein (GFP)	1:1000	Invitrogen, UK
Mouse anti islet 1 (4D5)	1:50	Developmental Studies Hybridoma Bank (DSHB), USA
Mouse anti hb9 (5c10)	1:100	DSHB, USA
Chicken anti β-Galactosidase	1:1000	Abcam, USA
Secondary Antibody		
AlexaFluor ®488 Goat anti Rabbit	1:1000	Invitrogen, UK
AlexaFluor ®594 Donkey anti Mouse	1:1000	Invitrogen, UK
Cy-3 Donkey anti Mouse IgG, subclass 1 specific	1:1000	Jackson Immuno Research laboratories Inc., USA
Cy-5 Donkey anti Mouse IgG, subclass 2b specific	1:500	Jackson Immuno Research laboratories Inc., USA
FITC conjugated Donkey anti Chicken	1:250	Jackson Immuno Research laboratories Inc., USA
AlexaFluor ®488 Donkey anti Goat	1:1000	Invitrogen, UK

Table 2.1: Primary and secondary antibodies used, indicating working concentrations and origin.

2.7 Preparation of Dioxygenin labelled antisense cRNA probes for *in situ* hybridisation

Dioxygenin (DIG) labelled antisense cRNA probes were used to detect mRNA expression relating to the target protein. Probes were transcribed from DNA plasmids which contain short sequences of cDNA or expressed sequence tags (EST) which represent portions of expressed gene mRNA sequences. A complete list of mRNA gene targets, restriction enzymes, RNA polymerases and buffers used to produce antisense probes is provided in table 2.2.

Target mRNA	Restriction Enzyme / Buffer used.	RNA polymerase
Fgf8	BamH1 (Promega, UK) Buffer 'E'.	T7 (Roche, UK)
N-cadherin	Not 1 (NEB, UK), Buffer '3'.	T7 (Roche, UK)
Cadherin 6b	Nco 1 (NEB, UK), Buffer '4'.	T7 (Roche, UK)
Cadherin 8	Hind III (NEB, UK), Buffer '2'.	T3 (Roche, UK)
Cadherin 11	Hind III (NEB, UK), Buffer '2'.	T7 (Roche, UK)
Cadherin 13	Hind III (NEB, UK), Buffer '2'.	T7 (Roche, UK)
Cadherin 20	Hind III (NEB, UK), Buffer '2'.	T7 (Roche, UK)
Cadherin 22	Hind III (NEB, UK), Buffer '2'.	T7 (Roche, UK)

Islet 1	EcoR I (Promega, UK), Buffer 'H'.	T7 (Roche, UK)
ɣ-catenin	Not 1 (NEB, UK), Buffer '3'.	T7 (Roche, UK)
Nav1.6	Not 1 (NEB, UK), Buffer '3'.	T3 (Roche, UK)
FGFR1	Not 1 (NEB, UK), Buffer '3'.	T3 (Roche, UK)
FGFR2	Not 1 (NEB, UK), Buffer '3'.	T3 (Roche, UK)
FGFR3	Not 1 (NEB, UK), Buffer '3'.	T3 (Roche, UK)
Spry4	Not 1 (NEB, UK), Buffer '3'.	T3 (Roche, UK)
Fhf1a	Not 1 (NEB, UK), Buffer '3'.	T7 (Roche, UK)
Fhf1b	Not 1 (NEB, UK), Buffer '3'.	T7 (Roche, UK)
Fhf2b	Not 1 (NEB, UK), Buffer '3'.	T7 (Roche, UK)
Fhf4a	Not 1 (NEB, UK), Buffer '3'.	T7 (Roche, UK)

Table 2.2: List of gene targets, restriction enzymes and RNA polymerases used to produce antisense cRNA probes for in situ hybridisation (see section 2.7.5 for details of plasmid origin).

2.7.1 Linearisation of DNA plasmid

Plasmids were linearised using the necessary restriction endonuclease (see table 2.2) in the following reaction mixture, added in sequence:

- 10µg plasmid, in Xµl of MB water.
- 10µl appropriate buffer.
- 10µl of 10X BSA.
- 77.5-Xµl MB water, to increase total volume to 97.5µl.
- 2.5µl Restriction endonuclease.

The reaction mixture was then incubated for 2 hours at 37°C.

2.7.2 Gel Electrophoresis

Following incubation 5µl of each mixture was used to check the linearisation of the plasmid via Gel electrophoresis.

2.7.3 Phenol Extraction

Following DNA plasmid linearisation a phenol extract was performed in order to purify the cut plasmid from the reaction mixture. Using the remaining reaction mixture, 50µl of phenol and 50µl of chloroform was added, this was then placed in a vortex (Fisherbrand™ Whirlmixer, Nickel electro ltd, UK) for 1 minute at RT. The sample tubes were then immediately placed in a centrifuge (MSE, Microsentaur, Jencons PLS Ltd, UK) and spun at 13,000 RPM for 5 minutes at RT.

During centrifugation the mixture separates into two distinct layers. The top or aqueous phase, which contains the DNA plasmid, is retained in a sterile 1.5ml eppendorf tube (Eppendorf, UK). The lower, phenol phase is discarded. DNA plasmid was then precipitated using ethanol precipitation (see section 2.4.2) and dissolved in 10µl of MB water.

2.7.4 DIG labelled RNA probe transcription

Antisense DIG labelled cRNA probes were transcribed from the linearised DNA plasmid template in the following reaction mixture, added in sequence.

- 2µl Transcription buffer.
- 1µg Cut DNA plasmid, in Xµl of MB water.
- 15-Xµl MB water, to increase total volume to 15µl.
- 2µl DIG labelled nucleotides (Roche, UK).
- 0.5µl RNAsin (Promega, UK).
- 1.5µl appropriate RNA polymerase.

The reaction mixture was incubated at 37°C for 2 hours. Following incubation 30µl of MB water was added to the mixture. Probes were purified from this mixture using a G-50 spin column (Amersham Biosciences, UK) as per manufacturer's

instructions. In order to verify the length of the probe in accordance with that expected, 2.5µl of the sample was retained and checked using gel electrophoresis (see section 2.7.2). The remaining solution was mixed with 150µl of Hybridisation solution to make the probe stock solution, which is stored at -20°C until required.

2.7.5 Plasmids used for *in situ* hybridisation protocol

Complementary antisense RNA *in situ* hybridisation probes were produced using plasmids encoding the cDNA sequence of the target gene. The Fgf8 probe, described by Ohuchi et al. 1997, contains a 495bp fragment of the chick Fgf8 gene inserted into a pBluescript II SK(-) backbone. Probes for *cadherin 20*, cadherin 6b, cadherin 8, cadherin 11, cadherin 13 and cadherin 22 were cloned by S.R. Price using either full length cDNA sequences or fragments inserted into the multiple cloning region of a pBluescript II SK (+) backbone.

Cloned fragments of Fhf1a (chick EST database identifier; 125e7), Fhf1b (485i23), Fhf2a (71F6), Fhf4a (793g10), Nav1.6 (380), and Spry4 (742e5) were ordered utilising the chickEST database (University of Manchester, UK) and supplied by Source Bioscience, UK. FGFR1 (CEK1), FGFR2 (CEK3), FGFR3 (CEK2) were a gift from C. Stern. Each fragment was inserted into a pBluescript II KS(+) vector and subsequently sequenced on site (UCL, UK).

2.8 *In situ* hybridisation histochemistry

Two *in situ* hybridisation protocols were used during this study; single hybridisation (section 2.8.1) and hybridisation with immunohistochemistry (section 2.8.2). Each protocol takes 3-4 days to complete and is performed on tissue sections which are prepared as detailed in section 2.5.2. Each part of the protocol was performed at RT unless otherwise stated.

2.8.1 Single *in situ* hybridisation

Stage I: Tissue preparation and hybridisation

Slides were fixed (4% PFA, 0.1M PB) for 10 minutes then washed 3 times in PBS (3 X 5 minutes each). Tissue was permeabalized in Proteinase K solution (1mg ml^{-1} PK, 50mM Tris-HCl pH7.5, 6mM EDTA) for 5 minutes and washed 3 times in PBS (3 X 5 minutes each). In order to reduce the background signal associated with non

specific cRNA probe binding, tissue was acetylated (1.3% Triethanolamine, 0.13% HCl, 0.19% Acetic Anhydride), for 10 minutes with constant stirring using a magnetic stirrer.

Following acetylation slides were washed 3 times in PBS (3 X 5 minutes each) and each then equilibrated in 0.5 ml hybridisation solution (50% Formamide, 5 X SSC, 5 X Denhardt's solution, 250µg ml^{-1} Baker's yeast tRNA, 500µg ml^{-1} Salmon sperm DNA) for 1 hour.

Probes were prepared for hybridisation by diluting 20µl of the stock probe solution into 1ml of hybridisation solution and then heating at 99°C for 5 minutes, in order to reduce cross binding of the cRNA. Slides were covered with 130µl of the appropriate probe and then a cover slip placed over each. Care was taken to ensure good distribution of the probe and minimise tissue damage. Slides were incubated overnight at 72°C in humidified chambers (50% Formamide, 5 X SSC). Each probe was incubated separately in order to prevent cross contamination.

Stage II: Washes and Primary Antibody incubation

Following overnight hybridisation cover slips were removed from the slides carefully in 5 X SSC which had been pre-heated to 72°C. Slides were then washed twice in 0.2 X SSC for 40 minutes, also at 72°C. In situ hybridisation dishes were immersed in a water bath (Grant Sub, Grant Instruments, UK) at 72°C in order to maintain temperature during washes.

Slides were washed once in 0.2 X SSC for 5 minutes, then equilibrated in B1 buffer (0.1M Tris-HCl pH7.5, 0.15M NaCl) for 5 minutes. Subsequent to equilibration the tissue was blocked in B1 buffer containing 10% Heat Inactivated Goat Serum (HINGS, Invitrogen, UK) for 1 hour. Blocking solution was removed by tapping the slides gently on tissue. Slides were then incubated in 0.5ml B1 buffer containing 1% HINGS and sheep FAB fragments anti-DIG Alkaline Phosphatase conjugated antibody (1:5000, Roche, UK) overnight at 4°C in a humidified chamber.

Stage III: In situ detection

Slides were washed 3 times in B1 buffer (3 X 5 minutes each) and then equilibrated in B3 buffer (0.1M Tris-HCl pH9.5, 0.1M NaCl, 0.05M $MgCl_2$) for 10 minutes. Visualisation of bound anti-DIG antibody is achieved using the NBT/BCIP Alkaline Phosphotase substrate kit (Vector Laboratories Inc., USA) prepared in B3 buffer

containing 0.1% Tween, to ensure good tissue penetration, as per the manufacturer's instructions. Excess B3 solution was removed and replaced with 500µl of the NBT/BCIP solution. The staining is then allowed to develop in a humidified darkened chamber for 2 to 24 hours until the desired staining intensity is achieved. Upon achieving the desired staining intensity slides are washed in distilled water for 10 minutes and then allowed to dry. To protect the tissue each slide was mounted with a cover slip using two drops of heated Dako Glycerol mounting medium (Invitrogen, UK). Once the mounting medium had solidified the slides can be stored indefinitely.

2.8.2 Hybridisation with Immunohistochemistry

Stage I: Tissue preparation and hybridisation

Slides were fixed (4% PFA, 0.1M PB) for 10 minutes then washed 3 times in PBS (3 X 5 minutes each). In order to reduce the background signal associated with non specific cRNA probe binding, tissue was acetylated (1.3% Triethanolamine, 0.13% HCl, 0.19% Acetic Anhydride), for 10 minutes at RT then washed 3 times in PBS (3 X 5 minutes each). Tissue was permeabalized in 1% Triton X-100 in PBS for 30 minutes and washed 3 times in PBS (3 X 5 minutes each). Slides were then equilibrated in 0.5 ml hybridisation solution (50% Formamide, 5 X SSC, 5 X Denhardt's solution, 250µg ml^{-1} Baker's yeast tRNA, 500µg ml^{-1} Salmon sperm DNA) for 1 hour.

Probes were prepared for hybridisation by diluting 20µl of the stock probe solution into 1ml of hybridisation solution and then heating at 99°C for 5 minutes, in order to reduce cross binding of the cRNA. Slides were covered with 130µl of the appropriate probe and then a cover slip placed over each. Care was taken to ensure good distribution of the probe and minimise tissue damage. Slides were incubated overnight at 72°C in humidified chambers (50% Formamide, 5 X SSC). Each probe was incubated separately in order to prevent cross reaction.

Stage II: Washes and Primary Antibody incubation

Following overnight hybridisation cover slips were removed from the slides carefully in 5 X SSC which had been pre-heated to 72°C. Slides were then washed twice in 0.2 X SSC for 30 minutes, also at 72°C. In situ hybridisation dishes were immersed in a water bath (Grant Sub, Grant Instruments, UK) at 72°C in order to maintain temperature during washes.

Slides were washed once in 0.2 X SSC for 5 minutes, then equilibrated in B1 buffer (0.1M Tris-HCl pH7.5, 0.15M NaCl) for 5 minutes. Subsequent to equilibration the tissue was blocked in B1 buffer containing 10% Heat Inactivated Goat Serum (HINGS, Invitrogen, UK) for 1 hour. Blocking solution was removed by tapping the slides gently on tissue. Slides were then incubated in 0.5ml B1 buffer containing 1% HINGS and the required Primary antibody (Mouse anti islet 1 (4D5), 1:50 or Mouse anti hb9 (5c10), 1:50, DSHB, USA) overnight at 4°C in a humidified chamber.

Stage III: Primary antibody detection

Following overnight incubation with primary antibody slides were washed 3 times in B1 buffer (3 X 5 minutes each). Slides were then incubated in 0.5ml of B1 buffer containing 1% HINGS plus Donkey anti Mouse horseradish peroxidase conjugated secondary antibody (1:500, Jackson Immuno Research laboratories Inc., USA) for 30 minutes in a humidified chamber.

Slides were washed 3 times in B1 buffer (3 X 5 minutes each) then incubated with 0.5ml of Vector ImmPACT DAB peroxidise substrate (Vector Laboratories Inc., USA) for 2 to 10 minutes until the desired staining intensity was achieved. To stop this reaction slides were washed 3 times in B1 buffer (3 X 5 minutes each).

Following washes the tissue was blocked in B1 buffer containing 10% Heat Inactivated Goat Serum (HINGS, Invitrogen, UK) for 30 minutes. Blocking solution was removed by tapping the slides gently on tissue. Slides were then incubated in 0.5ml B1 buffer containing 1% HINGS and sheep FAB fragments anti-DIG Alkaline Phosphotase conjugated antibody (1:5000, Roche, UK) overnight at 4°C in a humidified chamber.

Stage IV: In situ detection

Slides were washed 3 times in B1 buffer (3 X 5 minutes each) and then equilibrated in B3 buffer (0.1M Tris-HCl pH9.5, 0.1M NaCl, 0.05M $MgCl_2$) for 10 minutes. Visualisation of bound anti-DIG antibody is achieved using the NBT/BCIP Alkaline Phosphotase substrate kit (Vector Laboratories Inc., USA) prepared in B3 buffer containing 0.1% Tween, to ensure good tissue penetration, as per the manufacturer's instructions. Excess B3 solution was removed and replaced with 500µl of the NBT/BCIP solution. The staining is then allowed to develop in a humidified darkened chamber for 2 to 24 hours until the desired staining intensity is achieved. Upon achieving the desired staining intensity slides are washed in

distilled water for 10 minutes and then allowed to dry. To protect the tissue each slide was mounted with a cover slip using two drops of heated Dako Glycerol mounting medium (Invitrogen, UK). Once the mounting medium had solidified the slides can be stored indefinitely.

2.9 Imaging

Processed tissue was viewed using a NIKON eclipse 80i microscope (Nikon Instruments Inc., USA). Fluorescent images were taken using a Hamamatsu Orca-er (Hamamatsu, Japan) and IP-Lab software (Scanalytics, USA) used to introduce false colour to and merge multichannel fluorescent images. White light images were taken using a NIKON digital sight camera (Nikon Instruments Inc., USA). Where appropriate all exposure times and image enhancement remained constant.

2.10 Data Analysis

Cell counts, area analysis and signal intensity analysis were performed using ImageJ software (National Institutes of Health, USA). Statistical analysis was performed using Microsoft® Excell software (Microsoft ® Corporation, USA). Figures were compiled in Corel™ Draw (Corel ™ Corporation, Canada).

2.10.1 Cell counts

Embryos were sectioned and analysed in series of 4 across sufficient numbers of sections to encompass the entire region/neuronal nucleus of interest. Numbers of embryos or sections analysed for each experiment are indicated on the appropriate figure. Cell counts were performed on tissue following immunohistochemistry and *in situ* hybridisation protocols. The process of *in situ* hybridisation results in the deposit of a blue precipitate in the cytoplasm of cells containing target mRNA. As such positively labelled cells appear as a light circle of the cell nucleus surrounded by a halo of blue precipitate. *In situ* hybridisation with immunohistochemistry show double labelling; Addition of ImmPACT DAB peroxidase substrate results in the deposit of a brown precipitate in regions which are positively labelled with POD conjugated antibodies. The primary antibodies used in this study; Hb9 and Islet 1, label nuclear target proteins. As such double labelled cells appear as a dark brown circle surrounded by a halo of blue precipitate. Positively labelled cells were considered those which were stained in at least 50% of the cytoplasm.

Immunohistochemistry labels proteins found in both the nucleus and cytoplasm. Double labelling of cells was determined by analysing merged images of multichannel fluorescence.

2.10.2 Assessing levels of mRNA expression

In order to assess the relative levels of mRNA expression across nL the intensity of staining was assessed using ImageJ. Positively labelled cells were selected at equal distance at 5 points across nL and the average staining intensity measure over the entire cell. Measurements were normalised to a cell containing no visible staining.

2.10.3 Neuronal mixing index

A neuronal mixing index was performed as described in Price et al. 2002. Each neuron of the AccAb was scored according to the number of FMN neurons which surround it. These AccAb were then assigned to a distinct bin, determined by that number; as shown in figure 2.1. The percentage of neurons in each bin was then calculated and averaged to produce a mean figure. From the mean figure a students' T-test was used to establish statistical significance between control and experimental categories. Further to this a Neuronal coalescence index was performed, whereby an identified neuron surrounded by one or more neuron of the same type was placed in the ≥1 bin; neurons which are not surrounded by any neurons of the same type are placed in the 0 bin. Each neuron was marked to avoid double counting using ImageJ. A distance of one cell body as judged by eye was used to determine the proximity of such neurons. Statistical analysis was performed as for the neuronal mixing index.

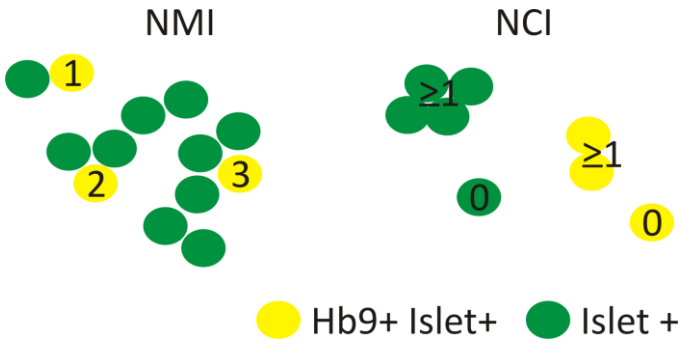

Figure 2.1: Schematic illustrating the neuronal mixing and neuronal coalescence indexes used. Neurons were identified and categorised based upon their differential expression of Hb9.

2.11 Axonal tracing

In order to assess the residual the connections to nL neurons following electroporation and axonal tracing strategy was attempted. Embryos at HH35 were removed from their shells and briefly decapitated in sterile L-15 medium (Sigma Aldrich, UK). The hindbrain region was dissected and then sectioned into 300µm sections in slicing buffer using a vibratome. A cut was then made through the midline of the hindbrain section and a small amount of rhodamine-dextran (Invitrogen, UK) crystals inserted in the midline. Shortly after this HRP-conjugated to alexa-488 (Invitrogen, UK) was microinjected into the region of the superior Olivary nucleus sing a drawn glass pipette. Slices were incubated at 38°C for 4 hours in oxygenated L-15 medium and then fixed and processed as usual.

3. Cadherins in cranial motor nucleogenesis

Nuclei are a prominent mode of neuronal organisation within the CNS which is evolutionarily preserved across all vertebrate species (Gilland & Baker, 2005). Neurons coalesce into clusters which occupy specific, stereotyped positions within the rostrocaudal, dorsoventral and mediolateral axes. Despite the prevalence of neuronal nuclei, the molecules which drive their formation are not currently fully understood.

Within rhombomere 5 (r5) of the embryonic chicken hindbrain there are four distinct motor nuclei; Abducens (Ab), Accessory Abducens (AccAb) and the Facial Motor Nucleus, which consists of dorsal (dFMN) and ventral (vFMN) divisions (Reviewed in Guthrie 2007). The early development of the motor neurons which will constitute these nuclei has been extensively studied; it is known that their differentiation in spatially restricted progenitor domains is determined by hox gene expression in the rostrocaudal and dorsoventral axes under the control of morphogens expressed at the MHB, paraxial mesoderm and floorplate of the developing neural tube. However the migration of these neurons in transverse sections and the molecules which potentially drive their coalescence in to distinct nuclei has not been studied.

3.1 The time course of cranial motor nucleus development in rhombomere 5

In the first instance it was necessary to study the normal developmental time course of nucleus development in r5. Both the Ab and AccAb nuclei consist of somatic motor (SM) neurons; vFMN and dFMN consist of branchiomotor (BM) neurons. These two neuronal subtypes are distinguishable by their expression of specific transcription factors; SM neurons express *Hb9* and *Islet-1* whilst BM neurons express *Islet-1* only, throughout nucleogenesis (Tanabe & Jessell 1996, Goulding 1998) (figure 3.1, D). I thus characterised the development of the AccAb, Ab and d/vFMN in r5 from HH20 to HH31 using immunofluorescence to visually distinguish SM and BM neurons.

Motor neurons exit the ventricular zone close to the midline and migrate towards the ventral hindbrain (Figure 3.1, A). At HH20 both SM and BM neurons are found in a mixed population. SM neurons can be seen contained within the main body of BM neurons (Figure 3.1, A). At HH26 the neurons are beginning to segregate and it is possible to distinguish potential individual nuclei. Ab remains as a loose cluster of cells coalescing near the medial dorsal region of the hindbrain. AccAb neurons are

still intermingled with the Islet+ neurons of the potential FMN. The divisions of the FMN are not yet distinguishable, but remain a large somewhat scattered population (Figure 3.1, B).

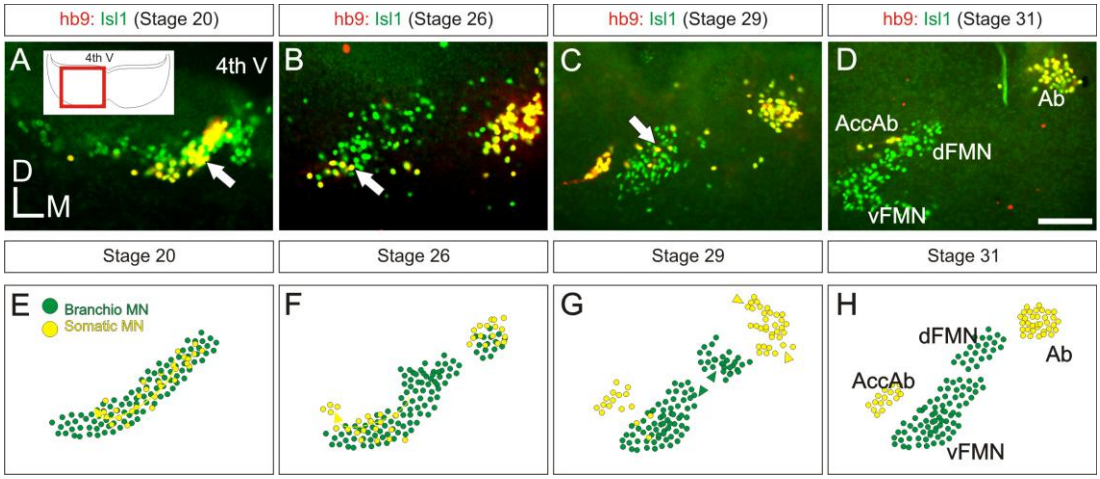

Figure 3.1: Time course of cranial motor nucleogenesis in r5. **A:** SM neurons are found mixed with BM neurons close to the midline at HH20. The red box illustrates the position represented in each image. 4th Ventricle is shown for orientation (4th V) **B:** By HH26 the nuclei have begun to segregate, the Abducens (Ab) population remains close to the midline in dorsal hindbrain, SM neurons of the Accessory Abducens (AccAb) are still mixed with BM of the Facial Motor Nucleus (FMN). **C:** AccAb neurons are nearly completely migrated laterally to FMN, however a few SM neurons remain in the FMN (indicated by arrow). **D:** By HH30/31 migration is complete. **E-H:** Summary of the migratory process. The SM neurons of AccAb migrate through the presumptive FMN to their final position. Scale bar 100µm.

At HH29 we see that the Ab has begun to coalesce. AccAb has almost completely segregated from the FMN, although a few isolated SM neurons remain in the FMN (Figure 3.1, C) and FMN itself begins to organise into its two distinct parts; vFMN and dFMN. By HH31 segregation of the motor neurons is complete and the nuclei have organised into their mature conformations. Ab is found in the dorsal hindbrain, close to the midline. AccAb sits laterally to the two aspects of the FMN, which are now visibly distinct (Figure 3.1, D).

This process is summarised in Figure 3.1, E-F, which illustrates the migratory pathways of the SM and BM neurons respectively. The development of these nuclei is highly stereotyped; SM and BM neurons are initially found in a mixed neuronal population. SM neurons which will constitute Ab remain close to the midline and segregate from the FMN before HH26. Those SM neurons which will constitute AccAb migrate through the FMN to their final position by HH29-31. In summary this

appears to be an active process of segregating different cell types from a mixed population into specific nuclei.

3.2 Differential cadherin expression in rhombomere 5 cranial motor nuclei

Cadherins are known to drive cell sorting both *in vitro* (Takeichi 1988, Fredette 1993) and *in vivo*; where combinatorial cadherin expression drives the sorting of motor neurons into distinct motor pools within the spinal cord (Price et al., 2002). Equally it appears that cadherins may also play a role in development of the auditory cranial nuclei of r5 (Chapter 5). As such they present an ideal candidate to drive cranial motor nuclei segregation. Focusing on the known position of the motor nuclei in r5 positive staining was assayed as neurons which in which the cytoplasm was at least 50% positively labelled with blue precipitate. Analysis of cadherin expression by in situ hybridisation in r5 at HH36 revealed at least 6 cadherins to be differentially expressed in the four cranial motor nuclei; *cadherin 20*, 6b, 13, 22, 8 and 11 (Figure 3.2, C-H). Importantly γ-catenin, which is required for cadherin function, is also expressed in these nuclei (Figure 3.2, B). Scattered positive staining was also seen for some of the cadherins assayed, for example cadherins 13 and 11, however this was not restricted to any specific region, and was notably lacking immediately juxtaposed to the motor nuclei (Figure 3,2, E, H). This demonstrates that cadherins are present and may be actively driving binding within the r5 motor nuclei.

Each of the motor nuclei can be distinguished by their specific differential cadherin expression profile, for example AccAb neurons express *cadherin 6b*, 11 and 13 whereas Ab expresses cadherin 11 and 8 only. Similarly the two division of the FMN also exhibit differential cadherin expression profiles; dFMN expresses cadherins 6b, 11, 13 and 20 whilst vFMN expresses cadherins 6b, 8, 11 and 22 respectively. Thus each of the r5 motor nuclei expresses a unique combination of cadherins. This data is summarised in Figure 3.2, I.

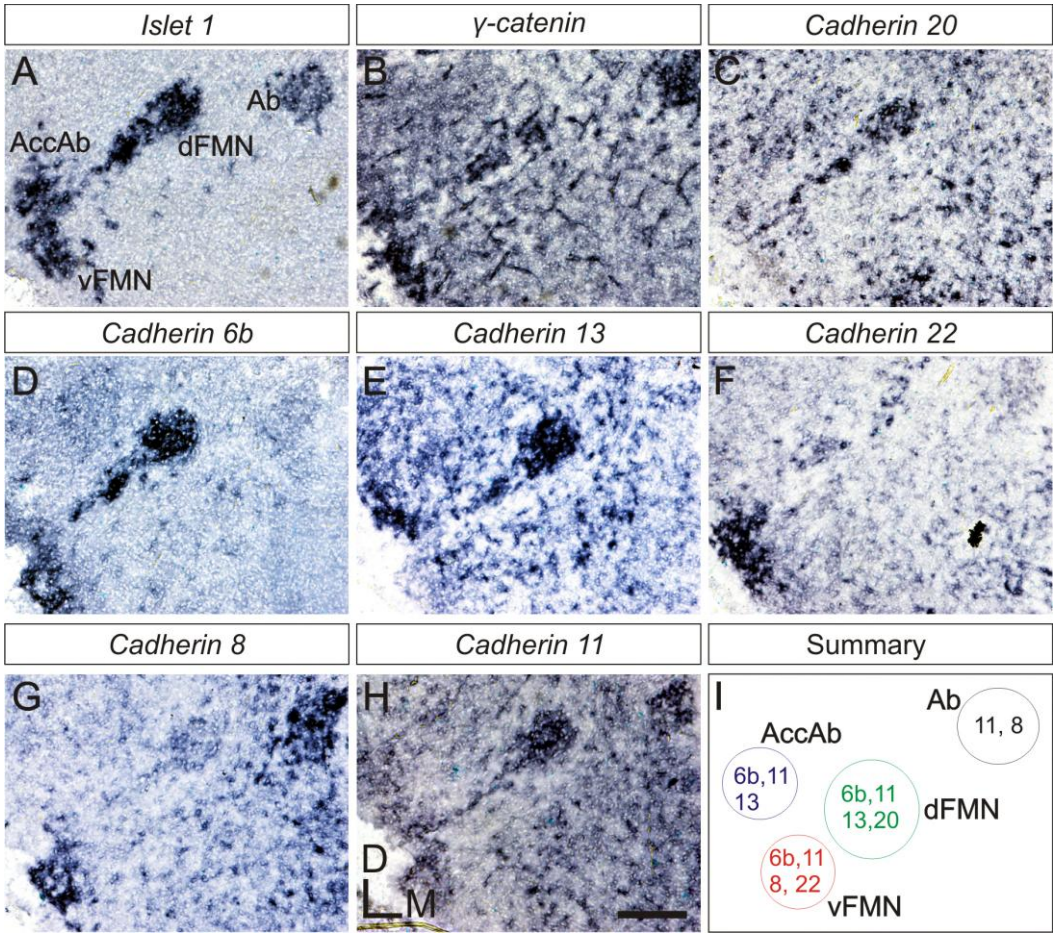

Figure 3.2: Cadherin and catenin expression in r5 motor nuclei. **A:** *Islet-1* expression in the motor nuclei of r5; AccAb, Ab, dFMN and vFMN. **B:** ɣ-catenin is expressed in r5 cranial motor nuclei. **C-H:** Expression patterns of *cadherin 20*, 6b, 13, 22, 8 and 11. **I:** Summary showing differential cadherin expression profile in each nucleus. Scale bar 100µm.

3.3 Cadherin function is important in r5 cranial motor nucleus development.

In order to assess whether cadherins have a functional role in motor nucleogenesis a dominant negative *N cadherin* isoform (NΔ390) was utilised. Lacking its extracellular domain, but still containing its intracellular catenin binding domains; NΔ390 inserts into the plasma membrane and competes with endogenous cadherin binding to ɣ/β-catenin. Its presence in the plasma membrane reduces the amount of available ɣ/β-catenin in the cytoplasm. In this manner NΔ390 is able to knock down cadherin-cadherin function between cells by disrupting the formation of a stable adherins complex (Kintner, 1992). Embryos were unilaterally co-electroporated with both NΔ390 and GFP plasmid constructs at HH18 and analysed at HH30. Successful electroporation was confirmed by the presence of GFP. As the plasmid construct is only inserted into one hemisphere of the hindbrain the non-electroporated hemisphere acts as an internal control for each embryo as a basis for comparison.

NΔ390 expression did not alter the number of SM or BM neurons in r5 (Figure 3.3, E, G), however did result in desegregation of the motor nuclei (Figure 3.3). Using the Neuronal Coalescence Index (NCI) (Methods 2.10.3) it is possible to quantitate this phenotype in terms of cell-cell juxtaposition. Neurons were placed into one of two bins dependent upon the number of other neurons of the same type with which each is juxtaposed; either zero or ≥one. Analysis of SM neurons showed a significant decrease in the percentage of *Hb9+*/*Islet-1+* neurons localised to one another, when compared with control (Figure 3.3, D), following NΔ390 expression. Due to the nature of this phenotype it is not possible to distinguish motor neurons of the Ab and AccAb as all the *Hb9+* neurons are scattered and are not found in their usual spatially discrete location. This suggests that knocking down normal cadherin function in r5 motor neurons inhibits the interactions which bind these cells into tight nuclei. As a result motor neurons are increasingly isolated from each other and the nuclei appear desegregated (Figure 3.3, B).

Analysis of BM neurons which constitute the FMN revealed a similar desegregation phenotype following NΔ390 expression (Figure 3.3, F). There is a significant increase in the percentage of BM neurons which are isolated following NΔ390 expression compared with the control (Figure 3.3, F). Again this is indicative of cadherins playing an active role in the coalescence of the r5 cranial motor nuclei. Knocking down cadherin function in motor neurons appears to inhibit normal

nucleus development and both SM and BM neurons are increasingly scattered and isolated from one another.

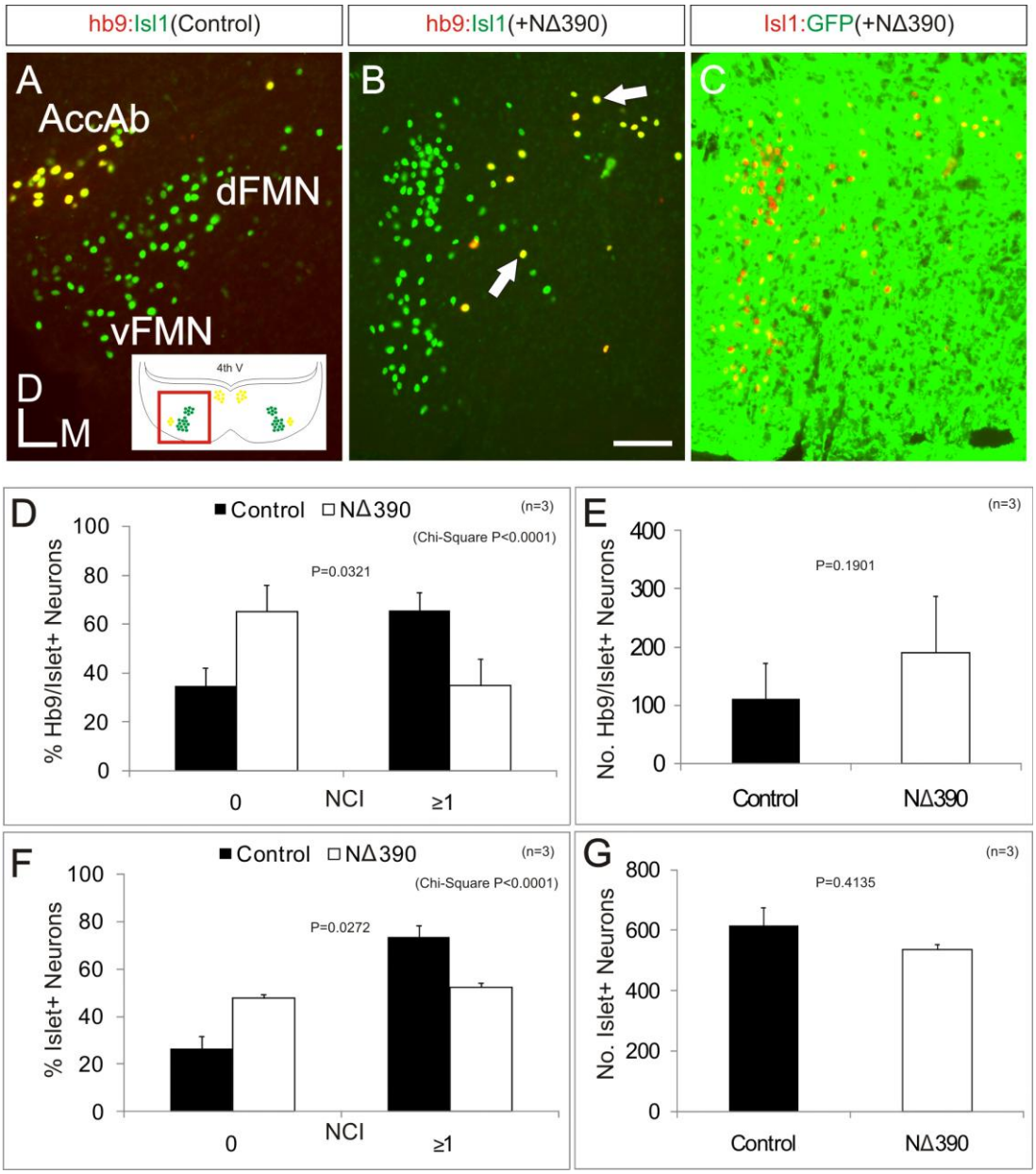

Figure 3.3: Cadherins are required for cranial motor nucleus development in r5. **A:** Isl1 and *Hb9* expression in control hemisphere showing AccAb (yellow) sitting lateral to the FMN. The red box illustrates the position represented in each image. 4th Ventricle is shown for orientation (4th V) **B:** Following NΔ390 expression the nuclei fail to coalesce correctly. Neurons of the AccAb are mispositioned and scattered throughout the hindbrain (indicated by arrows). **C:** GFP expression indicates successful electroporations. **D:** NCI analysis of SM neurons (*HB9*+/Isl1+). The percentage of neurons which coalesce into a coherent nucleus is significantly lower following NΔ390 expression. **E:** There is no significant alteration in SM neuron number following NΔ390 expression. **F:** There is a significant increase in scattering of BM neurons in r5 following NΔ390 expression as assayed by the NCI. **G:** Total BM number in r5 is not significantly altered following NΔ390 expression. Students T-test, Error bars indicate standard error, (n=3). Scale bar 100µm.

3.4 Normalising cadherin expression profiles between motor nuclei inhibits normal nucleus segregation

In the spinal cord combinatorial cadherin expression is known to drive motor pool segregation (Price et al., 2002) Given that the motor nuclei of r5 exhibit differential cadherin expression profiles and knocking down cadherin activity in those nuclei results in desegregation it is reasonable to predict that the combinatorial cadherin expression is crucial for normal nucleogenesis in r5. In order to investigate this possibility it is necessary to identify cadherin targets for manipulation. Looking at Figure 3.2 it is apparent that the dFMN expresses cadherins *6b, 11, 13* and *20*, whilst AccAb expresses *cadherin 6b*, *11* and *13* only. These two nuclei differ only in the expression of *cadherin 20*. The prediction therefore would be that misexpression of *cadherin 20* in AccAb neurons which normalises the expression pattern between the two nuclei will inhibit segregation.

As with previous experiments, a *Cadherin 20* construct (Price et al., 2002) was co-electroporated with GFP into one hemisphere of the hindbrain at HH18. Analysis at HH30 indicates that as predicted the AccAb motor neurons fail to segregate correctly from the FMN (Figure 3.4). Figure 3.4, B clearly shows *Hb9*+/*Islet-1*+ neurons of the AccAb are found mixed with *Islet-1*+ FMN neurons (Indicated by arrows). Quantitation using the Neuronal Mixing Index (NMI, See methods) demonstrates that there is a significant increase in the percentage AccAb neurons situated close to, and therefore aberrantly mixing with, at least one FMN neuron (Figure 3.4, D), from an average of 4.62% (±1.59) in control to 33.61% (±3.21) ($p=0.0004$, Student's T-test) following *cadherin 20* misexpression. This increase in juxtaposition between AccAb and FMN neurons is indicative of an increased intermingling between the two populations following *cadherin 20* misexpression. There is no alteration in the number of AccAb neurons between control and electroporated hemispheres (Figure 3.4, E) demonstrating that any phenotypic change is not as a result of a change in motor neuron number.

Misexpression of *cadherin 20* in AccAb neurons alters their expression profile to match that of dFMN. It is apparent that AccAb neurons appear initially to migrate correctly, through the FMN, but that segregation of those neurons now aberrantly expressing *cadherin 20* does not occur. A potential explanation for the desegregation phenotype is that in essence AccAb neurons appear on the cell

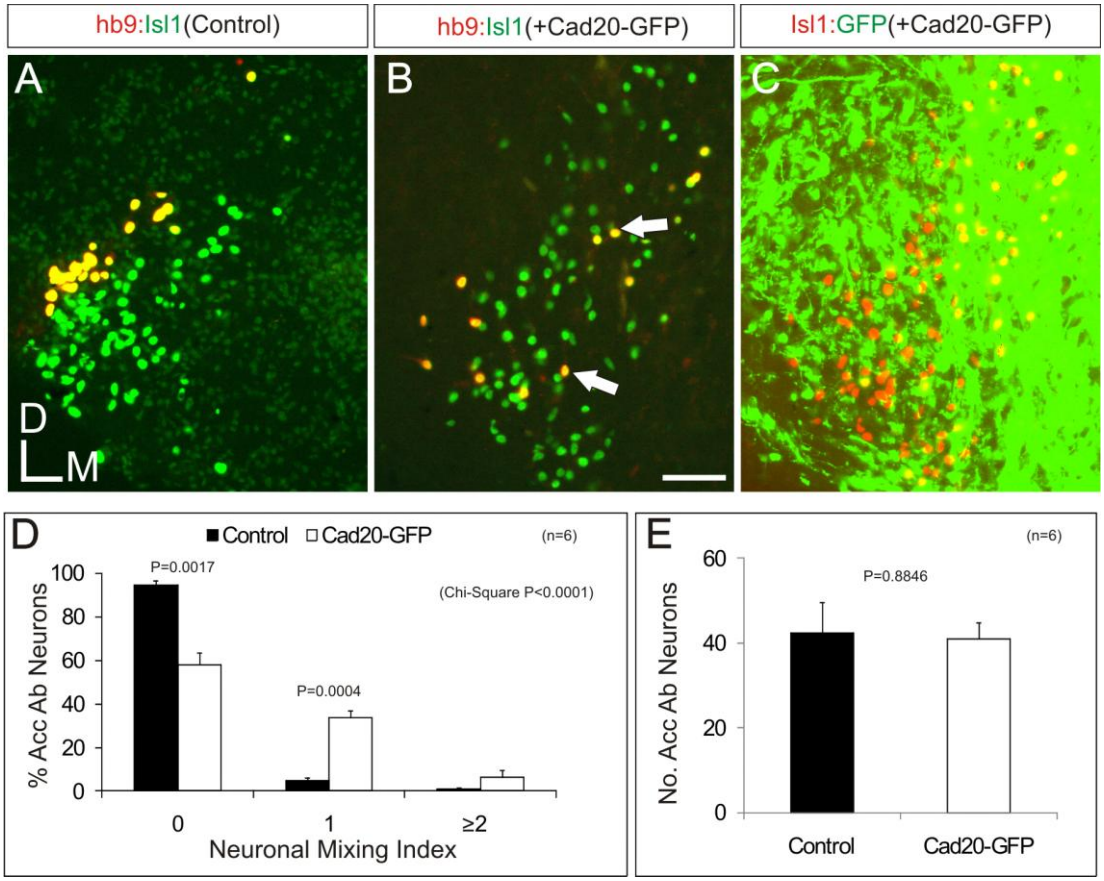

Figure 3.4: Normalising cadherin expression profiles between AccAb and dFMN via *cadherin 20* misexpression results in desegregation of the nuclei. **A:** Isl1 and *Hb9* expression in control hemisphere showing AccAb (yellow) sitting lateral to the FMN. **B:** *Cadherin 20* misexpression in AccAb results in failure of AccAb neurons to segregate from dFMN. AccAb neurons are visible mixed with FMN (indicated by arrows) **C:** GFP expression indicates successful electroporations. **D:** NMI analysis shows a significant decrease in the percentage of AccAb neurons which have coalesced with one another. **E:** There is not significant change in the number of AccAb neurons in r5 following *cadherin 20* misexpression. Paired Student's T-test, error bars indicate standard error (n=6). Scale bar 100µm.

surface as dFMN neurons as defined by their cadherin expression and can bind to each other.

One other method of equalising *cadherin 20* expression between these two nuclei is to knock down *cadherin 20* function in dFMN. A cytoplasm truncated version of *cadherin 20* (dnCad20) which acts as a dominant negative was used in order to knock down *cadherin 20* function in dFMN. This truncated version of *cadherin 20* will insert in to the plasma membrane where its extracellular domain will bind preferentially to *cadherin 20* on the opposing cell surface, competing with endogenous *cadherin 20*. However, as its cytoplasmic domain is truncated the cadherin-cadherin complex is not able to mediate the formation of a stable junction linked to the actin cytoskeleton, in this manner targeted disruption of *cadherin 20* function is achieved. Following dnCad20 electroporation at HH18 in FMN neurons AccAb and dFMN fail to segregate correctly by HH30 (Figure 3.5). Figure 3.5, B illustrates this; AccAb neurons are aberrantly positioned within dFMN (indicated by arrows). There is a significant increase in the percentage of AccAb neurons contacting at least one FMN neuron from 7.30% (±3.76) in control to 28.17% (±3.86) following dnCad20 expression. As assayed using the NMI the increase in AccAb neurons contacting one or more FMN neuron is indicative of increased mixing between the two neuronal populations following dnCad20 expression when compared with control. If the cadherin manipulations had no effect, one would expect the number of AccAb neurons found intermixed with FMN neurons to be unaltered. The percentage of AccAb neurons which are isolated from FMN neurons drops, from 91.47% (±4.04) in control to 55.32 (±5.42) ($p=0.0017$, Student's T-test). As with *cadherin 20* misexpression, there is no alteration the number of AccAb neurons following dnCad20 expression (Figure 3.5, E).

Thus, by knocking down *cadherin 20* function in dFMN the functional cadherin expression profiles of dFMN and AccAb are equalised leading to desegregation of the nuclei. AccAb neurons become bound to neurons of the dFMN and fail to migrate to their normal position lateral of the FMN.

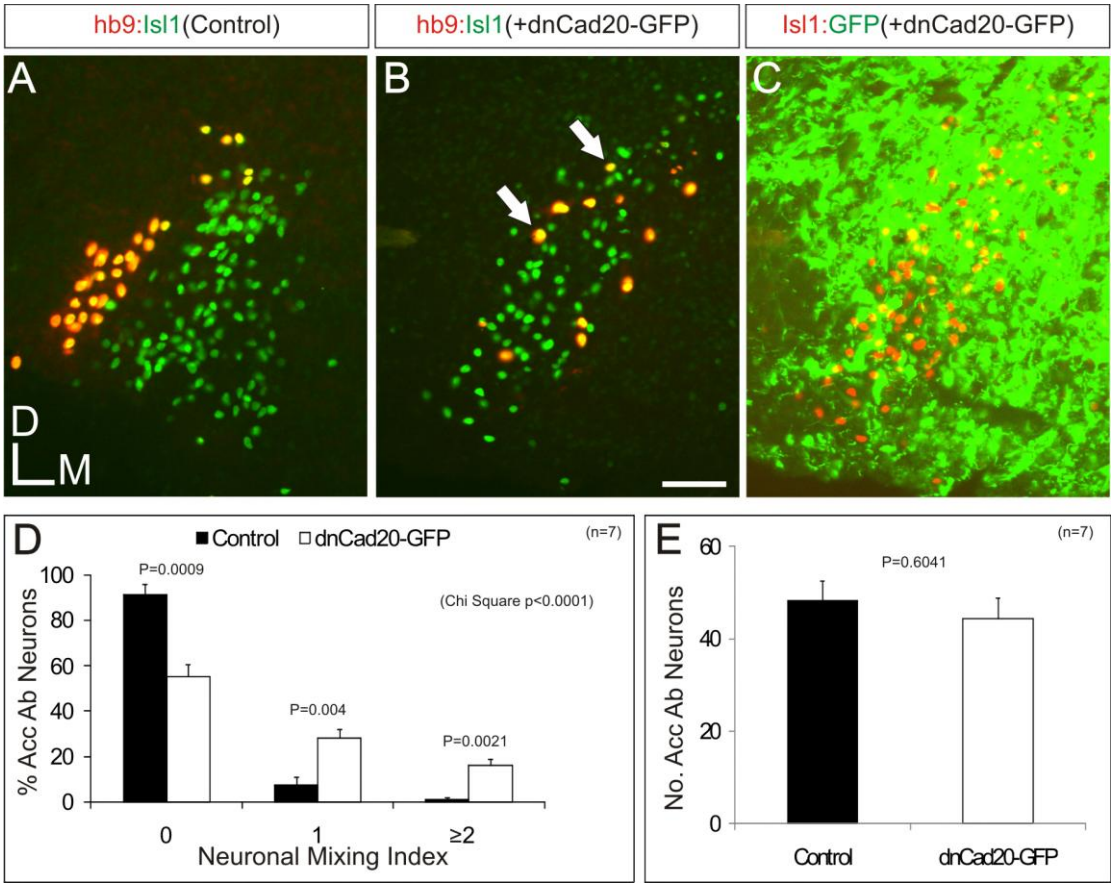

Figure 3.5: Normalising cadherin expression profiles between AccAb and dFMN using dnCad20 also results in desegregation of the nuclei. **A:** Isl1 and *Hb9* expression in control hemisphere showing AccAb (yellow) sitting lateral to the FMN. **B:** dnCad20 expression in FMN results in failure of AccAb neurons to segregate from dFMN. AccAb neurons are visible mixed with FMN (indicated by arrows) **C:** GFP expression indicates successful electroporations. **D:** NMI analysis shows a significant decrease in the percentage of AccAb neurons which have coalesced with one another. **E:** There is not significant change in the number of AccAb neurons in r5 following dnCad20 expression. Paired Student's T-test, error bars indicate standard error (n=7). Scale bar 100µm.

3.5 Misexpression of *cadherin 6b* or *N cadherin* has no effect on motor nucleogenesis in r5

To control for non specific effects of cadherin misexpression in general, we misexpressed cadherins 6b which is expressed in both FMN and AccAb and N cadherin, which is not expressed in any of the r5 cranial motor nuclei. Thus over expression of *cadherin 6b* or N-cadherin in each nucleus will have no destabilising effect on their combinatorial cadherin expression and nucleogenesis should proceed unperturbed.

Misexpression of *Cadherin 6b* at HH18 resulted in no significant alterations in segregation of the AccAb and FMN at HH30 (Figure 3.6). Following *cadherin 6b* misexpression, the AccAb and FMN segregate normally; AccAb is found lateral to FMN as in the control hemisphere (Figure 3.6, A, B). Significantly there is no increase in mixing between the two nuclei as assayed using the NMI (Figure 3.6, D). A few scattered AccAb cells do remain within the FMN; however there is no significant difference in the percentage of misplaced cells when compared with the control. For example the percentage of AccAb neurons juxtaposed to two or more FMN neurons is 3.99 (± 2.89) in control compared with 4.00 (±0.99) ($p=0.996$, Student's T-test) following *cadherin 6b* misexpression (Figure 3.6, D).

N cadherin, a type I cadherin, is not expressed in any of the r5 motor nuclei (Figure 3.2), and presents a good target for manipulation; misexpression of *N cadherin* should alter the cadherin expression profile of each nucleus identically and have no effect on nucleogenesis if combinatorial type II cadherin expression is driving the process of segregation. Using a doxycycline inducible N cadherin-GFP tagged construct embryos were unilaterally electroporated at HH18 and the construct induced at HH20. Analysis was performed at HH30.

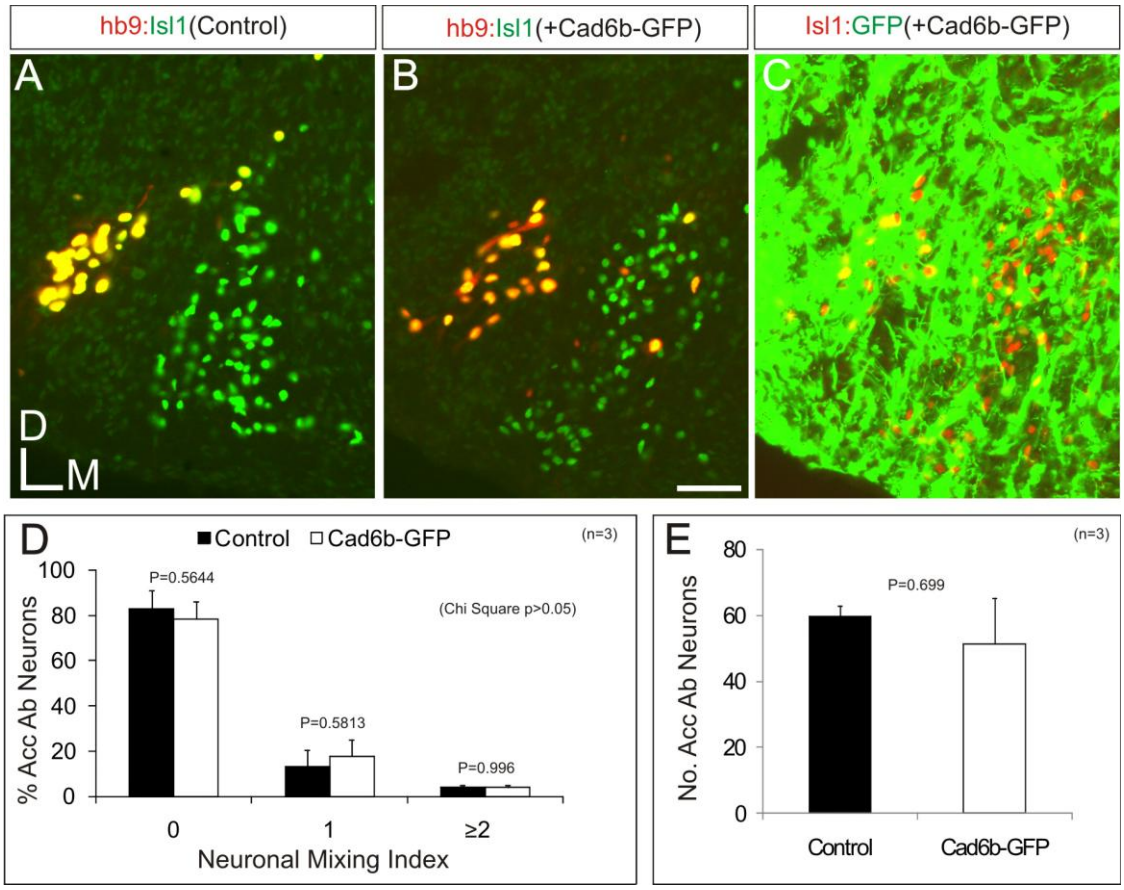

Figure 3.6: Over expression of *cadherin 6b* does not alter r5 cranial motor nucleogenesis **A:** Isl1 and *Hb9* expression in control hemisphere showing AccAb (yellow) sitting lateral to the FMN. **B:** following cad6b over expression the AccAb and FMN appear phenotypically unaltered when compared with the control hemisphere **C:** GFP expression indicates successful electroporations. **D:** NMI analysis shows no significant change in the percentage of AccAb neurons which have coalesced with one another following cad6b over expression **E:** There is not significant change in the number of AccAb neurons in r5 following cad6b over expression. Paired Student's T-test, error bars indicate standard error (n=3). Scale bar 100µm.

Misexpression of N cadherin, as with *cadherin 6b*, had no effect on nucleogenesis in r5 (Figure 3.7). AccAb and FMN segregate as expected, with AccAb found lateral to FMN (Figure 3.7, B). Analysis using the NMI shows that there is no significant changes in the percentage of AccAb neurons which are not in contact with any FMN; 89.88 (±0.29) in control against 84.61(±4.33) (p=0.3582, Student's T-test) following *N cadherin* misexpression (Figure 3.7, D). This indicates that the AccAb population is spatially separated from the FMN.

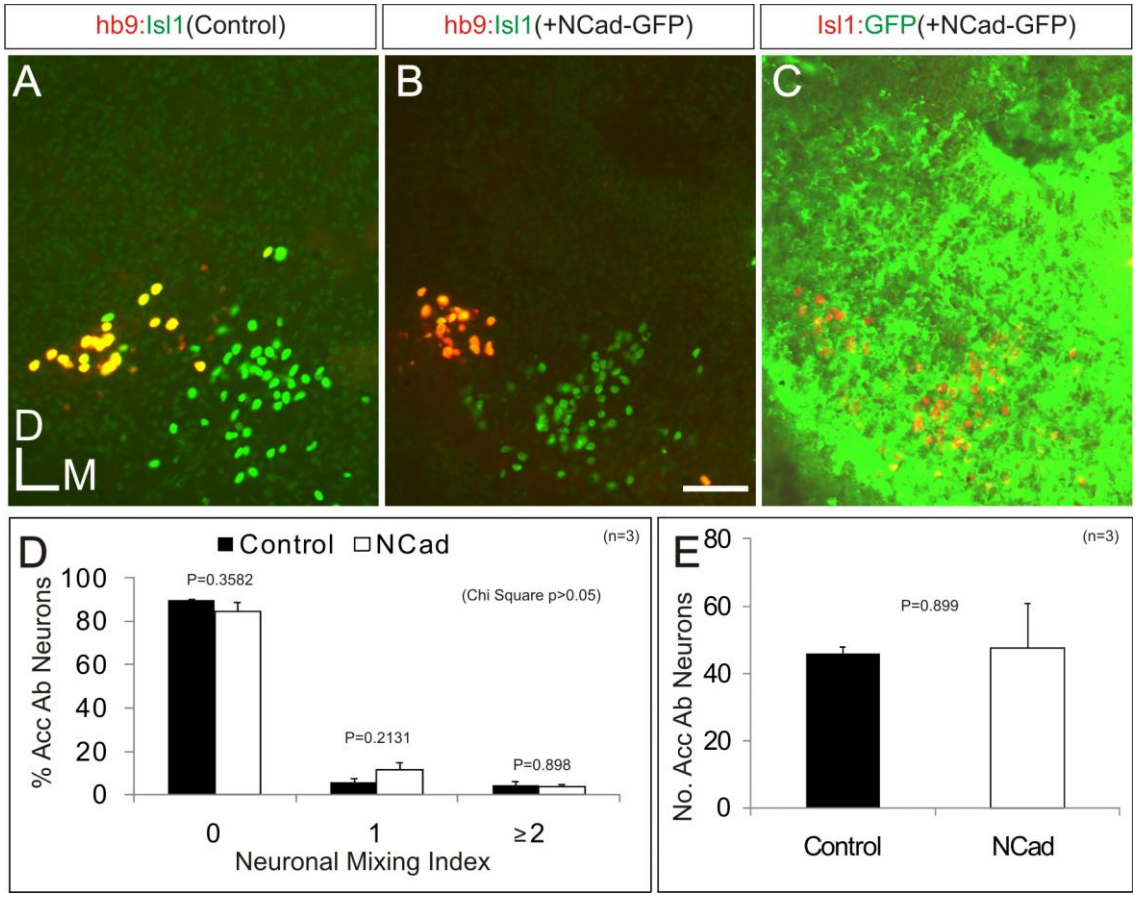

Figure 3.7: Misexpression of *N cadherin* does not alter r5 cranial motor nucleogenesis **A:** Isl1 and *Hb9* expression in control hemisphere showing AccAb (yellow) sitting lateral to the FMN. **B:** following NCad misexpression the AccAb and FMN appear phenotypically unaltered when compared with the control hemisphere **C:** GFP expression indicates successful electroporations. **D:** NMI analysis shows no significant change in the percentage of AccAb neurons which have coalesced with one another following NCad misexpression **E:** There is not significant change in the number of AccAb neurons in r5 following NCad misexpression. Paired Student's T-test, error bars indicate standard error (n=3). Scale bar 100µm.

Taken together this data suggests that up regulation of cadherin expression, whilst retaining a differential expression pattern within each nucleus, has no effect on r5 cranial nucleogenesis. Given that normalising cadherin expression patterns between AccAb and dFMN leads to desegregation of these nuclei, it is reasonable to suggest that differential cadherin expression is driving segregation of the r5 cranial motor nuclei during nucleogenesis.

3.6 Cadherin expression in rhombomere 8 cranial motor nuclei

As cadherins appear to drive segregation of the r5 cranial motor nuclei, and are known to drive motor pool sorting in the spinal cord, it is possible that cadherins play a role in nucleogenesis throughout the central nervous system. To establish whether a cadherin driven mechanism of nucleogenesis is conserved throughout the hindbrain an analysis of cadherin expression in rhombomere 8 was performed. In r8, motor neurons are divided into 4 distinct motor nuclei; Glossopharyngeal (Gl), Dorsal Vagus (DV), Ventral Hypoglossal (V Hypo) and Dorsal Hypoglossal (D Hypo). Similarly to the r5 cranial motor nuclei, there are two different motor neuron subtypes found in r8, SM and BM which are distinguishable by their respective expression of the transcription factors *Islet-1* and *Hb9*. The two Hypoglossal nuclei consist of SM neurons, whilst the Dorsal Vagus and Glossopharyngeal nuclei are formed from BM neurons (Reviewed in Guthrie 2007).

Analysis of the developmental time course of r8 motor nuclei reveals a similar picture to that seen in r5. At HH24, upon exiting the ventricular zone, both SM and BM neurons are found in a mixed population close to the midline (Figure 3.8, A). These neurons then undergo an active process of segregation, BM neurons of the DV and Gl nuclei migrate dorsally and laterally toward their respective final positions (Figure 3.8, B) whilst those SM neurons which will constitute the dorsal and ventral hypoglossal nuclei remain close to the midline. At HH27 the SM neurons are beginning to separate into two distinct populations. By HH29 the r8 motor nuclei have segregated and coalesced at their final positions; the ventral and dorsal hypoglossal sit close to the midline ventricular zone. DV is found dorsal to the D hypo, whilst the Gl is located laterally to the hypoglossal complex (Figure 3.8, C). In summary in a similar manner to that shown in r5 (Figure 3.1) SM and BM neurons are initially found in a mixed population and then, through a process of migration and cell sorting, segregate to form four distinct neuronal nuclei.

Analysis by *in situ* hybridisation of the cadherin expression in r8 cranial motor nuclei revealed a differential expression of *cadherin 6b* and 13 respectively (Figure 3.9). This data is summarised in Figure 3.9, C; DV expresses cadherin 13 only, Gl expresses *cadherin 6b* only, whilst the D Hypo expresses both. Most interesting is the V Hypo, where *cadherin 6b* is expressed throughout the nucleus, but cadherin 13 is restricted to a population of cells in the ventral aspect of the nucleus only. This

data points towards an anatomical specialisation within the nucleus which requires the separation of two populations.

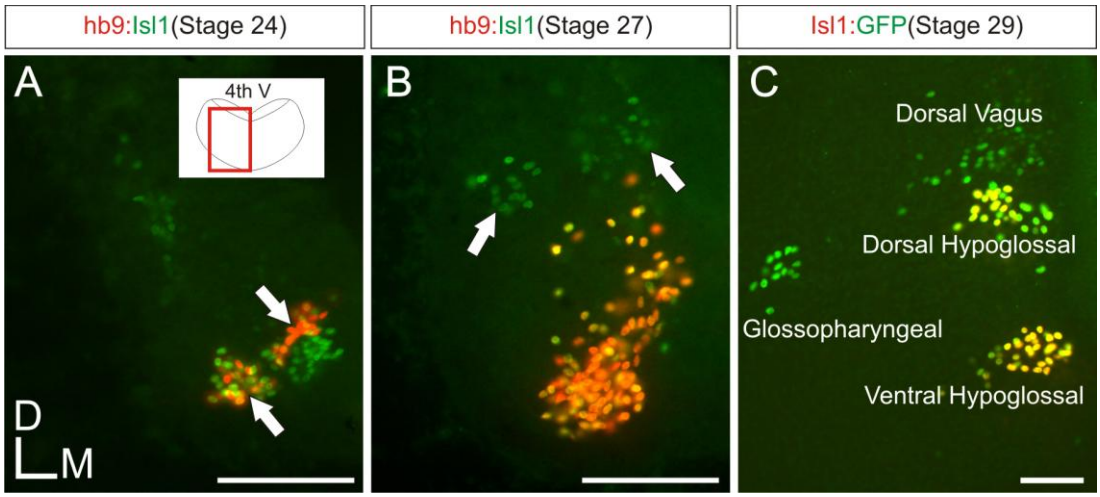

Figure 3.8: Developmental time course of r8 cranial motor nucleus development. **A:** At HH24 SM and BM motor neurons are found in a mixed population close to the midline. The red box illustrates the position represented in each image. 4th Ventricle is shown for orientation (4th V) **B:** By HH27 SM and BM neurons have begun to segregate. Dorsal Vagus and Glossopharyngeal neurons migrate towards their final positions (indicated by arrows). **C:** At HH29 migration and segregation is complete and the nuclei occupy their final positions. Scale bar 100µm.

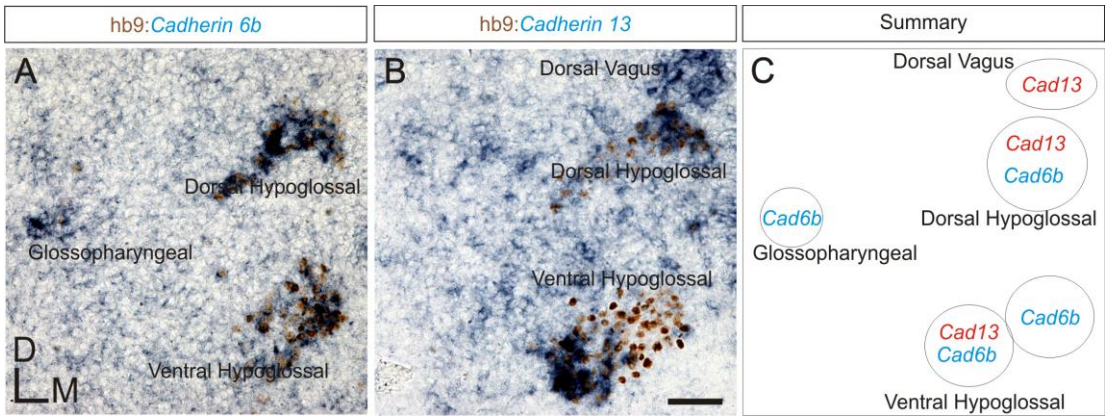

Figure 3.9: Cadherin expression in r8 cranial motor nuclei. **A:** *Cadherin 6b* is expressed in three cranial motor nuclei of r8; Dorsal Hypglossal, Glossopharyngeal and Ventral Hypoglossal. **B:** Cadherin 13 is expressed in Dorsal Vagus and Dorsal Hypoglossal nuclei, but is restricted to a ventral population of the Ventral Hypoglossal nucleus. **C:** Summary of differential cadherin expression patterns in r8 cranial motor nuclei. Scale bar 100µm.

3.7 Down regulation of cadherin function inhibits nucleogenesis in rhombomere 8

In order to assess a potential role for cadherins in nucleogenesis at r8, cadherin function was knocked down using the dominant negative *N cadherin* isoform, NΔ390. Embryos were unilaterally electroporated at HH18 and analysed at HH30. As seen in r5, the motor nuclei in r8 are not tightly coalesced following NΔ390 expression (Figure 3.10). Neurons belonging to the Hypoglossal and Dorsal Vagus nuclei appear mispositioned (Figure 3.10, B) and all nuclei appear to have failed to coalesce correctly.

Assayed using the NCI, and taking each in turn, each of the nuclei is significantly altered. Both ventral and dorsal aspects of the Hypoglossal show significant decreases in neuronal coalescence: Decreasing from 92.59% (±0.57) to 66.83% (±4.40) ($p=0.0261$) of total neurons coalesced with one or more neuron of the same type in Ventral Hypoglossal (Figure 3.10, D). In Dorsal Hypoglossal there is a similar phenotype following NΔ390 expression; the percentage of coalesced neurons drops from 91.33% (±1.89) in control to 64.75% (±5.54) ($p=0.0234$) (Figure 3.10, F). These decreases are indicative of a lack of neuronal cohesion due to cadherin function knock down.

In the Islet+ only populations of the Dorsal Vagus and Glossopharyngeal nuclei NΔ390 expression has the same effect. Cohesion of the Dorsal Vagus population is lost, accompanied by a loss of neuronal coalescence from 80.38% (±4.78) in control to 62.26% (±8.09) (Figure 3.10, H). Similarly the Glossopharyngeal nucleus fails to coalesce correctly; there is a decrease from 78.41% (±1.67) in control to 56.24% (±3.87) of total neuron number coalesced with one or more Islet+ neuron following NΔ390 expression (Figure 3.10, J). There is no decrease in total cell number following NΔ390 expression for any of the four neuronal populations (Figure 3.10, E, G, I, K).

Thus knocking down cadherin function in r8 leads to defects in neuronal development in the same manner as that seen at r5; Inhibiting cadherin function leads to a decrease in cohesion and coalescence between MN's and the nuclei appear scattered. Cadherins therefore appear to play a role in motor nucleus development throughout the hindbrain.

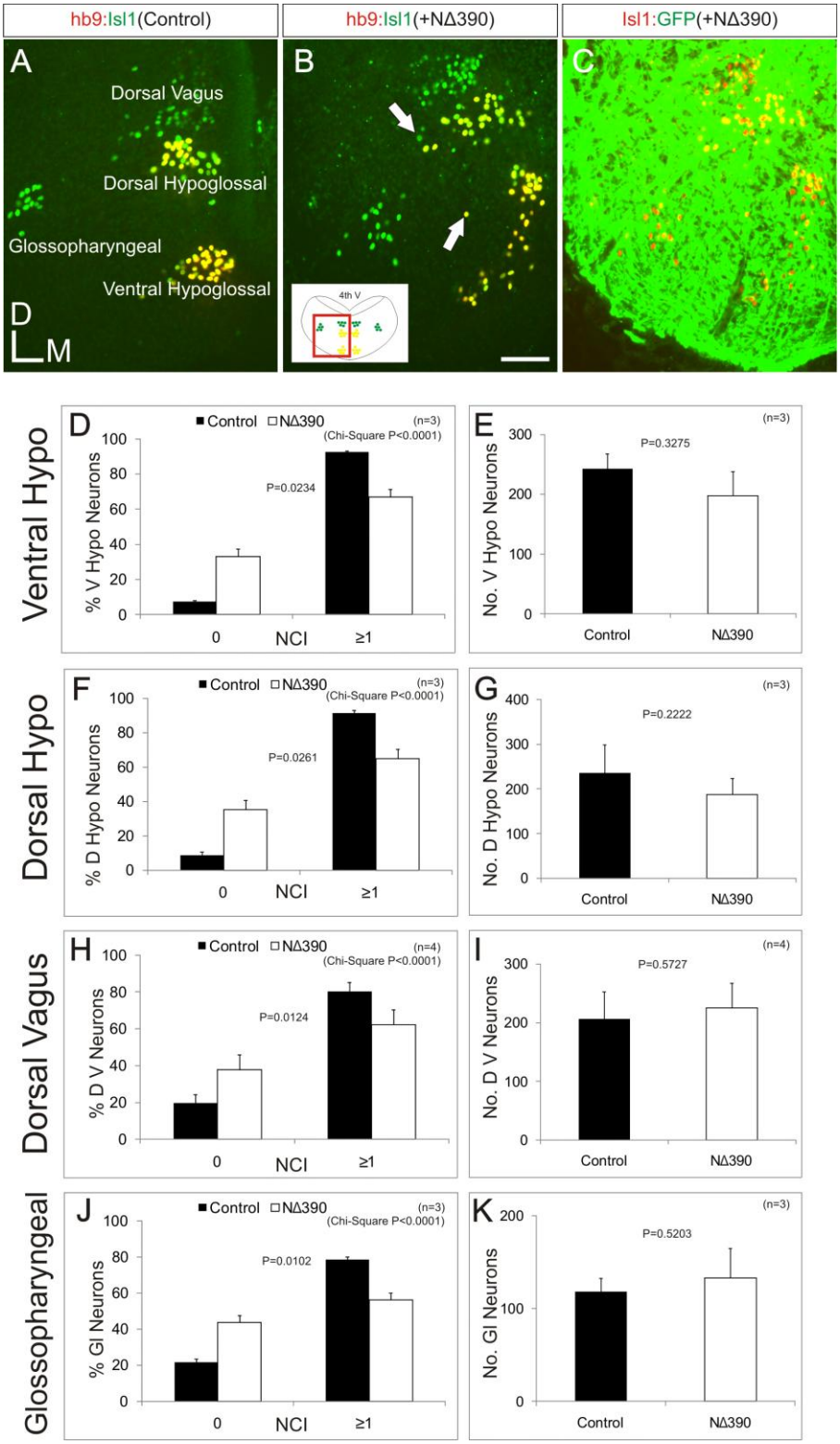

Figure 3.10: Cadherins are required for motor nucleus development in r8 **A:** Control hemisphere showing the positions of the four major r8 motor nuclei. **B:** Following NΔ390 expression the integrity of the nuclei is lost. Neurons appear scattered and have failed to coalesce correctly (indicated by arrows). The red box illustrates the position represented in each image. 4th Ventricle is shown for orientation (4th V)**C:** Successful electroporation was confirmed by the presence of GFP. **D-K:** NCI analysis indicates that the nuclei fail to coalesce following NΔ390 expression when compared with control hemisphere. There is no significant alteration in cell number following NΔ390 expression. Paired Student's T-test, error bars indicate standard error, Scale bar 100µm.

3.8 Cadherin expression is dynamic throughout nucleogenesis

The motor nuclei of r5 and r8 exhibit differential cadherin expression profiles (Figure 3.2, 3.8) in their mature configurations. The data suggests that cadherins are generally involved in coalescence of the nuclei and alterations in the differential cadherin expression can lead to desegregation of the nuclei. However prior to the segregation of the nuclei in r5 and r8 these MN are found in large mixed populations. Thus it is reasonable to predict that if cadherins drive, through their differential expression, nucleogenesis the*N cadherin* expression must be present throughout nucleogenesis. In order to assess this, cadherin expression was assayed at various stages throughout development in both r5 and r8.

The misexpression of *cadherin 20* in r5 leads to desegregation of the AccAb and FMN respectively, thus this provided the obvious target for analysis of developmental expression. In situ hybridisation analysis coupled with an antibody stain reveals that at HH20 *cadherin 20* is expressed in 80.99% (±0.60) of all *Islet-1*+ MN's of r5 (Figure 3.11, A, Table 3.1) however at HH30, when the nucleogenesis is complete, *cadherin 20* expression is restricted to AccAb only (Figure 3.11, B, C, F).Thus throughout the process of nucleogenesis in r5 *cadherin 20* expression is initially high in all MN's; 80.99 (±0.60) at HH20, but then this expression is refined to a subset of MN's which comprise the dFMN (Figure 3.11, D-E, Table 3.1). Thus the expression of *cadherin 20* in r5 is dynamic and it's restriction to the dFMN is key for the normal segregation of AccAb and dFMN neurons.

		HH20	HH24	HH29
% MN	**Islet+/Cad20+**	80.99 ±0.60	42.67 ±0.38	32.77 ±0.46

Table 3.1: Analysis of total *Cadherin 20* expression in all MN's of r5. Cadherin20 is initially expressed in 80.99% of all MN's at HH20. During nucleogenesis, as *cadherin 20* expression is refined, there is a concomitant decrease in total *cadherin 20* expression. Standard error is indicated (n=2).

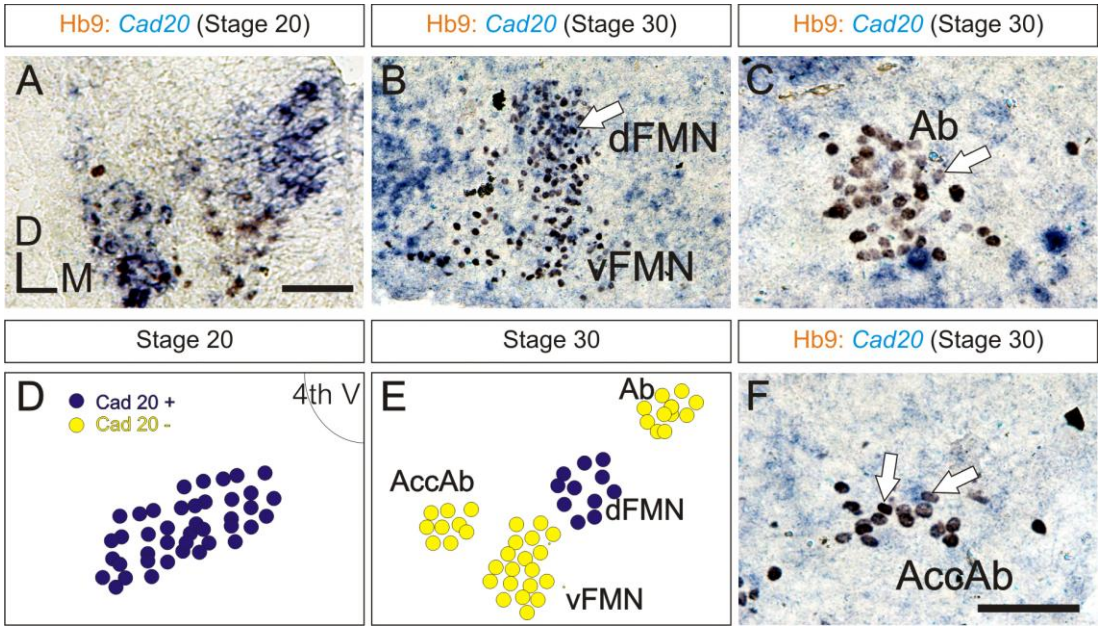

Figure 3.11: Analysis of *Cadherin 20* expression in r5 during nucleogenesis. **A:** Cadherin20 is initially expressed in 80.99% of all MN's at HH20. **B:** At HH30 *cadherin 20* expression is limited to the dFMN (arrow indicates *Cadherin 20* positive cells). **C:** *Cadherin 20* is not expressed in Ab at HH30 (arrow indicates *Cadherin 20* negative cells). **D-E:** *Cadherin 20*, initially expressed in a high proportion of r5 MN's at HH20 is later restricted to the dFMN by HH30. **F:** At HH30 *cadherin 20* is not expressed in AccAb. Scale bar 100µm.

In the r8 motor nuclei expression of Cadherins 6b and 13 was also assayed in the dorsal and ventral hypoglossal nuclei throughout development. At HH24 all the MN's of r8 are found in a mixed population close to the midline, analysis of *Hb9* and *cadherin 6b*/13 co expression shows that *cadherin 6b* is expressed in 16.09% of all *Hb9*+ MN's whilst cadherin 13 is not expressed (Figure 3.12, A,D, G). At HH27 as the nuclei are beginning to segregate into their final positions it is possible to differentiate between the two hypoglossal populations. Cadherin 13 is again absent from both divisions of the hypoglossal, however *cadherin 6b* expression increases. In the dorsal hypoglossal 69.33% of *Hb9*+ MN's express *cadherin 6b*, whilst in the ventral hypoglossal this percentage is lower at 21.21% (Figure 3.12, B, E, G). Thus the percentage of *Hb9*+/*cadherin 6b*+ MN's increases as nucleogenesis progresses, indicating an up regulation of *cadherin 6b* expression.

By HH29 motor nuclei of r8 have segregated and adopted their final positions within the hindbrain. At this stage both the ventral and dorsal hypoglossal express both cadherins 6b and 13. Interestingly ventral hypoglossal is found to express cadherin 13 in a ventrolateral subdivision only (Figure 3.12, F); the percentage of

Hb9+/cadherin 13+ MN's is just 30.26% which reflects this (Figure 3.12, G). Cadherin 13 is also expressed within 47.22% of the dorsal hypoglossal nucleus neurons; however this is not a spatially restricted expression pattern. *Cadherin 6b* expression decrease in the ventral hypoglossal to 54.23% when compared with HH27, whilst there is a concomitant increase in *cadherin 6b* expression in the dorsal hypoglossal to 52.19% of neurons compared with HH27 (Figure 3.12, C, G).

Thus within r8, as with r5, cadherin expression is dynamic within the motor neurons throughout nucleogenesis. In r8 *cadherin 6b* expression appears to fluctuate as the nuclei segregate from one distinct population from HH24-29, whilst cadherin 13 is not expressed within the hypoglossal until a time point between HH27-29. In r5 *cadherin 20* is expressed in all MN's and is refined to be expressed only in the dFMN, driving segregation between the FMN and the AccAb. In summary it is possible to suggest that cadherins, through their differential and dynamic expression, drive normal motor nucleogenesis in r5 and r8.

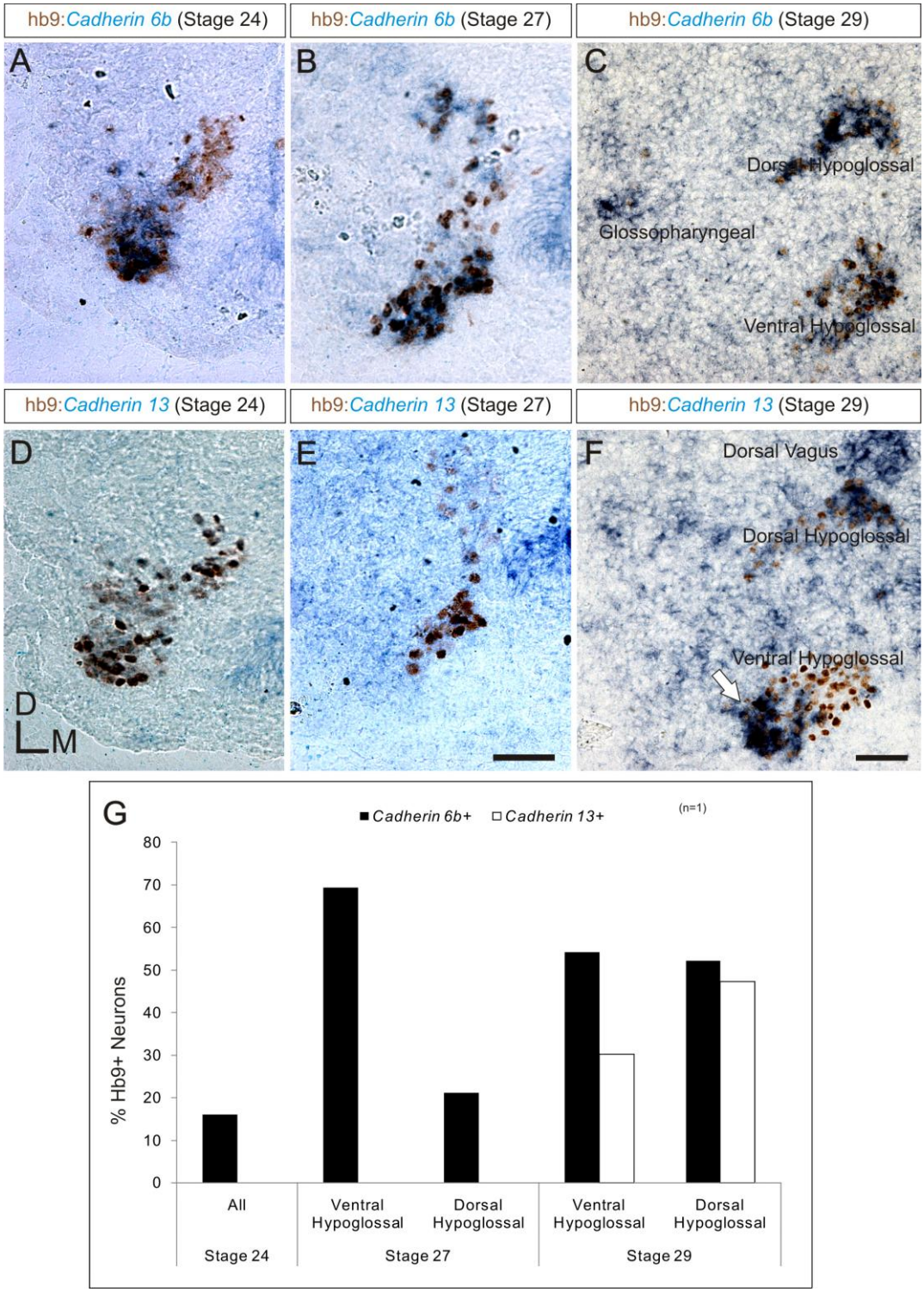

Figure 3.12: Analysis of Cadherin expression in r8 during hypoglossal nucleogenesis. **A:** Cadherin6b is initially expressed in a small number of *Hb9*+ SM neurons. **B:** At HH27 the two divisions of Hypoglossal are visible; *cadherin 6b* is highly expressed in ventral hypoglossal. Dorsal hypoglossal expresses *cadherin 6b*, but only in a small subset of neurons. **C:** *Cadherin 6b* is expressed in both Dorsal and Ventral Hypoglossal at HH29. **D-E:** Cadherin 13 is not expressed in r8 cranial motor nuclei at HH24 or HH27. **F:** By HH29 cadherin 13 is expressed in the Dorsal hypoglossal, but is restricted to a subset of neurons in ventral hypoglossal (arrow). **G:** Quantification of cadherin 13 and 6b expression in *Hb9*+ SM neurons during r8 nucleogenesis. Scale bar 100µm.

4. Fgf signalling in r5 cranial motor nucleogenesis

4.1 Fgf8 misexpression disrupts motor nucleogenesis in rhombomere 5

Cadherin expression in r5 and r8 motor nuclei appears to drive normal cranial motor nucleogenesis. Each of the nuclei studied here can be differentiated by its own differential cadherin expression profile which is established during nucleogenesis. Expression of certain cadherins is altered during development, for example the expression of *cadherin 20* in r5 which is initially found in all MN's but then refined to the dFMN only. What drives these dynamic changes in cadherin expression during nucleogenesis is currently unknown.

In the spinal cord combinatorial cadherin expression drives motor pool sorting and this combinatorial cadherin expression is mediated by certain transcription factors, which themselves are induced by exogenous factors. For example Haase et al. 2002 demonstrated that GDNF (Glial cell-line derived Neurotrophic Factor) expressed in the brachial plexus surrounding the spinal nerves is crucial for the expression of the ETS transcription factor Pea3. In the absence of GDNF spinal motor neurons fail to differentiate correctly and are perturbed in their positioning within the spinal cord (Haase et al. 2002). Importantly it is known that down regulation of Pea3 leads to defects in the expression of the Type II cadherins crucial for motor pool segregation (Livet et al. 2002). Taken together these studies suggest a model whereby GDNF expressed in the periphery acts to induce Pea3 expression in a subset of motor neurons which modulates cadherin expression crucial for motor pool sorting.

In the developing hindbrain it is possible that such an exogenous factor could induce the dynamic changes in cadherin expression which are crucial for motor nucleogenesis. Fgf8 presented itself as an ideal candidate molecule to drive this dynamic cadherin expression. Firstly there are two potential sources of Fgf8 for cranial motor neurons; the nucleus Laminaris and Magnocellularis both express Fgf8 within r5 providing a potential central Fgf8 source, also Fgf8 is highly expressed within the developing otic vesicle a region past which axons of the Ab, AccAb and FMN project in close proximity (Figure 4.1); FMN axons project through a large ventral exit point of the hindbrain passing immediately rostral to the otic vesicle, whilst Ab and AccAb axons project from a small ventral exit point (Guthrie,

2007). Secondly it is important to note that Fgf signalling alterations in r5 led to disruption of nL development with concomitant alterations in cadherin expression.

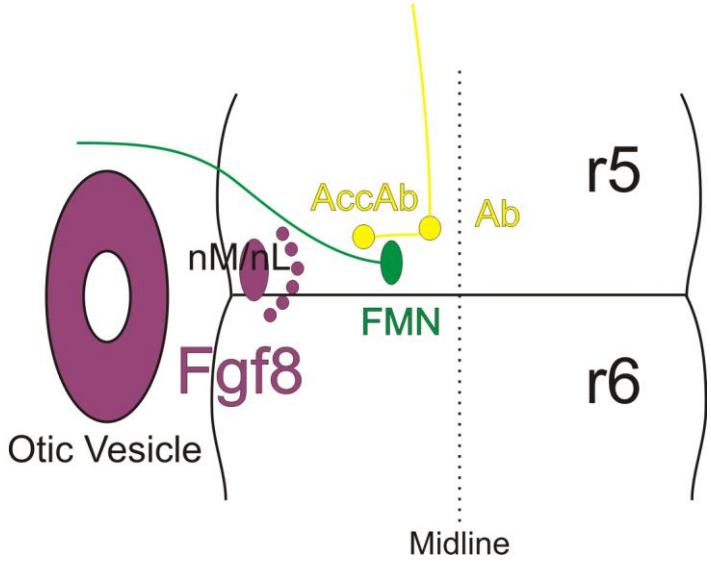

Figure 4.1: The otic vesicle and the auditory hindbrain nuclei provide peripheral and central sources of Fgf8 respectively.

In order to assess the potential impact of altering Fgf signalling levels on cranial motor nucleogenesis a murine Fgf8 (FGF8) construct was unilaterally driven into the hindbrain at HH18 via *in ovo* electroporation. The construct was co-electroporated with GFP to confirm successful tissue penetration (Figure 4.2, A, C). Analysis performed at HH30 shows that up regulation of Fgf signalling in this manner led to desegregation of motor nuclei in r5 only (Figure 4.2, B, D). Following mFfgf8 misexpression all MN's in r5 appear scattered and have formed no cohesive and distinct nuclei compared with control (Figure 4.2, B). However the motor nuclei of r8 remain intact following FGF8 misexpression, indicating that nucleogenesis has occurred normally (Figure 4.2, D).

Significantly this demonstrates that Fgf signalling is not acting to disrupt nucleogenesis in the hindbrain through gross morphological alterations, but is important in cranial nucleogenesis specifically in r5.

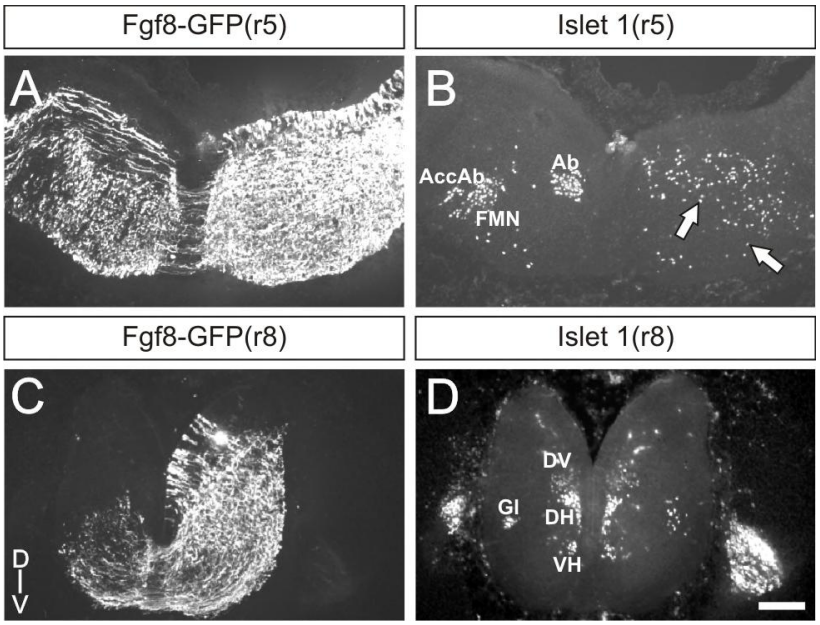

Figure 4.2: Fgf8 over expression disrupts motor nucleogenesis in r5, but not r8. **A:** GFP expression indicates successful electroporation. **B:** Following Fgf8 over expression the cranial motor nuclei fail to coalesce, MN's are scattered throughout r5 (indicated by arrows). **C:** Electroporation was also successful in r8. **D:** Development of r8 cranial motor nuclei appears unperturbed by Fgf8 over expression, when compared with control. DV: Dorsal Vagus. DH: Dorsal Hypoglossal. VH: Ventral Hypoglossal. GI: Glossopharyngeal. Scale bar 100µm.

4.2 Fibroblast growth factor receptors are expressed in cranial motor neurons throughout nucleogenesis in rhombomere 5

To investigate the potential role of Fgf signalling in r5 cranial motor nucleogenesis it was necessary to assay the expression patterns of members of the Fgf signalling pathway at various stages throughout development. Using *in situ* hybridisation the expression of FGFRs 1, 2 and 3 as well as Sprouty 4 in r5 cranial motor nuclei was characterised at HH35 (Figure 4.3). FGFR 4 was also assayed, but was not present in the r5 cranial motor nuclei (data not shown). FGFR1 is expressed in each nucleus; Abducens (Ab), Accessory Abducens (AccAb) and both dorsal and ventral Facial Motor Nuclei (dFMN, vFMN) (Figure 4.3, A). FGFR2 is expressed exclusively in dFMN (Figure 4.3, B), whilst FGFR3 is found in both dFMN and vFMN (Figure 4.3, C). As with FGFR1, Spry 4 is expressed in all 4 of the r5 motor nuclei. Thus at HH35 at least one FGFR is expressed in each nucleus and Fgf signalling appears to be active as demonstrated by Spry 4 expression (Summarised in Figure 4.3, E). FGFR's were not expressed in r8 cranial motor nuclei (data not shown).

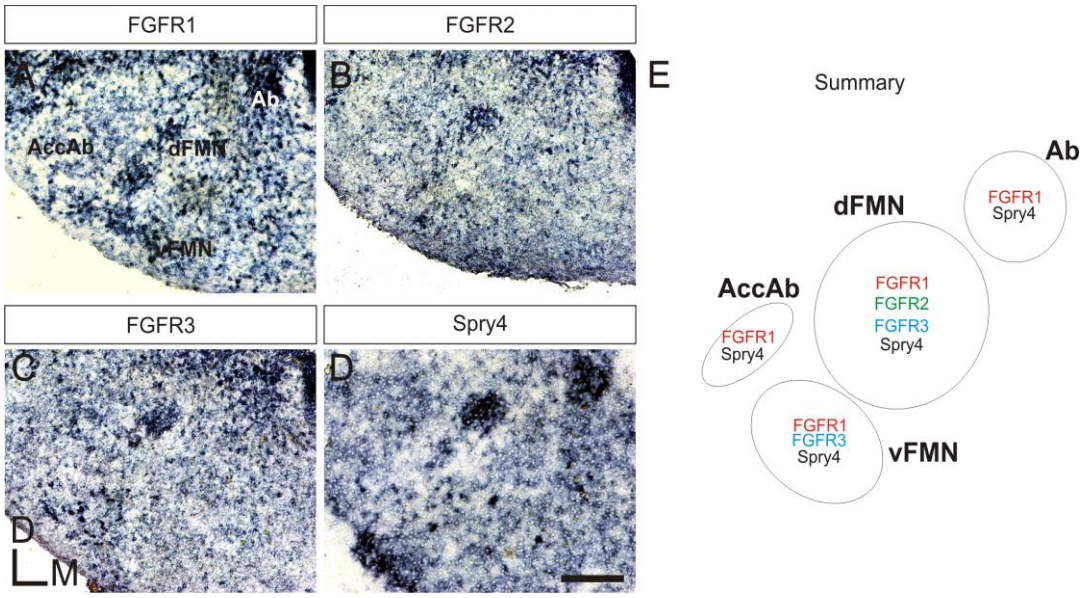

Figure 4.3: Fgf signalling pathway members found in cranial motor nuclei at HH36. **A-D:** The FGFR's 1,2 and 3 are differentially expressed in the cranial motor nuclei of r5. The downstream regulator of MAPK/ERK signalling Sprouty 4 (Spry4) is also expressed in all cranial motor nuclei in r5. **E:** Summary detailing the expression of each FGFR in each nucleus. Scale bar 100µm.

The segregation of Ab, AccAb, dFMN and vFMN occurs from HH26 to HH30 (Figure 3.1). If Fgf signalling is playing a role in nucleogenesis at r5 it would be predicted that the FGFRs and Spry 4 would be expressed prior to, and throughout, this process. As such expression of each FGFR and Spry 4 was analysed at HH25 and HH30 (Figure 4.4). Using *in situ* hybridisation coupled with antibody staining for Islet1 it is possible to quantify the percentage of r5 motor neurons which are expressing each receptor or Spry4; however it is not possible to differentiate between SM and BM populations.

At HH25 FGFR1 is expressed in 69.44% (±1.34) of Islet1+ MN's decreasing to 62.31% (± 0.03) by HH30 (Figure 4.4, A, H). Thus FGFR1 is expressed in a high proportion of MN's at HH25 and this expression is maintained through nucleogenesis to HH30 (Figure 4.4, E-G). FGFR1 is expressed in all of the nuclei, but not all MN's possibly due to overlapping expression of other FGFRs in BM neurons. FGFRs 2 and 3 are expressed at HH25 in a smaller percentage of MN's than FGFR1 (Figure 4.4, B, C, H). At HH30 FGFR2 is expressed in 53.76% (±1.83) of all MN's in r5, this is predicted as FGFR2 at HH35 is restricted to dFMN only. Similarly FGFR3 which is restricted to the dFMN and vFMN at HH35 is expressed in a smaller percentage of Islet1+ MN's at HH30; 45.86% (±5.13) (Figure 4.4, H).

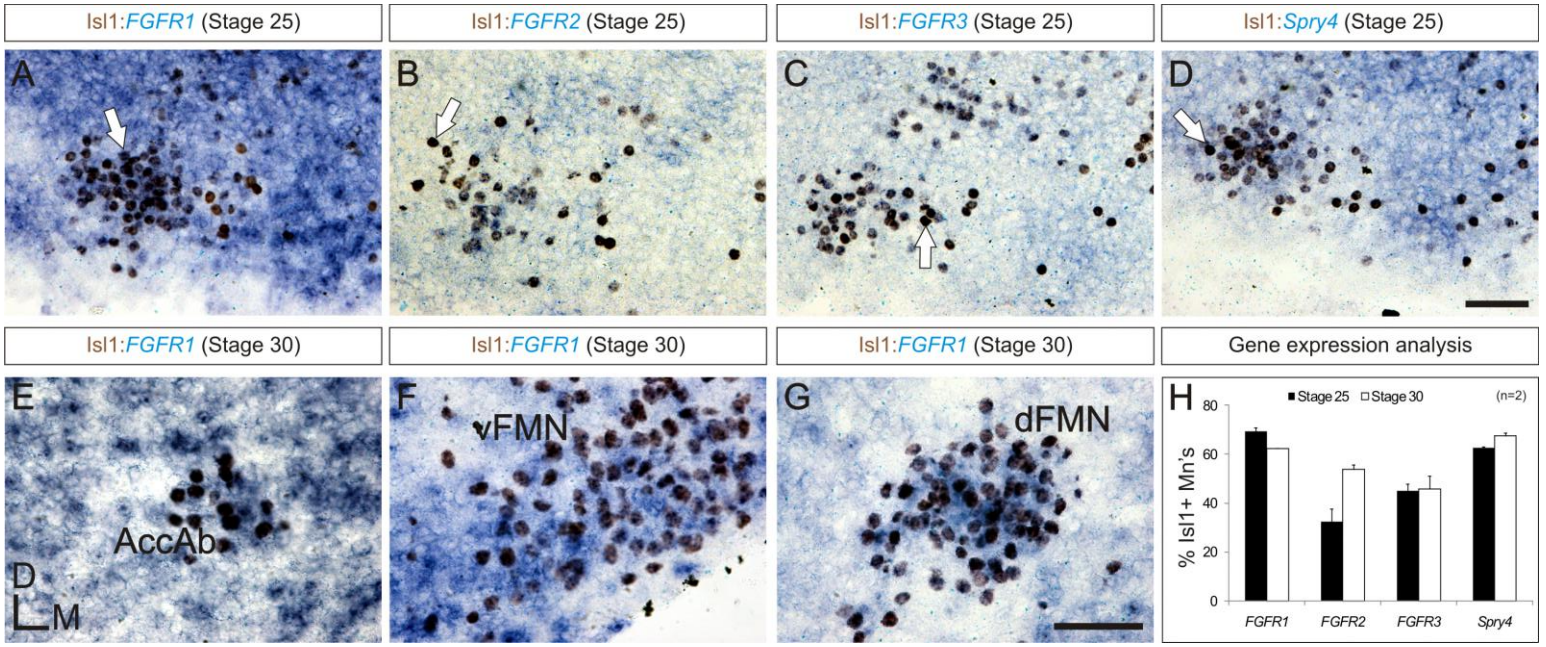

Figure 4.4: FGFR and Spry4 expression during r5 cranial motor nucleogenesis **A-D:** At HH25 all three FGFR's probed are expressed in the MN's, although in varying levels. Spry4 is also expressed in the MN's at HH25 (arrows indicate positively labelled neurons). **E-G:** Expression of FGFR1 is maintained in AccAb, vFMN and dFMN at HH30. **H:** Quantification of expression of each FGFR and Spry4 at HH25 and HH30. Error bars indicate standard error, (n=2). Scale bar 100µm.

Crucially Spry 4 is expressed in 62.20% (±0.37) of all r5 MN's at HH25 rising slightly to 67.39% (±1.27) by HH30 (Figure 4.4, H). Spry 4 is expressed in each of the r5 motor nuclei, but as with FGFR1, not all MN's. This may be due to the fact that Spry 4 is a negative feedback regulator of Fgf signalling and is expressed transiently in response to Fgf signalling; as such it may not be expressed in all MN's consistently. Taken together this data indicates that Fgf signalling is active at HH25 prior to nucleus segregation and is maintained throughout development until the nucleogenesis is complete.

4.3 Up regulation of the Fgf signalling pathway leads to desegregation of Accessory Abducens and dorsal Facial Motor Nuclei with concomitant alterations in *cadherin 20* expression.

Up regulation of Fgf signalling via FGF8 misexpression leads to motor nucleus desegregation in r5 (Figure 4.2), however this effect is not cell autonomous. To establish a role for Fgf signalling in cranial motor nucleogenesis the MAPK/ERK signalling pathway was targeted directly using aconstitutively active Raf construct (RafER). Fgf's signal through their receptors via the MAPK/ERK signal transduction pathway and a necessary activator in this intracellular signalling pathway is Raf. Raf is a MAP3K which once phosphorylated can activate MEK1 (Kyriakis et al,. 1992), leading ultimately to divergent cellular responses including gene transcription (Reviewed in Tsang et al. 2004). Raf presents an ideal target point for manipulation of this pathway. Using a Tamoxifen-inducible constitutively active Raf construct (RafER) it is possible to up regulate the MAPK/ERK pathway at any time point during development following *in ovo* electroporation (Samuels et al., 1994). As this Raf is constitutively active it cannot be inhibited by negative feedback involving Spry and thus acts to independently and consistently up regulate the pathway.

The RafER construct was driven unilaterally into the chicken embryonic hindbrain at HH18, and activated using Tamoxifen at HH22. GFP was used to confirm successful electroporations. At HH30 embryos were analysed using immunohistochemistry, to visualise mixing defects between SM and BM nuclei, and *in situ* hybridisation to investigate potential changes in the *cadherin 20* expression pattern.

Quantitation using the Neuronal Mixing Index (NMI) demonstrates that there is a significant increase in mixing between AccAb neurons and FMN neurons following RafER expression (Figure 4.5, D). Looking at Figure 4.5, B it is possible to identify *Hb9*+/Islet1+ neurons of the AccAb aberrantly positioned within the FMN (indicated by arrows). The percentage of AccAb neurons mixing with one FMN neuron increases from 10.81% (±2.75) in control to 26.29% (±3.82) (p=0.0125, Student's T-test) following RafER expression (Figure 4.5, D). Similarly there is a significant increase in the percentage of AccAb neurons found to be associated with two or more FMN neurons, demonstrating that the two nuclei have failed to segregate correctly. Importantly there is no difference in the total cell number of the AccAb between control and electroporated hemispheres (Figure 4.5, E).

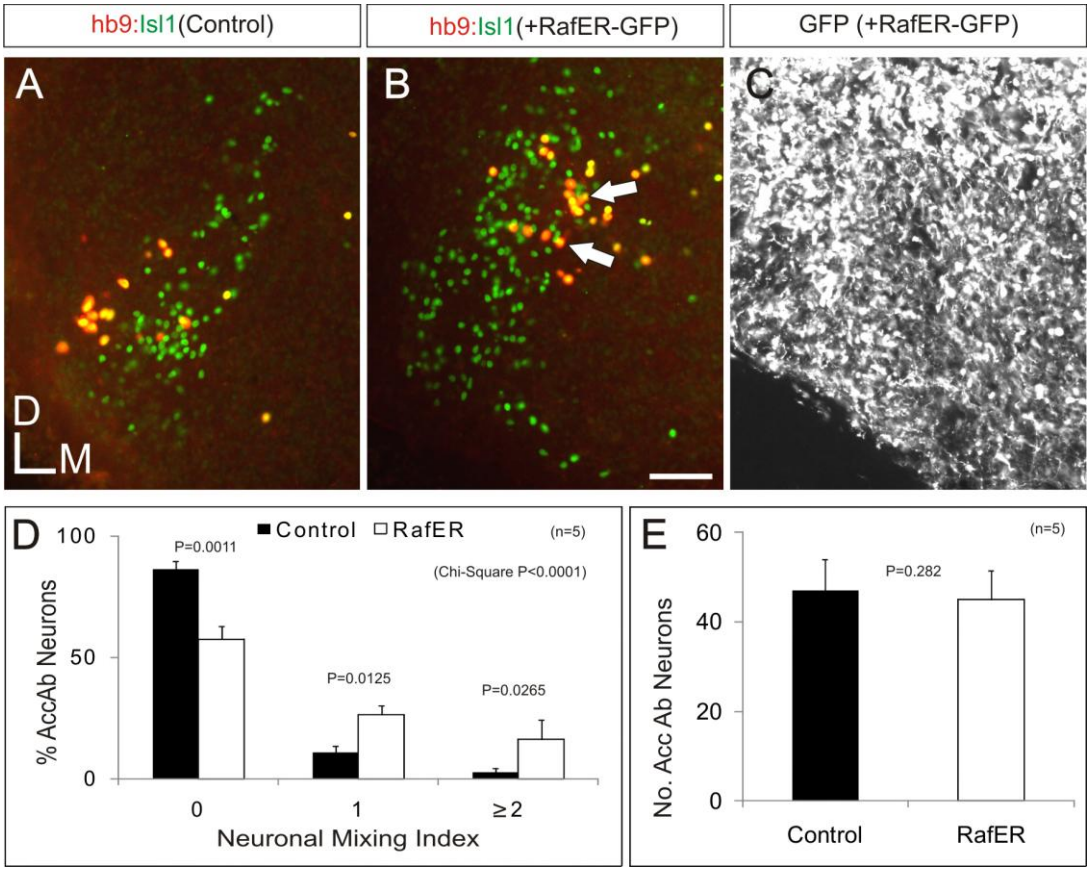

Figure 4.5: Up regulation of the MAPK/ERK signalling pathway using the RafER construct results in desegregation of the AccAb and dFMN. **A:** Isl1 and *Hb9* expression in control hemisphere showing AccAb (yellow) sitting lateral to the FMN. **B:** RafER electroporation results in failure of AccAb neurons to segregate from dFMN. AccAb neurons are visible mixed with FMN (indicated by arrows) **C:** GFP expression indicates successful electroporations. **D:** NMI analysis shows a significant decrease in the percentage of AccAb neurons which have coalesced with one another following RafER expression. **E:** There is not significant change in the number of AccAb neurons in r5 following RafER expression. Paired Student's T-test, error bars indicate standard error (n=5). Scale bar 100µm.

The phenotype identified following RafER expression is similar to that which is seen following both *Cadherin 20* and dn*Cadherin 20* misexpression (Figures 3.4 and 3.5). In each of those cases the AccAb and FMN fail to segregate as their differential cadherin expression profiles are normalised to one another. *Cadherin 20* is initially expressed in all r5 motor neurons, this expression is then refined to the dFMN only (Figure 3.11). In order to assess the potential impact of up regulating the MAPK/ERK signalling pathway analysis of *cadherin 20* expression following RafER expression was performed using *in situ* hybridisation coupled with antibody staining for either *Hb9* or Islet1 (Figure 4.5).

Following RafER expression the positioning of *Hb9*+ AccAb neurons is altered, as predicted based upon the NMI analysis, AccAb neurons are positioned medially in the location of the dFMN (Figure 4.6, G). Those *Hb9*+ AccAb neurons which are mispositioned are found to aberrantly express *cadherin 20* (Figure 4.6, H, indicated by arrows). Comparing *cadherin 20* expression in AccAb neurons following RafER expression with control reveals a 105.16% (±18.38) increase in the number of neurons expressing *cadherin 20* (Figure 4.6, E). There is also a 48.16% (±7.50) increase in the number of Ab neurons expressing *cadherin 20* (Figure 4.6, E) following RafER expression. This increase in *cadherin 20* expression in SM neurons is indicative that *cadherin 20* is not being down regulated following up regulation of the MAPK/ERK pathway in r5 MN's. As such the cadherin expression profiles of dFMN and AccAb are equalised and the nuclei fail to segregate normally. There is no difference in the number of SM neurons or indeed the total number of MN's as indicated by positive Islet1 staining (Figure 4.6, I, J).

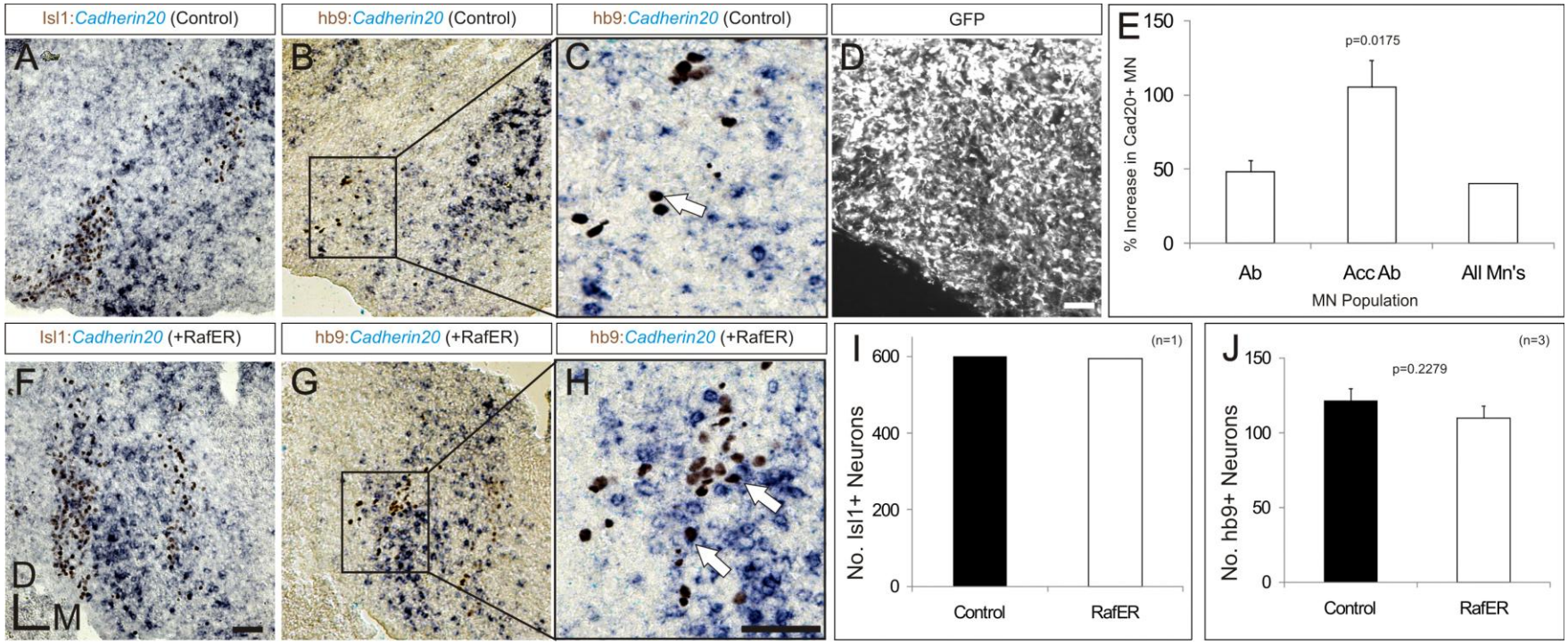

Figure 4.6: AccAb neuron positioning is altered following MAPK/ERK signalling up regulation. This is concomitant with an increase in *Cadherin 20* expression. **A-C:** Expression of *cadherin 20* in control hemisphere. *Cadherin 20* expression is restricted to the dFMN and is absent from the AccAb (magnified in C). **D:** GFP was used to confirm successful electroporations. **E:** *Cadherin 20* expression increases in all MN is compared with control. And is significantly increased in the AccAb, following MAPK/ERK signalling up regulation (n=3). **F-H:** *Hb9*+ AccAb neurons are positioned medially in the region of the dFMN and are found to aberrantly express *cadherin 20* (indicated by arrows in H). **I-J:** There is no significant difference in the total number of MN's (n=1) or the number of *Hb9*+ neurons (n=3) following RafER expression compared with control. Paired Student's T-test, error bars indicate standard error. Scale bar 100µm.

4.4 Down regulation of the Fgf signalling pathway also leads to desegregation of Accessory Abducens and dorsal Facial Motor Nuclei with concomitant alterations in *cadherin 20* expression.

Following up regulation of the MAPK/ERK signalling pathway, using the RafER construct, motor nucleogenesis is also disrupted as the SM and BM nuclei fail to segregate correctly. Tightly controlled Fgf signalling appears therefore to be crucial for normal nucleogenesis to occur. As a result it is reasonable to predict that down regulation of Fgf signalling in r5 motor neurons may also result in defects in nucleogenesis.

Down regulation of the Fgf signalling pathway was achieved using two DNA plasmid constructs via *in ovo* electroporation; a dominant negative FGFR1 (dnFGFR1) and a secreted form of FGFR3 (sFGFR3). Lacking its intracellular domain, dnFGFR1 inserts into the plasma membrane and binds Fgf's in the extracellular matrix; however downstream signalling is not initiated (Amaya et al., 1991). Unlike the RafER construct, this dnFGFR1 is non inducible. The sFGFR3 lacks its transmembrane domain and inserts into the plasma membrane, but is then secreted into the extracellular matrix where it sequesters Fgf8 protein, thus blocking Fgf8 from initiating its signalling pathway via the endogenous FGFRs (Fukuchi, 2001). As previously embryos were unilaterally electroporated at HH18 and analysed at HH30.

Following dnFGFR1 expression AccAb and FMN fail to segregate correctly; *Hb9*+ neurons of the AccAb are found to be mixed with the FMN (Figure 4.7, B). Analysis using the NMI reveals that the percentage of AccAb neurons which are isolated from the FMN drops to 50.44% (±5.02) compared to 90.26% (±5.15) ($p=0.0008$, Student's T-test) in control hemisphere following dnFGFR1 expression. The percentage of AccAb neurons found adjacent to at least one FMN neuron increases significantly to 26.23% (±3.08) following dnFGFR1 expression compared with 8.24% (±3.98) ($p=0.0079$, Student's T-test) in control hemisphere (Figure 4.7, D). There is no difference in AccAb cell number between electroporated and control hemispheres (Figure 4.7, E). It appears therefore that inhibiting the Fgf signalling pathway using the dnFGFR1 leads to desegregation of the AccAb and FMN as seen following up regulation of the MAPK/ERK pathway using the constitutively active Raf.

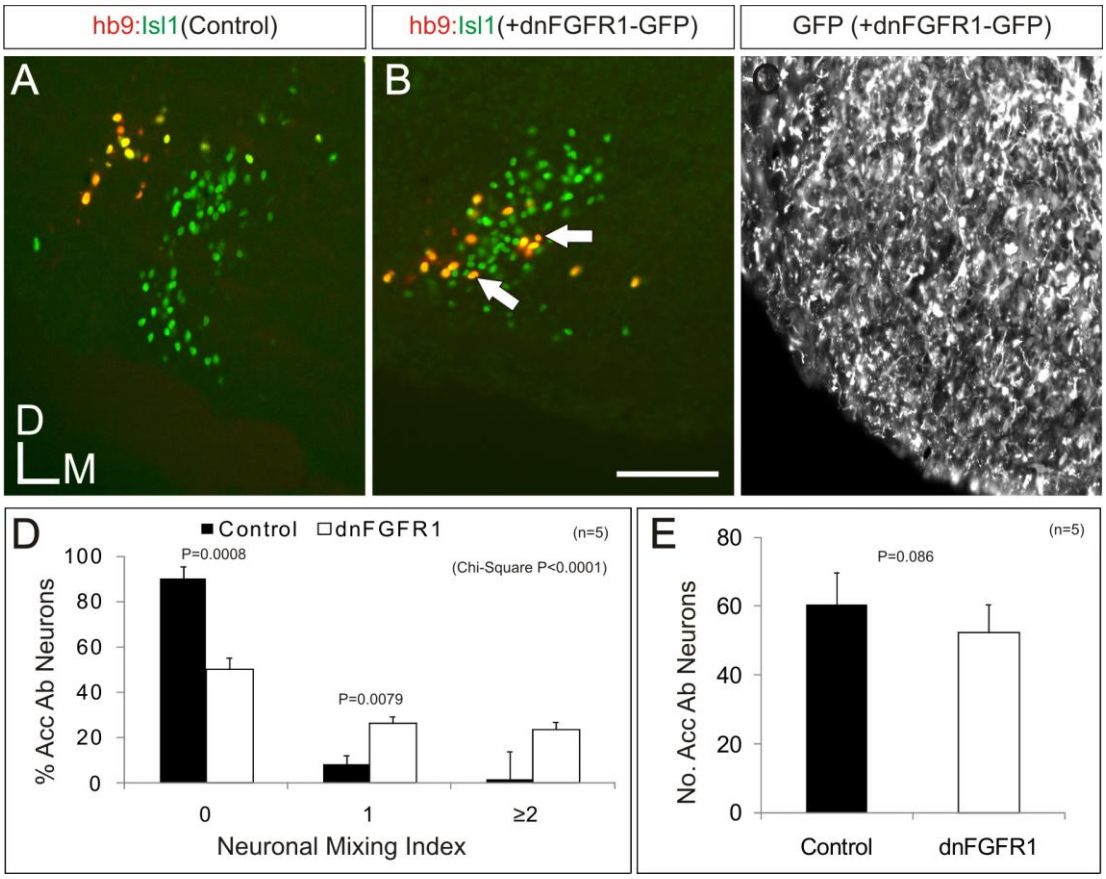

Figure 4.7: Down regulation of the Fgf signalling pathway using the dnFGFR1 construct results in desegregation of the AccAb and dFMN. **A:** Isl1 and *Hb9* expression in control hemisphere showing AccAb (yellow) sitting lateral to the FMN. **B:** dnFGFR1 electroporation results in failure of AccAb neurons to segregate from dFMN. AccAb neurons are visible mixed with FMN (indicated by arrows) **C:** GFP expression indicates successful electroporations. **D:** NMI analysis shows a significant decrease in the percentage of AccAb neurons which have coalesced with one another following dnFGFR1 expression. **E:** There is not significant change in the number of AccAb neurons in r5 following dnFGFR1 expression. Paired Student's T-test, error bars indicate standard error (n=5). Scale bar 100µm.

The failure of AccAb and FMN to segregate following MAPK/ERK signalling pathway up regulation is concomitant with increased *cadherin 20* expression in *Hb9*+ SM neurons (Figure 4.6). Following Fgf signalling down regulation via the dnFGFR1, the AccAb and FMN fail to segregate correctly. It is reasonable to predict, therefore, that *cadherin 20* would be aberrantly expressed in *Hb9*+ SM neuron following dnFGFR1 expression. Analysis of *cadherin 20* expression following dnFGFR1 expression reveals that *cadherin 20* is indeed highly expressed in *Hb9*+ AccAb neurons (Figure 4.8).

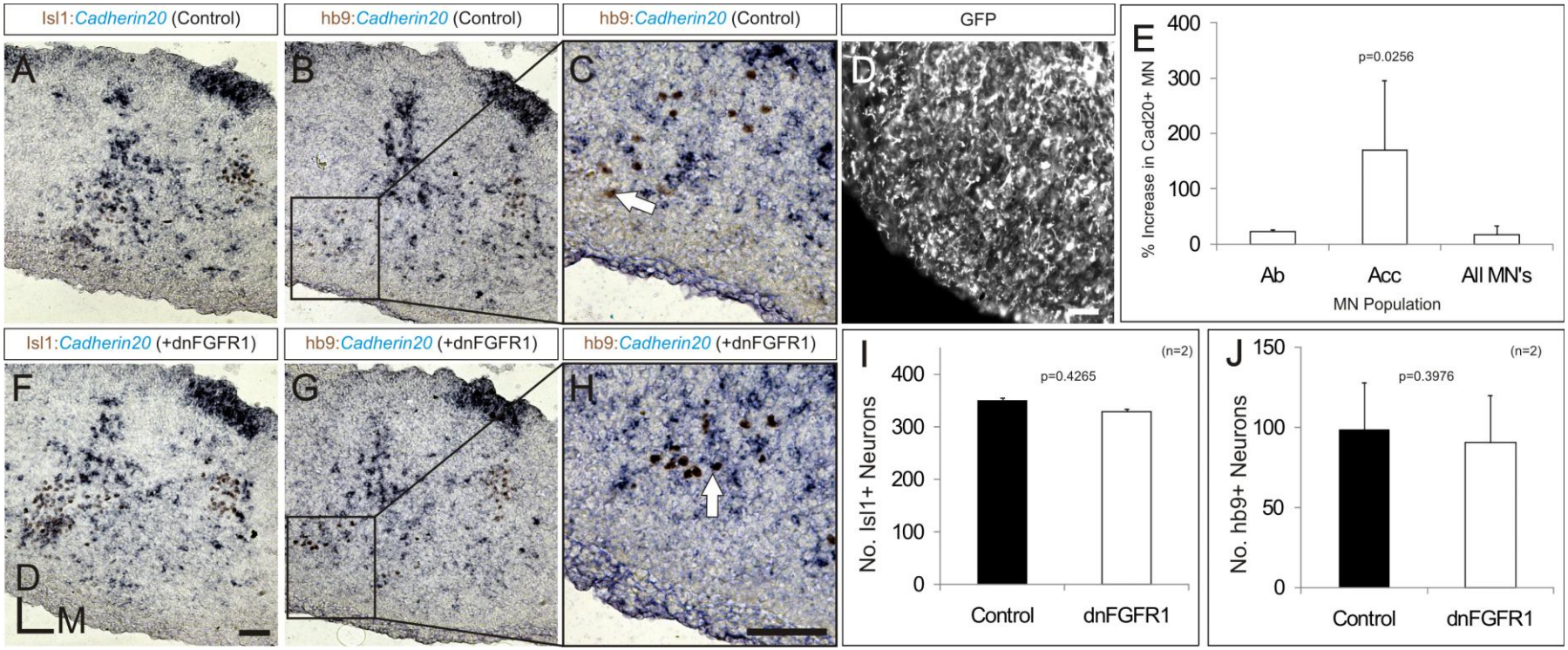

Figure 4.8: AccAb neuron positioning is altered following Fgf signalling pathway down regulation. This is concomitant with an increase in *Cadherin 20* expression. **A-C:** Expression of *cadherin 20* in control hemisphere. *Cadherin 20* expression is restricted to the dFMN and is absent from the AccAb (magnified in C). **D:** GFP was used to confirm successful electroporations. **E:** *Cadherin 20* expression increases in all MN are compared with control. Significantly in the AccAb, following Fgf signalling pathway down regulation (n=2). **F-H:** *Hb9*+ AccAb neurons are found to aberrantly express *cadherin 20* (indicated by arrows in H). **I-J:** There is no significant difference in the total number of MN's (n=2) or the number of *Hb9*+ neurons (n=2) following dnFGFR1 expression compared with control. Paired Student's T-test, error bars indicate standard error. Scale bar 100µm.

In control hemisphere *Hb9*+ AccAb neurons are located in the lateral aspect of the hindbrain, they do not express *cadherin 20* highly and are spatially segregated from the FMN (Figure 4.8, A, B, C). Following dnFGFR1 expression however *Hb9*+ neurons are positioned such that they are intermixed with the FMN neurons (Figure 4.8, F, G); those mispositioned *Hb9*+ neurons aberrantly express *cadherin 20* (Figure 4.8, H, indicated by arrows). Analysis of the number neurons expressing *cadherin 20* express reveals an increase of 169.92% (±126.29) (p=0.0256, Student's T-test) of *cadherin 20* positive AccAb neurons following dnFGFR1 expression (Figure 4.8, E). This is concomitant with an overall expected increase in *cadherin 20* expression of 16.5% (±8.62) in all r5 MN's (Figure 4.8, E). There is no difference in either total MN number as indicated by Islet1+ staining or in the number of SM neurons in r5 (Figure 4.8, I, J), demonstrating that the difference in cadherin expression levels is true and not an artefact of an increase in cell number following dnFGFR1 expression.

To test the integrity of this result a second down regulation of Fgf signalling was performed using the sFGFR3 isoform. The sFGFR3 sequesters available Fgf8 in the extracellular matrix thus inhibiting activation of the Fgf signalling pathway via the FGFRs. This provides a robust assay as it is non cell autonomous; it does not require MN's to be electroporated in order to mediate the desired effect.

Following sFGFR3 expression, consistent with the observed dnFGFR1 data, the AccAb and FMN fail to segregate correctly (Figure 4.9). *Hb9*+/Iset1+ neurons of the AccAb are visibly mixed with the dFMN and have failed to migrate to their stereotypical position lateral of the FMN (Figure 4.9, B). Quantification of this phenotype using the NMI assay reveals a significant increase in the percentage of AccAb neurons juxtaposed with at least one FMN neuron from 8.87% (±2.61) in control to 27.72% (±5.24) (p=0.0229, Student's T-test) following sFGFR3 expression (Figure 4.9, D). There is no difference in the number of AccAb neurons between control and sFGFR3 electroporated hemispheres (Figure 4.9, E).

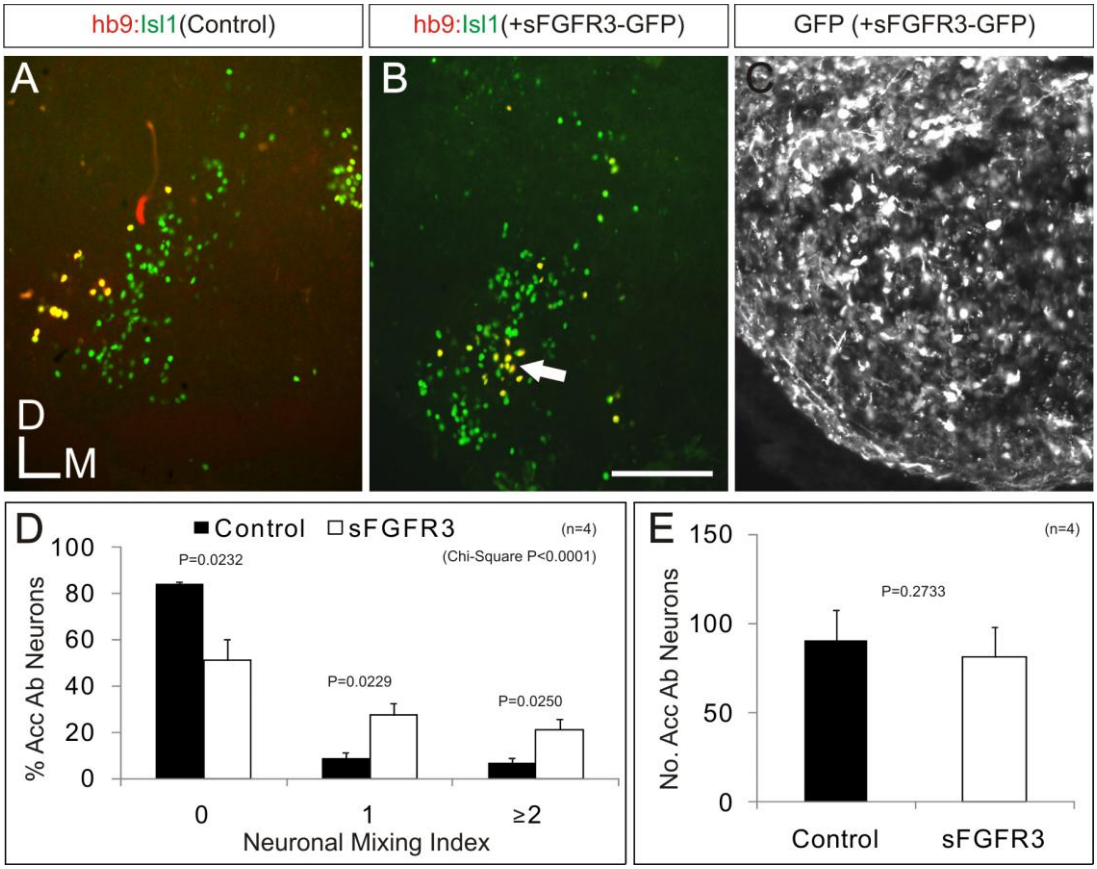

Figure 4.9: Down regulation of the Fgf signalling pathway using the sFGFR3 construct results in desegregation of the AccAb and dFMN. **A:** Isl1 and *Hb9* expression in control hemisphere showing AccAb (yellow) sitting lateral to the FMN. **B:** sFGFR3 electroporation results in failure of AccAb neurons to segregate from dFMN. AccAb neurons are visible mixed with FMN (indicated by arrows) **C:** GFP expression indicates successful electroporations. **D:** NMI analysis shows a significant increase in the percentage of AccAb neurons which have coalesced with one or more FMN neuron following sFGFR3 expression. **E:** There is not significant change in the number of AccAb neurons in r5 following sFGFR3 expression. Paired Student's T-test, error bars indicate standard error (n=4). Scale bar 100µm.

Cadherin 20 expression is increased in *Hb9*+ SM neurons following sFGFR3 expression; resulting in the desegregation of AccAb and FMN (Figure 4.10). AccAb neurons appear mispostioned relative to the FMN following sFGFR3 expression (Figure 4.10, F, G) when compared to the control hemisphere (Figure 4.10, A, B). This alteration in positioning is concomitant with a comparative increase in *cadherin 20* expression in AccAb neurons of 313.90% (n=1) compared with control (Figure 4.10, E) and a 50.00% increase in *cadherin 20* expression in the Ab. Thus it appears, as following Fgf signalling alterations using either the RafER or dnFGFR1

constructs, that *cadherin 20* expression is aberrantly maintained in SM neurons throughout nucleogenesis leading to AccAb and FMN desegregation.

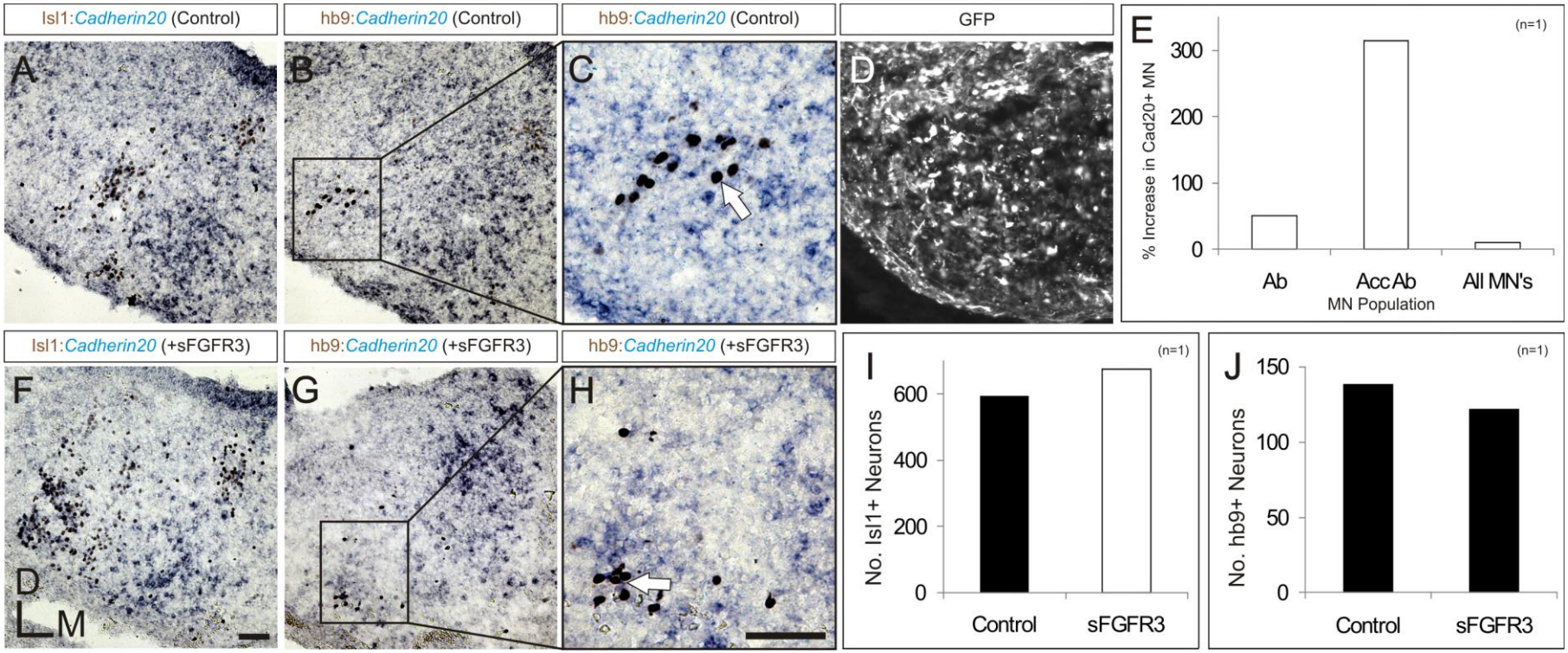

Figure 4.10: AccAb neurons aberrantly express *cadherin 20* following Fgf signalling pathway down regulation using the sFGFR3 construct. **A-C:** Expression of *cadherin 20* in control hemisphere. *Cadherin 20* expression is restricted to the dFMN and is absent from the AccAb (magnified in C). **D:** GFP was used to confirm successful electroporations. **E:** *Cadherin 20* expression increases in all MN are compared with control. The greatese increase is seen in the AccAb, following Fgf signalling pathway down regulation (n=1). **F-H:** *Hb9*+ AccAb neurons are found to aberrantly express *cadherin 20* (indicated by arrows in H). **I-J:** There is no significant difference in the total number of MN's (n=1) or the number of *Hb9*+ neurons (n=1) following RafER expression compared with control. Scale bar 100µm.

4.5 Strictly controlled Fgf signalling is required for normal motor nucleogenesis in r5

Disruptions in normal Fgf signalling leads to desegregation of the AccAb and dFMN, these two populations remain mixed and AccAb fails to migrate and coalesce in its usual position lateral to the FMN. This desegregation appears to be concomitant with an increased number of AccAb neurons expressing *cadherin 20* compared with control. This increased *cadherin 20* expression normalises the differential cadherin expression profiles between AccAb and dFMN which would otherwise drive their segregation.

This data suggests a model for nucleogenesis in r5 whereby differential cadherin expression profiles drive the segregation of MN's into their distinct nuclei. In the case of the AccAb and dFMN this segregation is driven specifically by the down regulation of *cadherin 20* in AccAb neurons. Up or down regulation of Fgf signalling leads to a failure of *cadherin 20* down regulation in AccAb neurons and subsequent defects in nucleogenesis. Thus a strictly controlled level of Fgf signalling appears to be crucial for cadherin driven motor nucleogenesis in r5 (Figure 4.11).

Interestingly there is no change in development of the abducens nucleus (data not shown), following Fgf signalling disruption. This is consistent with a model whereby Fgf signalling specifically refines the expression of cadherins within AccAb and FMN neurons as they migrate laterally to their final positions, as the Ab nucleus does not normally follow this tangential migration pathway, but instead these neurons settle in position immediately juxtaposed to their exit point from the ventricular zone (see discussion).

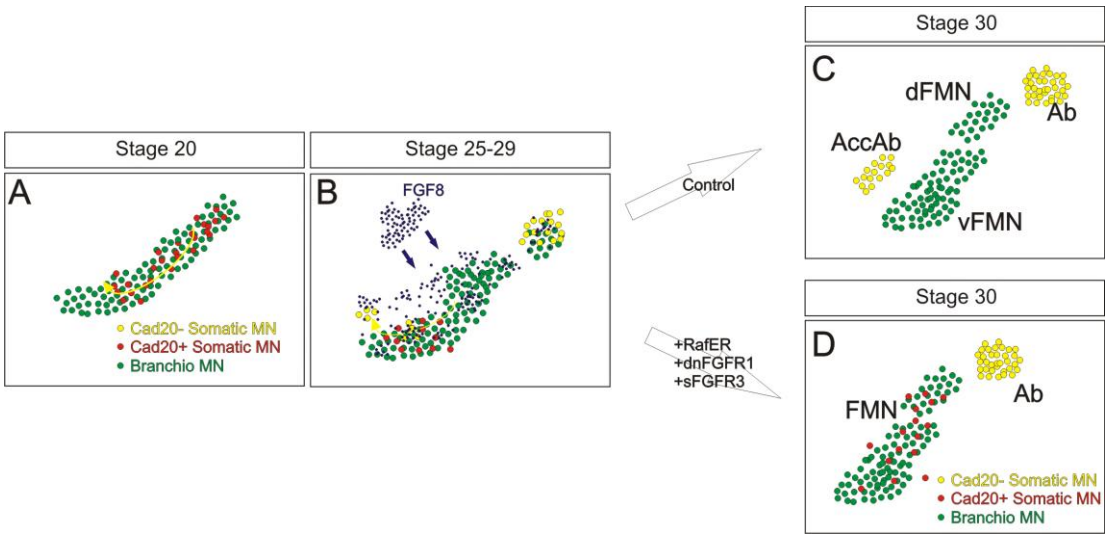

Figure 4.11: A model for nucleogenesis in r5, driven by Fgf regulated cadherin expression. A: At HH20 Cad20+ SM neurons are mixed with a Cad20+ BM population. B: Between HH25-29 exposure to Fgf8 results in a gradual decrease of Cad20 expression in the SM neurons as they migrate through the BM neurons of the FMN. C: This refinement of *cadherin 20* expression to the dFMN results in segregation of the AccAb. Nucleogenesis occurs as normal if the levels of MAPK/ERK signalling are unaltered. D: Up or down regulation of the Fgf/MAPK/ERK signalling pathway leads to a failure of cadherin refinement in MN's. SM neurons of the AccAb continue to express *cadherin 20* leading to desegregation of the nuclei.

5. Cadherins and Fgfs in the auditory hindbrain.

5.1 Cadherin expression in the auditory hindbrain.

The development of auditory cranial nuclei has been extensively studied however, little is known of the molecules which drive nucleogenesis in this region. Cadherins appear to drive cranial motor nucleogenesis in r5 (Chapter 3) and as such present an ideal target for investigation of auditory nucleus development. A comprehensive *in situ* hybridisation analysis of cadherin expression in the auditory hindbrain nuclei was performed and at least three members of the classical cadherin subfamily were found to be expressed here.

Cadherins 22, 13 and *N-cadherin* are all expressed in the nL (Figure 5.1). These cadherins are found to be expressed throughout auditory hindbrain development from HH29 onwards (Astick, 2007; Smith, 2011) as part of the auditory anlage. Expression of *cadherins 22* and *13* is restricted to nL upon segregation of the neurons into distinct nuclei.

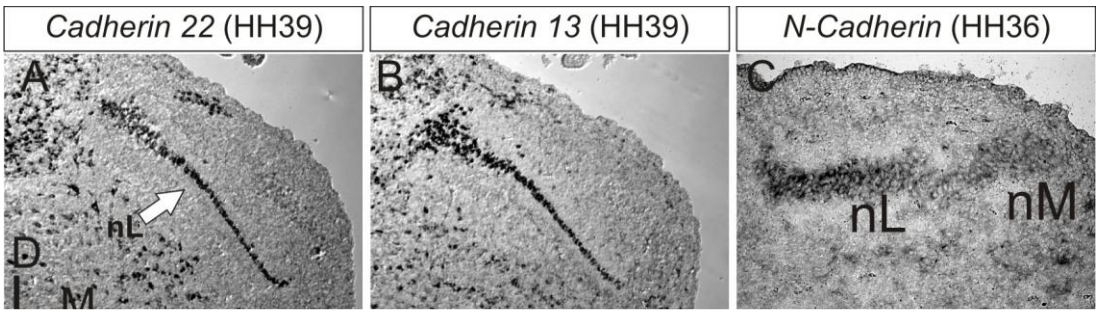

Figure 5.1: Cadherin expression in the auditory hindbrain. **A-b:** Cadherins 22 and 13 respectively are expressed in nL only (HH39). **C:** N Cadherin is expressed in both nL and nM (HH36)

5.2 Fgf, Spry4 and FGFR expression in the auditory hindbrain

Given that Fgf signalling appears to be important in cranial motor nucleogenesis, potentially acting to modulate cadherin expression, it is possible that a similar mechanism could be utilised by the auditory hindbrain nuclei of r5. Analysis using in situ hybridisation shows that *Fgf*8 is expressed within both nL and nM (Figure 5.2), marking both as potential sources of *Fgf*8 within r5. Significantly Fibroblast Growth Factor Receptors (*FGFR*) 1 and 2 are also expressed within this region at HH36, as well as the downstream inhibitor of the Fgf signalling pathway, Sprouty 4 (*Spry 4*)

(Figure 5.2). This suggests that Fgf signalling is active in this region throughout nL-nM development. Taken together with the data from section 5.1, this indicates that both Fgf signalling and cadherins could potentially be involved in nL-nM development and as such present ideal targets for manipulation.

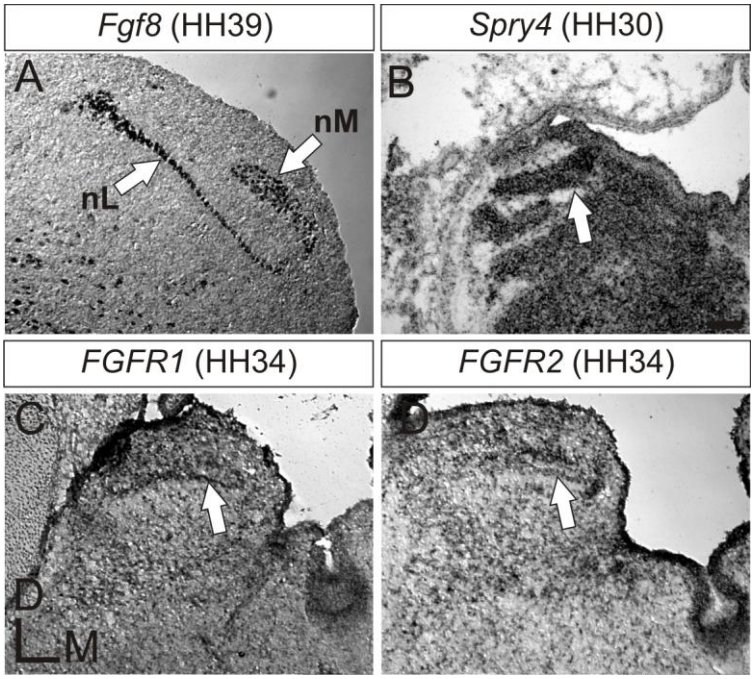

Figure 5.2: *Fgf*, *Spry4* and *FGFR* expression in the auditory hindbrain **A:** *Fgf*8 is expressed in both nL and nM. **B:** *Spry4* is expressed in the developing nL. **C-D:** *FGFR*'s 1 and 2 are expressed in the developing nL.

5.3 Up regulation of the Fgf signalling pathway causes defects in normal auditory hindbrain development.

The cells which constitute nL differentiate around HH21-23 whilst the cells of nM differentiate slightly earlier around HH17-19 (Cramer et al., 2000). The chicken embryonic hindbrain around HH18-20 is readily accessible for genetic manipulation via *in ovo* electroporation.

Utilising this technique a DNA plasmid construct containing the murine *Fgf*8 (m*FGF*8) cDNA protein coding region (the murine and chick *Fgf*8 genes retain a high sequence homology, particularly within the protein regulatory region, Haworth et al., 2005) was driven unilaterally in combination with a GFP plasmid constuct in to the r5 target region at HH18. Electroporated cells secrete m*FGF*8 protein increasing the amount of *Fgf*8 found in the extracellular matrix and subsequently up regulating Fgf signalling (Mahmood et al., 1995).

The expression of endogenous *Fgf*8, *cadherin 22* and *cadherin 13* in r5 was assayed and analysed at HH34 using *in situ* hybridisation following electroporation (Figure 5.3). At HH34, nL and nM are near to segregation and nL begins to develop its characteristic linear appearance (Figure 5.3, A). The average number of cells found to be expressing *Fgf*8 upon over expression of m*FGF*8 is significantly reduced from 151.2 (±22.0) to 67.7 (±11.4) (p= 0.0106, Student's T-test) per section (Figure 5.3, G), those cells which are *Fgf*8 positive do not coalesce to form a coherent structure (Figure 5.3, B). Reduction in endogenous *Fgf*8 expression may be due to the negative feedback loop known to regulate *Fgf*8 expression; increased MAPK/ERK pathway signalling leads to the induction of Spry 2 and 4 which act to inhibit *Fgf*8 production (Hanafusa et al., 2002; Fürthauser et al., 2001).

In the control hemisphere at HH34 cadherins 22 and 13 are found to be expressed in fewer cells compared with *Fgf*8 (Figure 5.3, G). Given that later in development *cadherin 22* and 13 are restricted to nL only, this indicates that their expression could be restricted to presumptive nL cells prior to nL-nM segregation. Upon over expression of m*FGF*8 the average number of cells expressing *cadherin 22* rises significantly from 93.1 (±15.6) to 144.1 (±20.4) (p=0.0087, Student's T-test) per section, indicating that a greater proportion of neurons may be expressing *cadherin 22*; expression is not restricted to a subset. The *cadherin 22* positive cells fail to coalesce into a single nucleus, but are scattered throughout the hindbrain (Figure 5.3, D).

Interestingly the mean number of *cadherin 13* positive cells per section decreases from 68 (±9.3) to 15.3 (±4.8) (p=0.0001, Student's T-test) when compared with control (Figure 5.3, F-G). *Cadherin 13* positive cells are sparse within r5 following m*FGF*8 over expression and do not form any cohesive groups. Using *cadherin 22* and 13 as potential markers for nL neurons this data suggests that nL has failed to develop correctly. The characteristic linear arrangement of nL as marked by *Fgf*8 or cadherin expression is absent, and number of cells expressing *cadherin 13* or 22 are altered. Changes in the number of *Fgf*8 positive cells are indicative of endogenous *Fgf*8 expression inhibition, however *Fgf*8 itself cannot be considered a reliable marker for nL or nM neurons in this case as its expression will be altered by up of down regulation of the Fgf signalling pathway as part of the *Fgf* synexpression group.

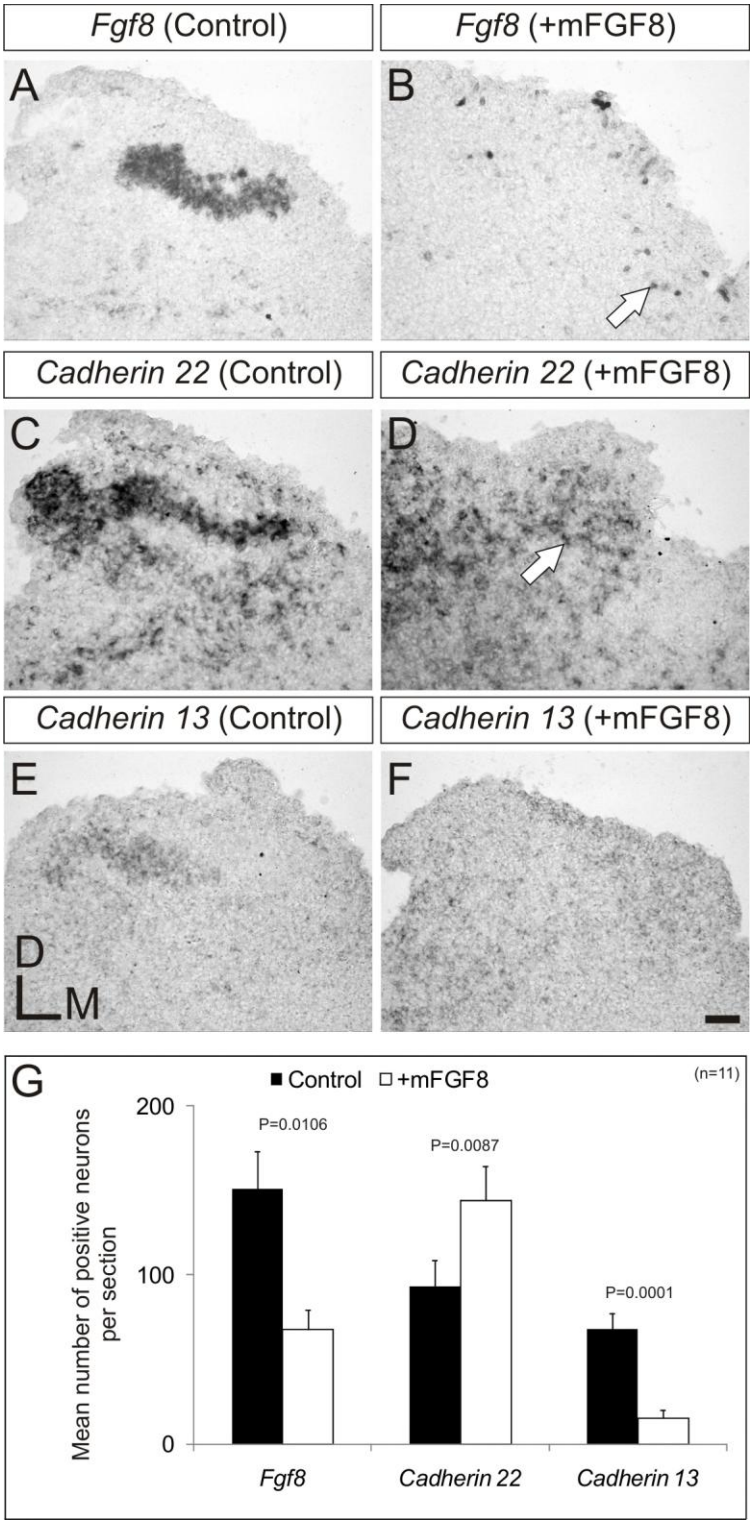

Figure 5.3: Expression of *Fgf*8, *cadherin 22* and 13 is altered, at HH34, following Fgf signalling up regulation via m*FGF*8 misexpression.

A: *Fgf*8 positive cells of the nL and nM are clearly visible in a linear conformation in the dorso-lateral region of the hindbrain.

B: *Fgf*8 positive cells are scattered following m*FGF*8 electroporation (indicated by arrows).

C: *Cadherin 22* expression in nL of the control hemisphere.

D: Cells expressing *cadherin 22* appear partially scattered throughout the hindbrain following m*FGF*8 expression. The distinctive laminar structure of nL is absent.

E: *Cadherin 13* expression is restricted to a sub population within nL in control.

F: The number of cells expressing *cadherin 13* appears severely reduced following m*FGF*8 expression.

G: Quantification of the number of cells expressing each marker gene per section. Paired Student's T-test, error bars indicate standard error. (n=11).

As over expression of m*FGF*8 leads to failure of nL and nM to develop correctly, it is reasonable to predict that up regulation at any point on the MAPK/ERK signalling pathway should lead to similar disruptions in normal auditory hindbrain development.

Embryos were electroporated with the RafER construct at HH18 and Tamoxifen added at HH23, by which stage the neurons of nL and nM have differentiated. At HH29 the auditory anlage is established as a mixed population of nL and nM neurons. *Fgf*8 and *cadherin 22* are highly expressed in this area (Figure 5.4, A, C) whilst a small number of cells are also found to express *cadherin 13* (Figure 5.4, E).

Following RafER misexpression the number of *Fgf*8 positive neurons is unilaterally significantly decreased ($p=0.0332$, Student's T-test), however there remains a small cluster of neurons in the "correct" position within the hindbrain (Figure 5.4, B, G). There is no difference in the number of neurons expressing *cadherin 22* between electroporated and control hemispheres (81.75 ± 9.0 and 81 ± 14.2 respectively). There is a clear cohesive group of *cadherin 22* positive cells found in the dorso-lateral aspect of the hindbrain (Figure 5.4, D, G). Additionally, the average number of cells expressing *cadherin 13* following RafER electroporation decreases); this decrease is not statistically significant (Figure 5.4, F, G).

The presence of *Fgf*8 and *cadherin 22* positive clusters of neurons in the position of the auditory anlage suggests that early development of the auditory anlage may have occurred, following RafER electroporation. Potentially this may suggest role whereby Fgf signalling and cadherin expression in nL development is important during segregation and maturation of the nuclei as opposed to early neuronal survival and migration. However, a great deal more evidence would be required to support this.

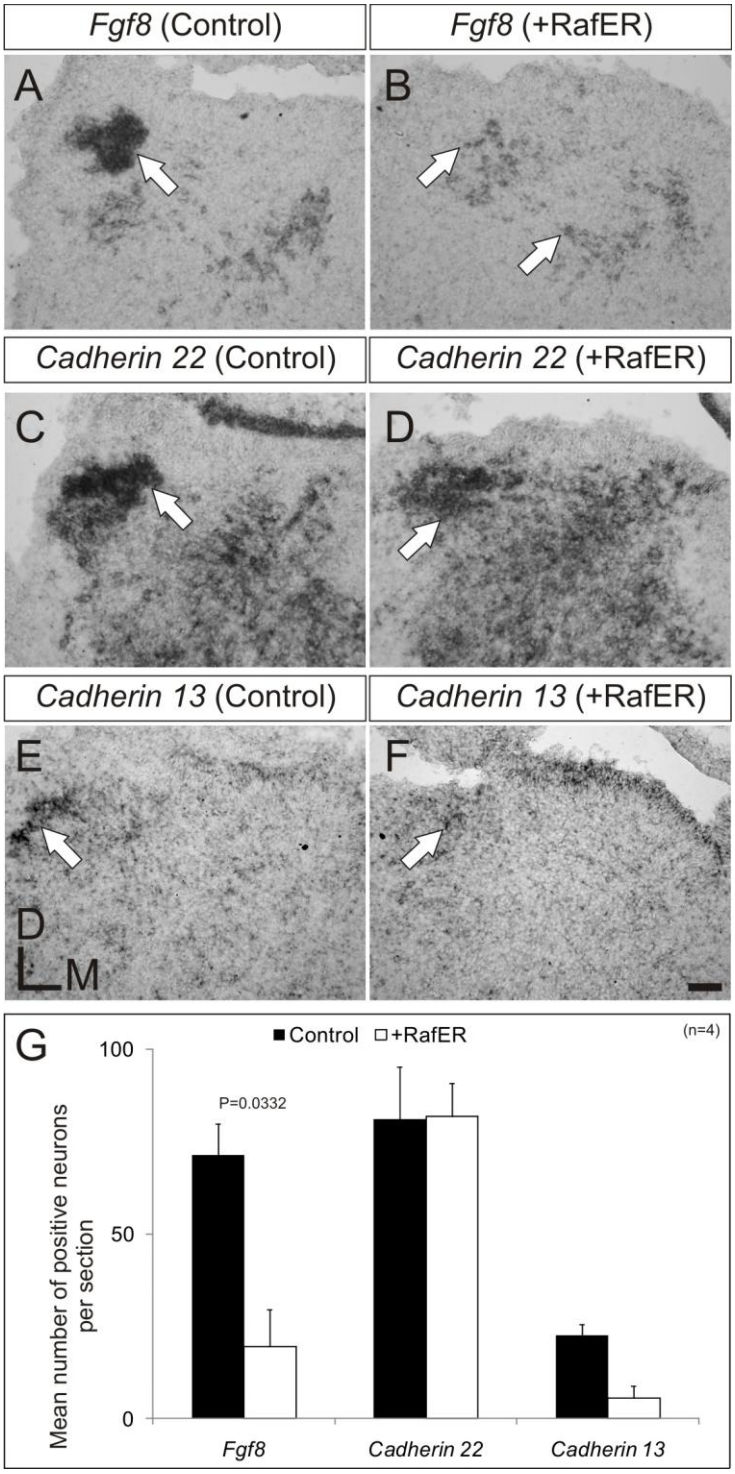

Figure 5.4: Expression of *Fgf*8, *cadherin 22* and 13 at HH29 following MAPK/ERK signalling up regulation via RafER expression.

A: The auditory anlage is visible as a small cluster of *Fgf*8 positive cells in the dorsal region of the hindbrain (indicated by an arrow).

B: *Fgf*8 positive cells are reduced in number and appear scattered following RafER electroporation (indicated by arrows).

C: *Cadherin 22* is expressed in the auditory anlage at HH29.

D: Following RafER expression there remains a cluster of *cadherin 22* positive cells in the dorso-lateral region of the hindbrain (indicated by arrows).

E: There is a small population of *cadherin 13* positive cells found in the auditory anlage.

F: This population of *cadherin 13* positive cells appears to decrease in number following RafER expression; however a small cluster of cells does remain (indicated by arrows).

G: Quantification of the number of cells expressing each marker gene per section in both control and electroporated hemispheres. Paired Student's T-test, error bars indicate standard error. (n=4).

In order to investigate this further, RafER was induced at HH28 immediately prior to auditory anlage formation. Analysis of *Fgf*8 expression at HH34 shows that the the number of neurons expressing *Fgf*8 following RafER misexpression drops from 74.4 (±12.6) to 13.5 (±6.1) per section compared with control (Figure 5.5, C). However a small cluster of *Fgf*8 positive neurons remains in the dorso-lateral aspect of the hindbrain (Figure 5.5, B). This cluster is smaller than, and does not take on the linear appearance of, the developing nL-nM at HH34 (Figure 5.5, A). This suggests that the nL-nM neurons have coalesced into the auditory anlage, but further development and segregation of both nuclei has failed to occur as a result of up regulating MAPK/ERK signalling. The timing of exposure to *Fgf*8 as well as the level of *Fgf* driven MAPK/ERK signalling therefore appear to be significant for cadherin refinement accompanying normal nL-nM development to occur.

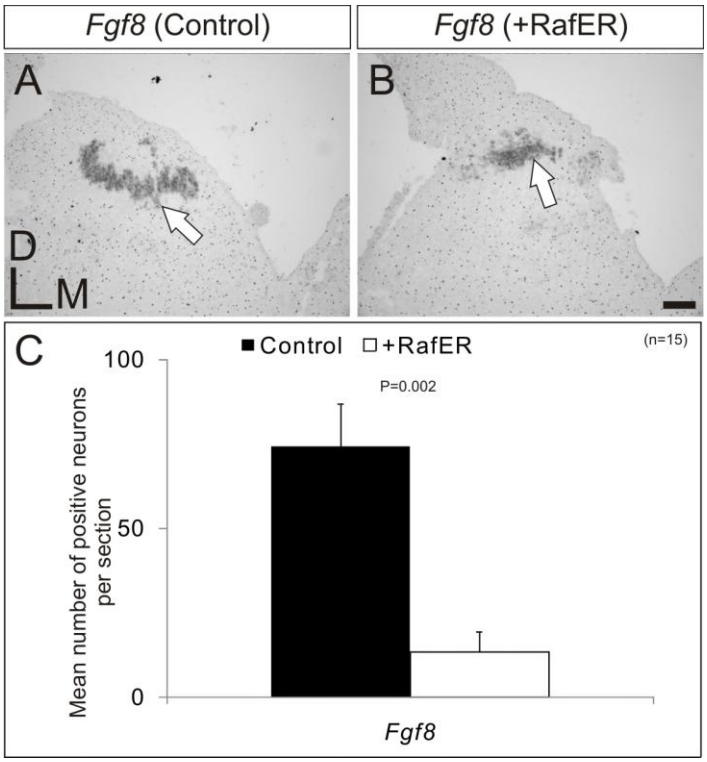

Figure 5.5: Expression of *Fgf*8 at HH34 following RafER induction at HH28, immediately prior to auditory anlage coalescence. **A:** *Fgf*8 positive cells of the nL and nM are clearly visible in the dorso-lateral hindbrain (indicated by an arrow). **B:** Following RafER expression there remains a small cluster of *Fgf*8 positive cells in the dorso-lateral aspect of the hindbrain (indicated by an arrow). **C:** Quantification of the number of *Fgf*8 positive cells in control and following up regulation of the MAPK/ERK signalling pathway via RafER expression. Paired Student's T-test, error bars indicate standard error. (n=15).

5.4 Down regulation of the Fgf signalling pathway also causes defects in normal auditory hindbrain development.

In order to assess the effect of down regulating Fgf signalling on auditory nucleogenesis the dominant negative FGFR1 (dnFGFR1) construct was used. Embryos were electroporated at HH18 and analysed at HH31.

There is a significant decrease in the number of neurons expressing *Fgf*8 per section following dnFGFR1 expression compared with control ($p=0.0477$, Student's T-test) (Figure 5.6, E). Furthermore, those neurons which are *Fgf*8 positive following dnFGFR1 expression are scattered and do not coalesce into a distinct nucleus (Figure 5.6, B). There is no significant change in the number of *cadherin 22* positive neurons following dnFGFR1 expression (52.4±12.64) compared with control (31±26.1) per section (Figure 5.6, E). However as with *Fgf*8 positive neurons, *cadherin 22* positive neurons appear scattered following dnFGFR1 expression (Figure 5.6, D). The apparent down regulation of endogenous Fgf expression following dnFGFR1 expression is potentially due to two factors; either the neurons which constitute the auditory hindbrain are missing or expression of Fgf8 is dependant itself upon Fgf signalling from another source as part of the Fgf syn-expression group. Lacking a reliable nL/nM marker, it is impossible to correctly attribute this effect to one or other circumstance.

Together, both up and down regulation of Fgf signalling via the MAPK/ERK signalling pathway results in disruption in normal nL-nM development. This data is summarised in Figure 5.7; At HH29 neurons of the presumptive nL and nM coalesce in a mixed population (the auditory anlage). *Cadherin 22* is highly expressed in this region whilst *cadherin 13* is also expressed in a small number of cells. Subsequently, the auditory anlage alters its shape and begins the process of segregation into two distinct nuclei (HH29-34). This process is accompanied by proportional decrease in relative *cadherin 22* and increase in *cadherin 13* expressions.

Altering the levels of Fgf signalling in r5 using m*Fgf*8, RafER or dnFGFR1 constructs, leads to defects in nL and nM development. *Cadherin 22* expression does not decrease, whilst *cadherin 13* expression levels remain low. Those cadherin positive neurons which do remain fail to develop into the distinct linear structure of nL, but are scattered or remain in a cluster similarly positioned to the auditory anlage. Suggesting that normal nL development has been disrupted.

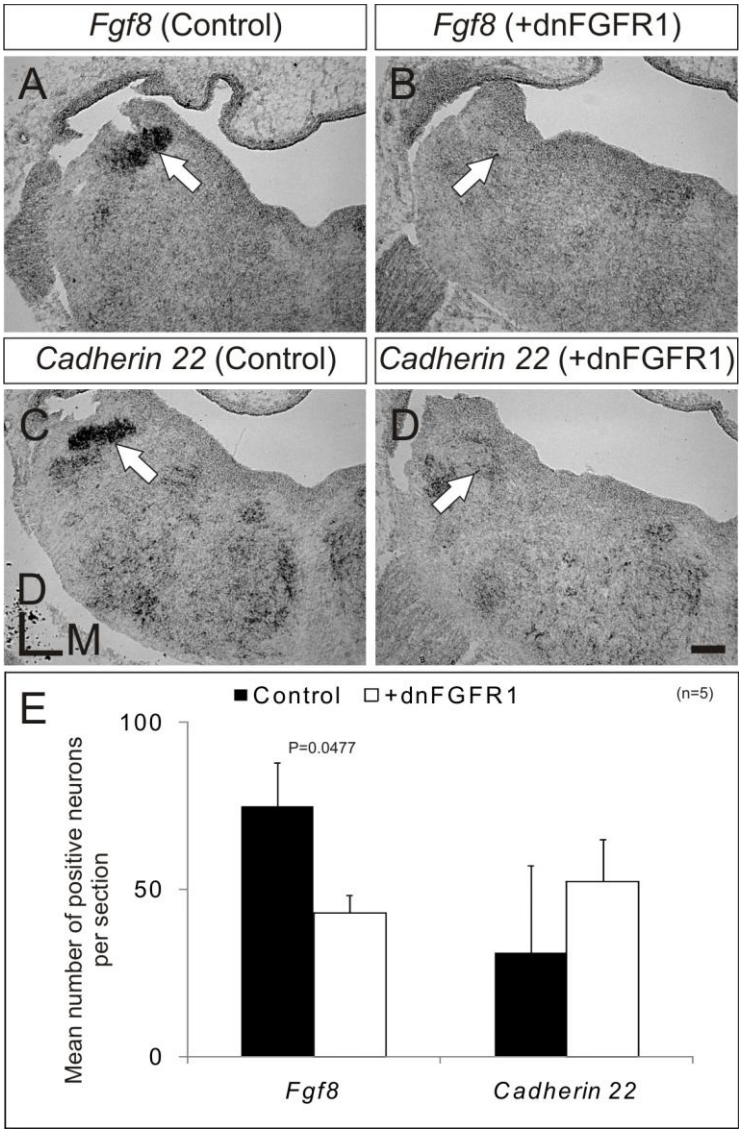

Figure 5.6: Expression of *Fgf*8 and *Cadherin 22* at HH31 is altered following MAPK/ERK signalling down regulation using a dnFGFR1 construct.

A: *Fgf*8 positive cells of the auditory anlage are visible clustered in the dorso-lateral hindbrain (indicated by an arrow).

B: Following dnFGFR1 expression, *Fgf*8 expressing cells are fewer and appear scattered throughout the hindbrain.

C: *Cadherin 22* is highly expressed in the auditory anlage of the control hemisphere.

D: Following dnFGFR1 expression the number of *cadherin 22* positive appears to fall. Those which remain appear scattered (indicated by an arrow)

E: Quantification of the number of *Fgf*8 or *cadherin 22* positive cells per section in control and following dnFGFR1 expression. Paired Student's T-test, Standard Error is shown (n=5).

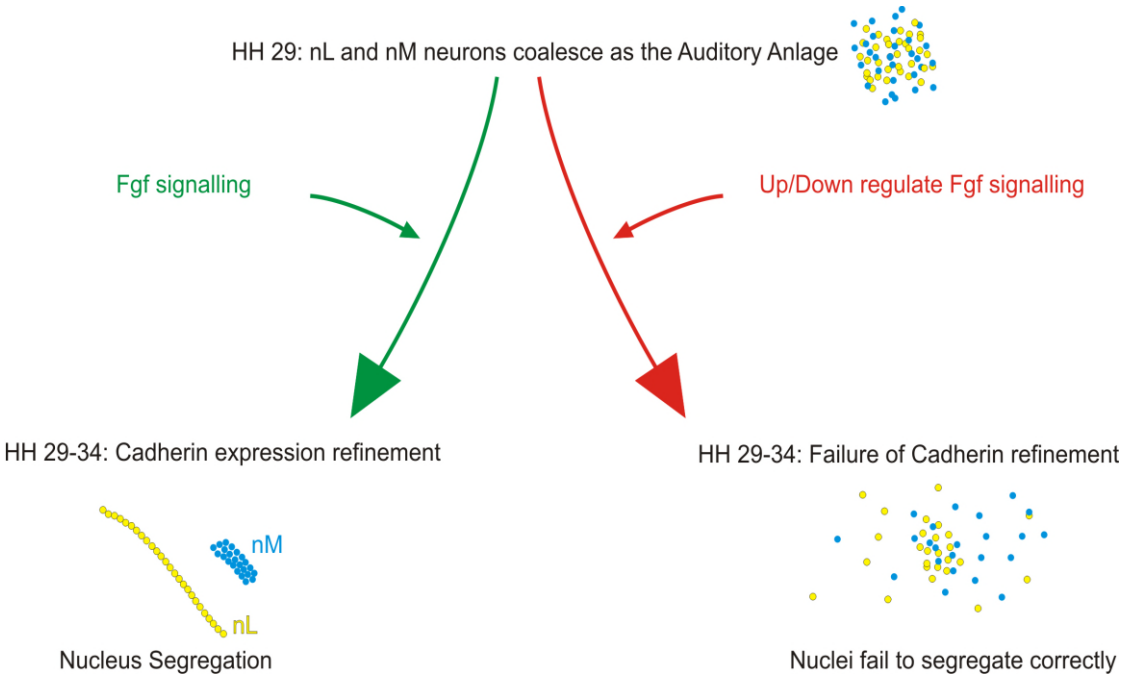

Figure 5.7: A model for *Fgf* regulated cadherin expression, driving cranial auditory nucleogenesis.

5.5 Analysing cell positioning defects in scattered nL neuronal population.

It is difficult to ascertain the nature of the developmental disruption following Fgf signalling disruption due to the lack of a reliable marker, for nL or nM neurons. The expression of *cadherin 22* and 13 would indicate that the neurons which will make up the cranial auditory nuclei are indeed present; however these cadherins are expressed in other regions of the hindbrain, which makes quantification difficult in a scattered population.

Previous studies have attempted to define a molecular marker for auditory hindbrain neurons (Smith, 2011), however to date none has been identified which is independent of Fgf signalling. One approach to identify nL neurons in a scattered population is to use anatomical tracing experiments focused upon input to the nL. nM neurons appear to project their axons across the midline to the region of the contralateral nL following m*FGF*8 misexpression (Figure 5.8, A). It is reasonable to suggest therefore that the ITD circuitry of nL-nM may remain, in part, intact. In wild type embryos nL receives a broad synaptic inhibitory input from neurons of the Superior Olivary Nucleus (SON) (Burger et al., 2005) as well as input from

contralateral nM neurons as part of this ITD neuronal circuitry. Thus using these two nL inputs it may be possible to identify misplaced nL populations in scattered populations.

Micro injections of Alexa 488 conjugated cholera toxin B into the cells of the SON provides an anterograde labelling of SON input to nL. Combined with insertion of dextran tetramethylrhodamine crystals at the midline; which labels contralateral nM afferents, allows visualisation of nL (Figure 5.8, B). The position of the juxtaposition of these markers indicates the position of nL (Figure 5.8, C). This presents a potential solution to the problem of identifying nL neuronal position following Fgf signalling alterations.

Alternatively it is possible to identify the region of nL using a nuclear marker such as DAPI. There appears a cell body sparse region surrounding nL which is rich with the dentrites of nL neurons (Figure 7, D). At HH34 this region is less clear as the nuclei have not established their mature conformations, however there is a region of the hindbrain which appears to contain a low concentration of cell bodies (Figure 5.8, E). Following RafER misexpression this region is absent, although a small region which could potentially be the position of the residual AA is present (Figure 5.8, F). Importantly this indicates that the linear structure of nL has failed to develop, ruling out the possibility that nL remains intact but with altered cadherin and *Fgf*8 expression.

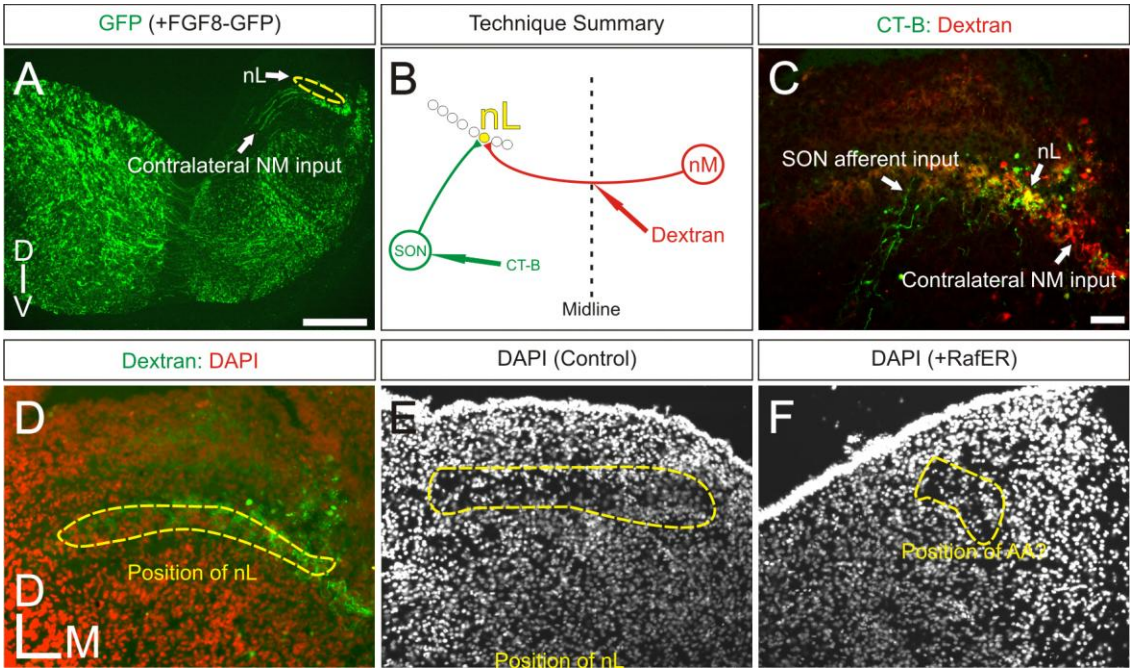

Figure 5.8: Attempting to locate nL neurons in a scattered population. **A:** GFP expression in nM afferent axons, following unilateral *in ovo* electroporation, shows the location of nL contralaterally (indicated by the yellow dotted line). **B:** A novel technique to idenify the position of nL neurons, using cholera toxin B (CT-B) microinjections to SON and Rhodamine dextran (dextran) inserted at the midline, as anterograde axonal tracers. **C:** An example of the technique demonstrates the position of the nL (yellow) at the juxtaposition of CT-B (green) and Dextran (red) labelling. **D:** Dextran labelling in combination with DAPI illustrates the cell sparse region surrounding the nL. **E:** In control hemisphere the cell sparse region indicates the position of the nL. **F:** Following RafER expression there appears a small cell sparse region as indicated by DAPI staining which could potentially be a remnant of the auditory anlage.

6. FHFs and Nav1.6 in nucleus Laminaris

6.1 FHF and Nav1.6 expression in nucleus Laminaris

Fibroblast Growth Factor's 11-14 are also known as Fibroblast Growth Factor Homologous Factors 1-4 (FHFs). They are a non secreted sub family of Fgf's which are FGFR independent (Review see Goldfarb 2005). FHFs 2 and 4a are reported intracellular binding partners of *Nav1.6*, the sodium channel which is known to mediate excitability of nL neurons (Wittmack et al., 2004, Lou et al., 2005). Following the identification of Fgf expression in nL, an analysis of wild type (WT) chicken hindbrains at HH36 by *in situ* hybridisation revealed that FHFs 1a and b, 2 and 4a were all expressed with nL (Figure 6.1 A-D). *Nav1.6* as previously reported (Kuba et al., 2006) was also expressed in nL (Figure 6.1, E).

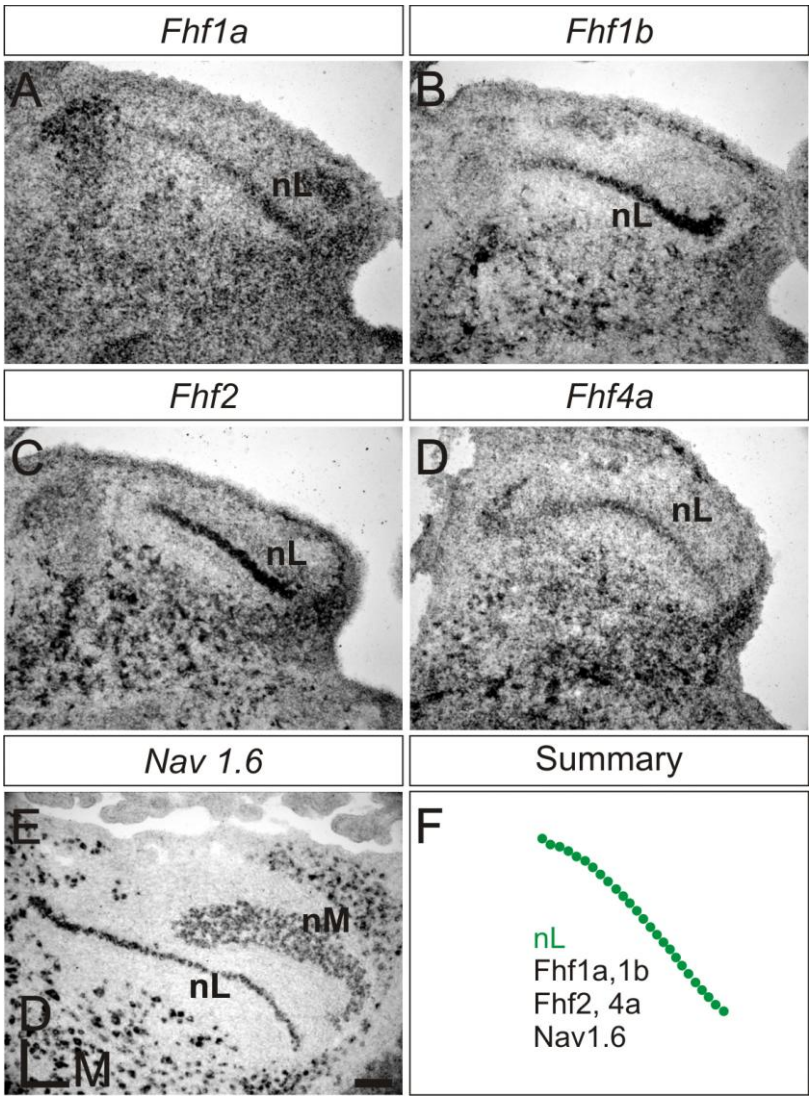

Figure 6.1: Fhf and *Nav1.6* in nL. **A-D:** FHFs 1a, 1b, 2 and 4a are all expressed in nL (HH36). **E:** *Nav1.6* is expressed in both nL and nM (HH39). **F:** Summary.

The nL is organised such that high and low frequency cells occupy distinct positions along the rostromedial to caudolateral axis (Smith & Rubel 1979; Smith 1981). Analysis was performed in order to investigate if a graded expression of FHF and/or *Nav1.6* existed across this frequency axis. Focussing on *Fhf2* and 4a, mRNA expression levels were assayed by analysing the intensity of staining at regular intervals throughout nL (Methods 2.10.2). Potentially an expression of *Nav1.6* intracellular binding partners could have implications for nL neuronal firing across the frequency axis. Given the roles performed by FHF's in terms of altering the dynamics of sodium channel inactivation (Goldfarb, 2012), it would be reasonable to predict that a gradient or differential expression of these genes may exist across the frequency axis.

6.2 FHF 2 and 4a are differentially expressed along the frequency axis of nucleus Laminaris

At HH36 the nL is approaching its final conformation and extends as a sheet, approximately 2-3 cells in diameter, along the rostrocaudal axis. Synapse formation between nL and nM has begun (Saunders et al., 1973) and the dendritic architecture of nL neurons is beginning to mature (Smith, 1981). Analysis of FHF expression at HH36 shows that *Fhf2* and *Fhf4a* exhibit different expression patterns within the nL (Figure 6.2).

The established tonotopic organisation of the nL across the rostro medial to dorso lateral axis results in a visible gradient of dendritic length associated with the characteristic best frequency of each neuron across the medial to lateral gradient. As such analysis across transverse sections should present a gradient of expression, if one were present, relative mRNA expression levels were determined as described in section 2.10.2, by measuring the intensity of staining of entire cells at regular intervals across the nL.

In transverse sections of the rostral nL, *Fhf2* is indeed expressed in a medial to lateral gradient; signal intensity is highest in the medial regions (~90%) and falls laterally (~40%) (Figure 6.2, A, C). This pattern of expression is maintained in medial sections of nL (Figure 6.2, D) where the difference in signal intensity from medial to lateral nL is greater (Figure 6.2, F). *Fhf2* expression appears to fall in the most caudal region of nL, but is maintained across the array (Figure 6.2, G). Taken together this indicates an expression pattern such that *Fhf2* is highly expressed in the rostromedial nL neurons and this expression decreases in caudolateral neurons.

Thus *Fhf2* appears to be highly expressed specifically in the high frequency nL neurons when compared with low frequency nL neurons.

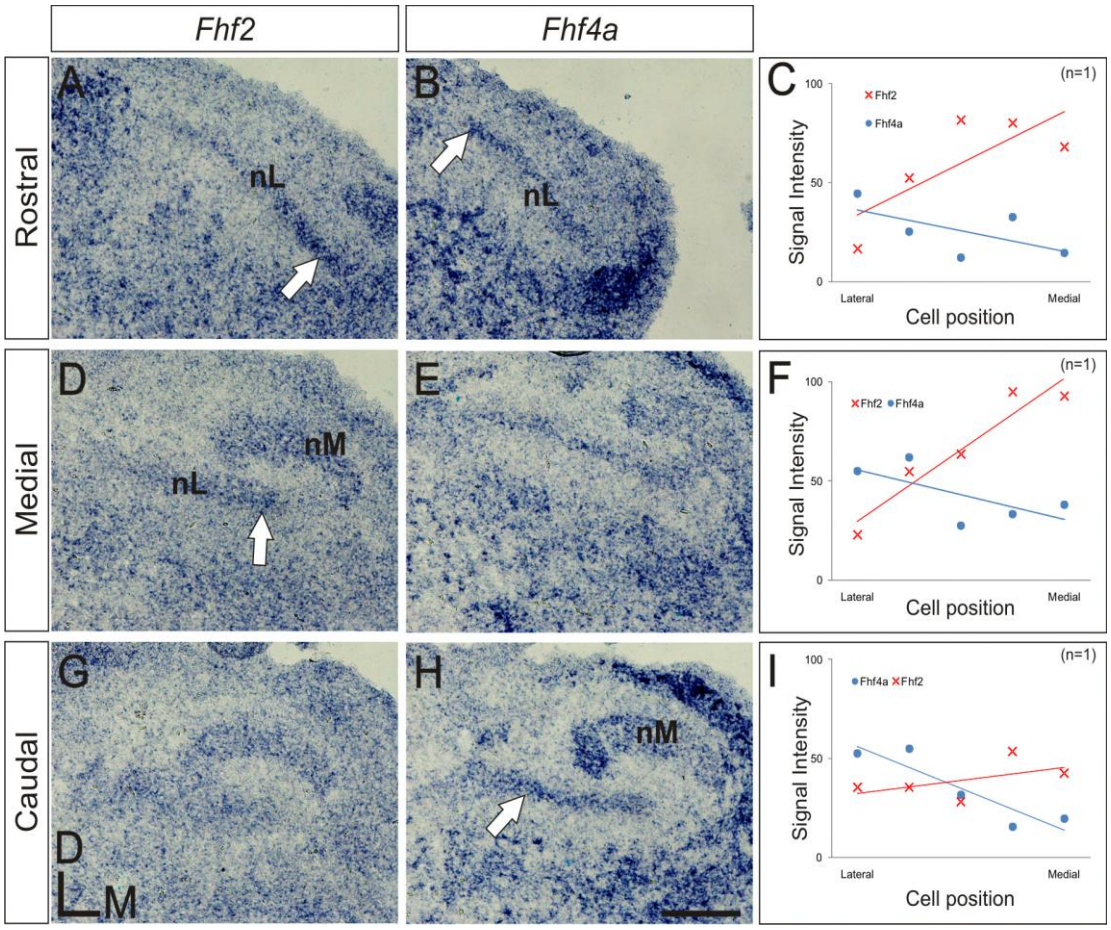

Figure 6.2: *Fhf2* and *Fhf4a* are differentially expressed in nL: A-C: *Fhf2* and 4a are expressed in complementary gradients across the medial to lateral axis of the rostral nL. Peak expression for both *Fhf2* and 4a is indicated by arrows. **D-F:** The gradient of both *Fhf2* and 4a expression seen in rostral nL is maintained in medial regions. *Fhf2* expression is highest medially. **G-I:** *Fhf2* expression decreases in caudal region, conversely *Fhf4a* expression is highest in this region. *Fhf4a* is most highly expressed in caudolateral nL.

Conversely *Fhf4a* shows the opposite gradient of expression. In rostral nL *Fhf4a* signal intensity decreases from ~40% laterally to ~10% medially (Figure 6.2, C), this profile is maintained along the rostrocaudal axis, with *Fhf4a* consistently expressed at higher levels in lateral compared with medial nL (Figure 6.2, F, I). Whilst notably, the peak of expression appears to be found in the most caudal regions (Figure 6.2, H, I). This data suggests that *Fhf4a* expression is higher in low frequency neurons

of the caudolateral nL. It should be noted that both *Fhf2* and *Fhf4a* are expressed across the entire nL, but significantly their gradient of expression is complementary.

At HH36 nM-nL synapse formation is initiated but these synapses are not functionally active until HH38. Analysis of nL at HH38 therefore will demonstrate if this graded expression is maintained following synapse formation. The average signal intensity along the rostrocaudal length of nL was analysed. As predicted, when we analyse signal intensity, *Fhf2* expression is higher in medial neurons of nL compared with those found laterally (Figure 6.3, A, C and E). *Fhf4a* is found to be expressed in a complementary gradient; its highest expression is found in the lateral aspect of nL and decreases medially (Figure 6.3, B, D and E). This data indicates, as with analysis at HH36, that *Fhf2* is expressed at a higher level in the high and middle frequency nL neurons. *Fhf4a* is expressed in the opposite gradient. Importantly this gradient of expression is established prior to the establishment of active synapses and maintained, suggesting a functional role across the frequency axis.

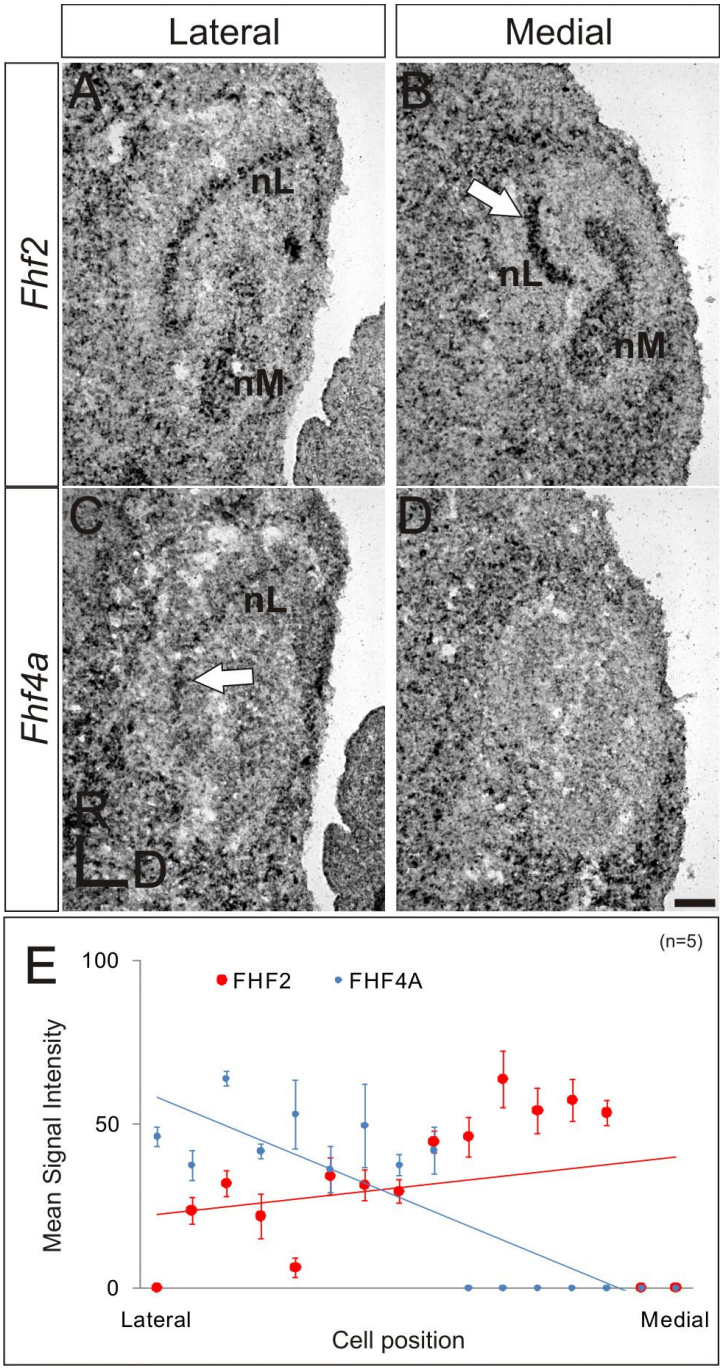

Figure 6.2: Sagittal sections through nL demonstrate showing *Fhf2* and *Fhf4a* expression.

A-B: *Fhf2* is expressed throughout nL in the medial to lateral plane. *Fhf2* expression is highest, however, in medial regions (indicated by arrow).

C-D: *Fhf4a* expression is complementary to *Fhf2*. The peak of *Fhf4a* expression is in the lateral region of nL (indicated by arrow). In the medial nL, *Fhf4a* is absent.

E: Mean signal intensity taken from 5 points along the rostrocaudal axis of nL in each section. *Fhf2* expression is highest in the medial nL sections and absent at the extreme lateral nL. *Fhf4a* is expressed in lateral nL, but is absent in the medial nL neurons. (n=5).

Nav1.6 is the predominant channel mediating action potential initiation in nL neurons. *Nav1.6* channels are found at the axon initial segment (AIS) but are sparse on the soma of nL neurons (Kuba et al., 2006) Analysis at HH36 found expression of *Nav1.6* mRNA to be constant across nL, with no discernable gradient of expression in either the mediolateral or rostrocaudal axes; signal intensity of *Nav1.6*

expression is consistent across the medial to lateral axis in rostral, medial and caudal sections of nL remaining around ~50% throughout (Figure 6.4). There are no sharp gradients as with *Fhf2* or *Fhf4a* expression. This indicates that there is no change in level of *Nav1.6* expression associated with any frequency specific sub population of nL neurons.

Taken together this data indicates that there is constant *Nav1.6* expression across the entire nL, but that *Fhf2* and *Fhf4a* are expressed in contrasting rostromedial to caudolateral gradients. This is summarised in Figure 6.5. Potentially this holds functional implications for nL and ITD analysis.

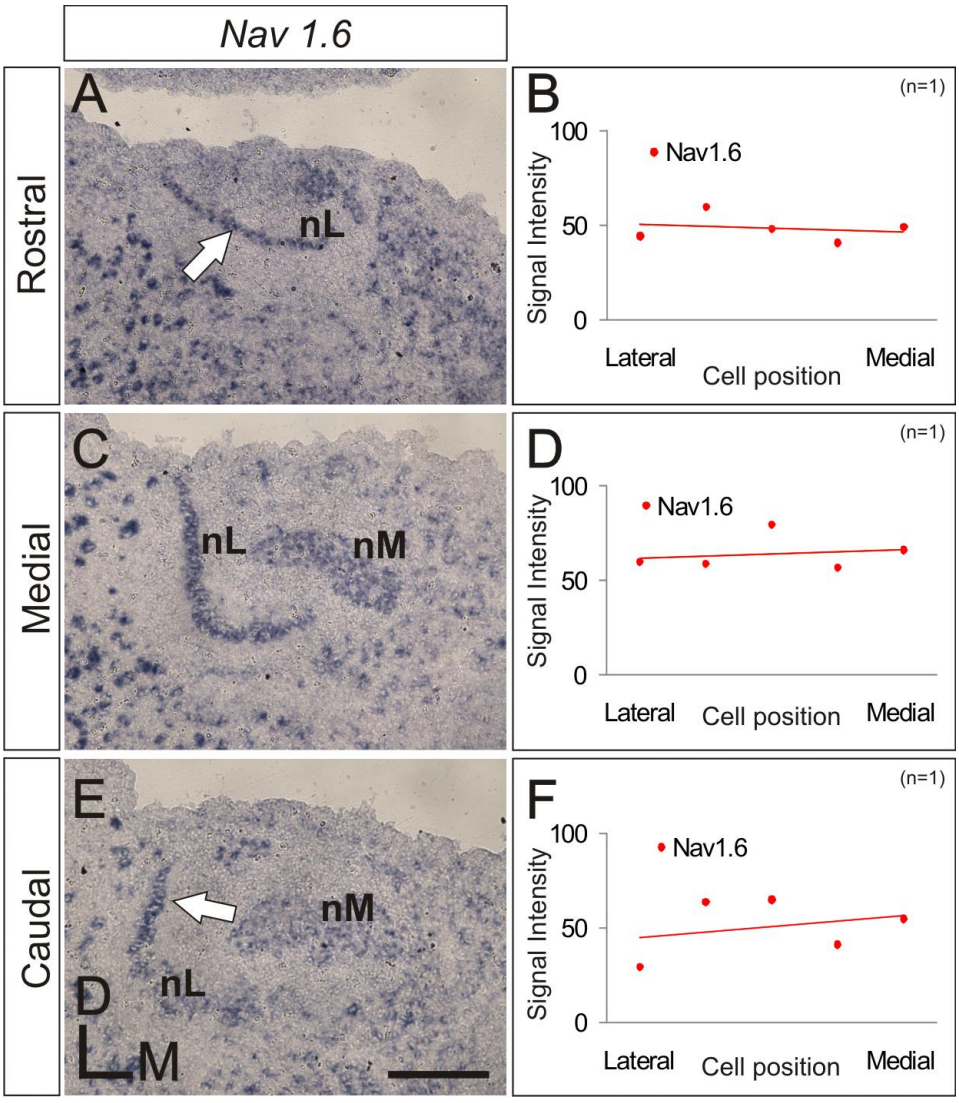

Figure 6.4: *Nav1.6* expression is constant across the entire nL. **A-F:** *Nav1.6* is expressed at a constant level across the lateral medial axis. It shows not large increases or decreases associated with different best frequency neurons along the rostrocaudal axis.

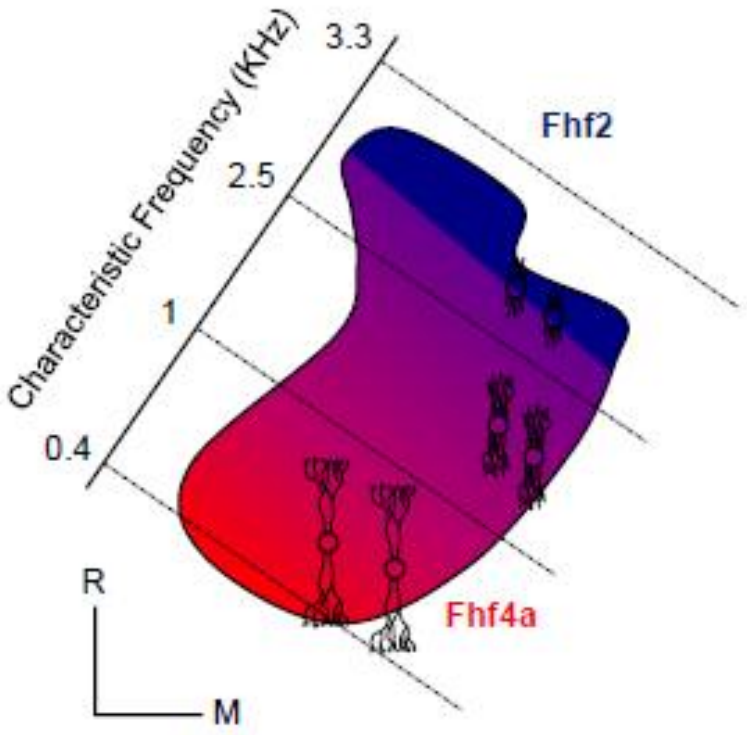

Figure 6.5: Summary: There is a complementary gradient in expression of *Fhf2* and *Fhf4a* along the frequency axis of nL. *Fhf2* (Blue) expression is highest in the rostromedial nL which contains high frequency neurons. *Fhf4a* (red) expression is highest in the caudolateral of nL, occupied by low frequency neurons.

6.3 The role of FHFs in nL

The FHFs are expressed in the chick embryo throughout embryogenesis, and through to adulthood. The expression of the FHFs, which are a non secreted sub family of the Fgfs, in the nL has important functional implications for auditory information processing. FHFs are intracellular binding partners of voltage gated sodium channels; they bind to the C-terminus of region of these channels where they act to alter the dynamics of channel opening. It has been demonstrated that FHFs act to raise the voltage dependence of fast channel inactivation, enabling constant repetitive firing of Action potentials. The nL is tonotopically arranged such that each region along the rostro caudal axis receives phase locked input at a

specific frequency matched to the positional of stimulation at the cochlea. The role of nL in processing of interaural time differences requires that each neuron is able to respond to coincident input with a high degree of fidelity, that is it is crucial that action potentials are only elicited in response to the correct stimulus. The membrane and channel properties which mediate AP firing are therefore crucial.

The nL has many specialisations which allow it to perform this function however, the novel discovery of FHF expression in nL neuron may illustrate another adaptation. *Fhf2* and *4a* were found to be expressed in complimentary gradients along the rostrocaudal axis. *Fhf2*b was highly expressed in the rostral nL where high best frequency neurons reside. *Fhf2* binds the C terminus region of Nav1.6, which is expressed at the same level throughout the nL, where it alters channel dynamics allowing repetitive firing of action potentials mediated by Nav1.6. In mice cerebellar slices it has been shown that *Fhf2* and *4a* act to decrease the recovery time of Nav1.6 channels from inactivation, helping to maintain repetitive action potential firing. That it also raises the voltage dependence of channel inactivation is indicative that *Fhf2* helps to prevent action potential generation in nL neurons which do not receive precisely time coincident input; only when a certain voltage threshold is reached will the Nav1.6 channels open, eliciting an AP. If the input to the nL neuron is only slightly mis-timed then the raised voltage threshold cannot be reached and Action potentials are not elicited.

The expression gradient of *Fhf 4a* is complimentary to that of *Fhf2*, indicating that the two may have different roles in high and low frequency neurons. In the caudal nL specialisations allow for the low input frequency of coincident input, and it would seem that a raised voltage dependence of channel opening and inactivation here may be a disadvantage. However, these neurons are also required to fire repetitively and so the role of FHFs here may also be to act as a filter preventing aberrant nL neuronal firing. The role of FHFs in sodium channel binding is a fairly recent discovery and studies as to its exact function have not differentiated a role for the different FHF family members. This data suggests that they may have different roles to play dependent upon the neuron in which they are expressed. Further electrophysiological investigation would be required to determine the exact implications of the gradients of expression discussed here.

7. Discussion

Cranial nucleogenesis requires that neurons are able to migrate to their correct spatially distinct position, where they will recognise and coalesce with molecularly identical neurons into functionally related clusters; neuronal nuclei. Analysis of the development of the cranial motor nuclei in r5 and r8 demonstrated that Somatic and Branchiomotor neurons exit the ventricular zone at similar time points and positions and are found in mixed populations prior to the onset of nucleogenesis. The initial intermixing of the two populations has not previously been reported and suggests a requirement for controlled cellular adhesive interactions in order for nucleogenesis to occur. In r5, for example, at HH20 both BM and SM neurons are located in a mixed population close to the midline adjacent to the ventricular zone. These neurons begin to segregate into distinct groups dependent upon their molecular identity by HH26. The process of segregation and nucleogenesis is not complete until HH30. The question asked in this study is what can drive this two part process of segregation and coalescence of distinct neuronal subtypes?

7.1 A model for Cranial Nucleogenesis

The data presented in this thesis suggests that differential cadherin expression under the control of Fgf signalling may play an important role in mediating the organisation of motor neurons in to distinct nuclei. Within r5, each of the motor nuclei expresses a unique combination of type II cadherins; this is the first family of molecules which has been demonstrated to define the identity of specific cranial nuclei and significantly differentiates between different divisions of the FMN. Notably, the Accessory Abducens and dorsal Facial Motor nuclei differ only in their expression of *cadherin 20*; a mosaic misexpression of *cadherin 20* in r5 MN's resulted in defects in the normal development of AccAb and dFMN.

The time course of r5 motor nuclei development illustrates that the AccAb and FMN are intermixed at HH26 during embryogenesis, however these two nuclei are completely segregated by HH31. Early in development (HH20) *cadherin 20* is expressed in a high percentage of all MN's, by HH29 however, it is restricted to the dFMN. it appears that the down regulation of *cadherin 20* expression in AccAb MN's as they migrate through and segregate from the FMN MN's between HH24-29

prevents these AccAb neurons from interacting with and potentially aberrantly adhering to dFMN MN's.

A potential extrinsic factor which could affect changes in the hindbrain is Fgf8; which is known to act as a secreted morphogen and can induce differential gene expression in a concentration dependant manner. Up or down regulation of Fgf signalling leads to desegregation of the AccAb and dFMN, in a manner which is phenotypically identical to alteration in *cadherin 20* expression in these two nuclei. Analysis of *cadherin 20* expression in r5 MN's following changes in Fgf signalling levels revealed that *cadherin 20* is aberrantly expressed in mispositioned AccAb neurons.

Thus a model is presented, such that the dynamic expression of cadherins under the control of Fgf signalling facilitates the segregation of a mixed population of MNs into spatially discrete neuronal nuclei. In the particular case of the r5 motor nuclei this process is dependent upon a tightly controlled down regulation of *cadherin 20* during the critical stages of AccAb and FMN nucleogenesis; that is the time point when these two populations separate from one another and coalesce in their final positions. Fgf signalling appears to be critical for the modulation of cadherin expression in r5 as disruption in Fgf signalling leads to alterations in cadherin expression with concomitant defects in nucleogenesis (Figure 7.1).

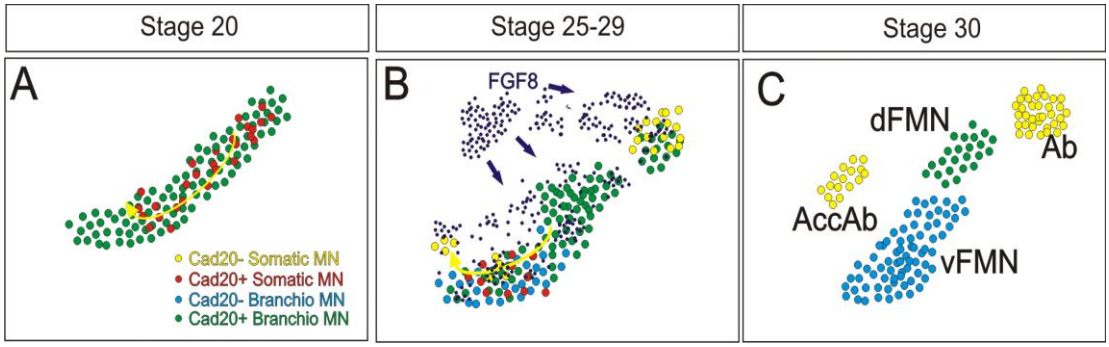

Figure 7.1: A model for cranial motor nucleogenesis in r5. **A.** Initially Somatic and Branchiomotor neurons express cadherin 20 and are mixed in one population. **B.** As development proceeds cadherin 20 expression is refined, such that it is down regulated in all motor nuclei, except those that will form the dFMN. This process is possibly dependent upon tightly controlled Fgf signalling, initiated by Fgf8 found in the extracellular matrix. **C.** By HH31 nucleogenesis is complete, only the dFMN expresses cadherin 20. Ab, Abducens; AccAb, Accessory Abducens; dFMN, dorsal Facial Motor Nucleus; vFMN, ventral Facial Motor Nucleus.

7.2 Type II cadherins mediate cell sorting in vivo

Cadherins are a family of calcium dependant adhesion molecules, which have been shown to mediate the sorting of different cell types in vitro (Nose et al., 1988). In the central nervous system their spatially and temporally restricted expression is important in the organisation and patterning of neurons into distinct regions and circuits. The morphogenetic functions of cadherins have been attributed to the classical type I and II cadherins (Nollet, 2000).Type I cadherins have broad expression patterns associated with, for example, the segregation of embryonic epithelial layers (Nishimura et al., 1999). Type II cadherins appear to have overlapping expression patterns in relatively small regions, particularly within nervous system; it is known that combinatorial type II cadherin expression drives the segregation of MNs in to distinct motor pools in the spinal cord (Price et al., 2002). The mechanisms which underpin the specificity of cadherin binding and associated cell sorting are now beginning to be elucidated.

Each type I or II cadherin possess 5 repeated 110 amino acid extracellular domains (EC1-5) (Reviewed in Tanabe et al., 2004). Binding of Type I cadherins is mediated at the EC1 domain by exchange of a β strand between two partnering EC1 domains; this exchange is anchored by the insertion of a side chain of a conserved Trp2 residue into a complementary hydrophobic pocket. This mechanism is believed to mediate binding of cadherins presented on the cell surface of two opposing cells. Importantly the EC1 domain has been shown to determine the specificity of type I cadherin binding in vitro (Nose et al., 1990).

The binding mechanism which mediates binding of type II cadherins, however, is significantly different. Binding between type II cadherins is also mediated via the EC1 domain, however it involves the exchange of two tryptophan residues (Trp2 and 4) into a larger hydrophobic pocket than that found in the type I cadherin EC1 domain (Patel et al., 2006). Thus there is a structural incompatibility between type I and type II cadherins which will prohibit adhesion between these two cadherin types. In vitro aggregation assays using wild type or chimeric type I/II cadherins, where the EC1 domain is switched, support this (Patel et al., 2006; Katsumba et al., 2009).

Interestingly aggregation assays involving only type II cadherins have so far failed to recapitulate the cell sorting effect seen using in vivo systems; cells expressing different type II cadherins at the cell surface will form mixed aggregates, whereas

under the same conditions differential expression of type I cadherins will drive segregation of two populations (Patel et al., 2006; Nose et al., 1990; Shiyoyama et al., 2000). Evidence presented here suggests that differential type II cadherin expression in cranial motor nuclei, as in spinal motor pools, is sufficient to drive the segregation of neuronal populations in vivo. Each of the r5 motor nuclei expresses a unique combination of type II cadherins, normalising the expression profile between two nuclei is sufficient to inhibit their segregation. Importantly no type I cadherins are expressed here; misexpression of the type I, N-cadherin in this system has no effect on nucleus development, suggesting a specificity of action imparted by type II cadherin interactions.

However, if type II cadherins are unable to drive segregation in vitro in the same manner as type I cadherins, then how are they able to drive this process in vivo? Firstly it should be noted that in vitro assays so far have used the expression of only one type II cadherin in each cell; in vivo, neurons express multiple type II cadherins. This indicates that combinatorial type II cadherin expression is important in cell sorting in vivo. In addition the strength of cadherin interactions has been shown to be variable between both type and individual cadherins. The affinity of homophilic interactions between the type I cadherins *N* and *E cadherin* have been shown to be slightly different, where the affinity of binding between two N cadherin dimers is greater than that of *E cadherin*. These two cadherins have been demonstrated to form heterophilic bonds in vivo (Volk et al., 1987); however the affinity of this interaction is less than that of the homophilic N cadherin interaction (Katsamba et al., 2009). The authors suggest that cell layer separation is still expected in the presence of heterophilic interactions if the affinity of one type of homophilic interaction is greater. Similarly, recent data has suggested that when the difference in binding affinity between two cadherins is relatively low, cell sorting in vitro does not occur. However, two-dimensional differences in binding affinity greater than 5 fold correlate with cell segregation in vitro (Tabdili et al., 2012).

The affinity of homophilic *cadherin 6* (a type II cadherin) was found to be an order of magnitude greater than that of N-cadherin (Katsamba et al., 2009), as would be predicted from the known larger interfacing surface area within the EC1 domain (Patel et al., 2006). Whilst data for adhesive affinity between chicken type II cadherins is not currently available the idea that each cadherin within the family has subtly different binding affinities which may translate into strength of adhesion may help to explain the role of type II cadherins in vivo. For example in the hindbrain

motor nuclei the adhesive strength of *cadherin 20* may be greater than that of the other type II cadherins expressed. One could propose a model whereby *cadherin 20* is initially expressed in all MNs as they migrate, as the dominant cadherin mediating aggregation of a mixed population. At a certain time point *cadherin 20* will be down regulated in subsets of MNs and other cadherin interactions will predominate to drive coalescence of discrete nuclei.

It has also been shown that the level of cadherin expression within cells is significant in the process of cell sorting; cells expressing high levels of *E- cadherin* will preferentially aggregate with those expressing a similarly high level as opposed to cells exhibiting low level *E-cadherin* expression (Nagafuchi et al., 1987). Thus there appears a mass action effect of cadherin binding is also important in the process of cell sorting. It is difficult in vivo to assess the relative contribution of each type II cadherin to the overall adhesive properties of individual neurons. However, taken together, it is possible that the specificity and affinity of cadherin interactions driven by their EC1 domains in combination with the level of cadherin expression at the cell surface could have profound effects on the overall adhesion of two neuronal populations. For example a subtle difference in binding affinity between two type II cadherins may not be sufficient to mediate cell sorting; however increasing the level of expression of one cadherin amplifies such a difference as a result of mass action. It is likely that, as well as the combinatorial expression of cadherins in the r5 cranial motor nuclei, the specificity and strength of homophilic type II cadherin interactions is crucial for nucleogenesis.

7.3 Cadherins in cranial nucleogenesis

Differential cadherin expression appears therefore to be important in normal cranial nucleogenesis, so far I have discussed the potential mechanisms by which cadherins mediate cell sorting in vivo with a particular focus on the r5 motor nuclei. Further to this analysis of classical cadherin expression in the developing chick embryonic hindbrain revealed that cadherins are expressed in both developing motor nuclei of r8 and the developing auditory hindbrain nuclei. Disruptions of cadherin function in either r5 or r8 using a dominant negative N-cadherin results in a loss of neuronal nuclei adhesion and associated scattering of neurons. This suggests that the coalescence of neuronal nuclei is dependent upon cadherin mediated cell-cell adhesion. Cadherins however, have other potential roles in

cranial nucleogenesis and their presence in cranial motor nuclei has many functional implications.

Cadherins are known to play active roles in the migration of neurons from their progenitor domains. For example classical cadherins are known to regulate the tangential migration of precerebellar neurons, which express *cadherins 8, 11* and *6*, to both the external cuneate nucleus and lateral reticular nucleus of the cerebellum. Knock down of cadherin adhesive function using a dominant negative has been shown to slow down this migration (Taniguchi et al., 2006). Cadherins have also been shown to be involved in the correct targeting of Purkinje cells to their respective cerebellar compartments through early decision making events regulated by cadherin expression (Luo et al., 2004). Similarly in the spinal cord the migration of LMC neurons from the ventricular zone is dependent upon cadherin function; the lateral migration of these neurons is inhibited following cadherin function deregulation using a dominant negative catenin, and they remain juxtaposed to their ventricular exit point (Bello et al., 2012). In the spinal cord LMC migration all MNs initially express the same cadherins, prior to refinement later in development once their lateral migration is almost complete (Price et al., 2002).

Early in the development of the r5 cranial motor nuclei all of the MNs are found in a mixed population immediately juxtaposed to the ventricular zone adjacent to the midline. Looking at the time course of nucleogenesis in this region it is apparent that the MNs which will constitute the FMN and AccAb appear to undergo a stereotyped lateral migration towards their final settling positions in the ventrolateral hindbrain. Disruption in normal cadherin expression pattern causes desegregation of the FMN and AccAb nuclei, associated with defects in cell sorting. The position of FMN appears unaltered by disruption of this combinatorial cadherin expression, whilst the AccAb neurons appear aberrantly intermixed with that population. Importantly the Abducens nucleus appears unaltered following mosaic expression of *cadherin 20* or a dnCad20. If MN migration in this region, as in the spinal cord, is driven by cadherin interactions with radial glia it would be predicted that the Ab would be unaffected by disruption to this system as those MNs do not migrate from their position upon exiting the ventricular zone. The phenotype ascribed to the failure of correct neuronal FMN and AccAb nucleogenesis may also be a result of the failure of AccAb MNs to complete migration driven by interaction with the radial glia, coupled with the altered cadherin based cellular adhesion as discussed previously.

A further role for cadherins in the development of cranial motor nuclei is in the outgrowth of the cranial nerves themselves. In fact cadherin expression has been shown to be an important regulator of axonal outgrowth and fasciculation (Marthiens et al., 2005; Shiga et al., 1991; Fredette & Ranscht, 1994). Marthiens et al, 2005 demonstrated that *cadherin 11* expression in motor axons is required for fasciculation, knock down of *cadherin 11* function blocks interaction between each axon and rapid extension of the axonal growth cone. Similarly Barnes et al., 2010 demonstrated that *cadherin 7* enhances motor neuron axon outgrowth whilst suppressing multiple axon formation in early stages of BM motor neuron development; subsequently down regulation of *cadherin 7* is followed by an up regulation in *cadherin 6b* expression. *Cadherin 6b* is able to promote motor axon branching in vitro, consistent with the phenotype of mature motor neurons (Barnes et al., 2010). However the actions of cadherins alone do not drive the behaviour of cranial motor axons independently, but are one of several mechanisms which are involved in cranial motor axon pathfinding.

For example it has been shown that repellent cues such as semaphorin D and Netrin 1 secreted from the floorplate act as repulsive cues to developing BM motor axons, which project their axons from large dorsal exit points. Abducens axons which project their axons from small ventral exit points were unaffected by Netrin 1 expression (Varela-Echavarria et al., 1997). This differential responsiveness of motor axons to guidance cues is significant in terms of this study, as they indicate a requirement for different cell adhesion and repellent systems to be expressed within developing MNs. For example in the spinal cord, selected MN pools are known to express *Sema3e* whilst their appropriate proprioceptive sensory afferents express the high affinity receptor *Plexin-D1*, this system is believed to be important for correct target recognition and synapse formation (Pecho-Vrieseling et al., 2009).

Similarly in the spinal cord the Eph receptor and ephrin ligand signalling system play an important role in the topographic relationship between LMC axonal guidance and motor neuron cell body positioning centrally. As mentioned LMCl and LMCm motor neurons map to either dorsal or ventral limb targets respectively, this action is mediated, in part, by forward ephrin:Eph signalling (which mediates repulsion) or reverse Eph:ephrin signalling (which mediates attraction). The distribution of respective Eph and their ephrin binding partners in either axon or limb mesencyme cooperate to drive the correct mapping of axons to their targets (Reviewed in Kao et al., 2012). Significantly for the development of cranial motor nuclei Feng et al., 2000

demonstrated that the Eph ephrin signalling pathway is important in mapping of the spinal accessory nerve and positioning of certain motor neurons in the caudal hindbrain. Eprhin A2 and A5 are expressed in the rostral muscle groups which are innervated by the spinal accessory nucleus, mutant mice lacking both of these ephrins show topographic axonal mapping defects as well as a mispostioning of the motor neurons which innervate the acromiotrapezius muscle; motor pools were shifted caudally and extended over a greater distance in mutant mice (Feng et al., 2000).

Similarly in the spinal cord the signalling pathways which mediate axonal guidance via Eph ephrin signalling can be directly linked to the positioning of LMC motor pools. Palmersino et al., 2010, investigated the potential links between Reelin signalling and the topographic mapping of LMC neurons to peripheral muscle targets. They established that Reelin, expressed in the ventral spinal cord, is necessary for the tangential migration of LMC neurons. This action is mediated downstream of Lhx1, in LMCl neurons; acting to increase the expression of the adaptor protein Dab1 which, in turn, determines the final settling position of both LMCl and LMCm in the ventral spinal cord. This effect is important in terms of mapping the central topography of MNs and their peripheral targets as the expression of Eph/ephrins in MN columns is controlled by *Lhx1/FoxP1* expression (Palmersino et al., 2010).

In terms of the cranial motor nuclei this presents a wider question for nucleogenesis. For example in r5, following deregulation of the central positioning of the AccAb by cadherin misexpression, will there be a defect in targeting or branching of axons to their muscle targets? Also it would be useful to establish a topographic link between the positioning of cranial motor nuclei in the absence of, or disruption of axonal guidance to, muscle targets. Importantly the role of reelin signalling in the ventral spinal cord in coupling these two processes, presents another potential role for Fgf signalling within r5 itself.

7.4 Fgf signalling drives cranial nucleogenesis

The down regulation of *cadherin 20* expression which mediates the segregation of AccAb and dFFM nuclei is a key step in nucleogenesis in r5. Data presented in this thesis suggests that this key step is controlled by the Fgf signalling pathway. Fgf8 is

expressed in the auditory hindbrain nuclei of r5; nL and nM, as well as in the otic vesicle directly adjacent to r5. Fgf8 is established as a secreted morphogen which can induce differential gene expression in a concentration dependant manner. Up or down regulation of Fgf signalling led to desegregation of the AccAb and dFMN, in a manner which is phenotypically identical to mosaic misexpression of *cadherin 20* in these two nuclei. Analysis of *cadherin 20* expression in r5 MN's following changes in Fgf signalling levels revealed that *cadherin 20* was aberrantly expressed in mispositioned AccAb neurons. Thus, Fgf signalling appears to specifically alter the cadherin expression profile of r5 cranial MNs during nucleogenesis, how is this achieved?

The specific effect of altering Fgf signalling only effects nucleogenesis in r5; r8 cranial motor nuclei showed now defects in nucleogenesis following Fgf8 misexpression. Thus Fgfs in this region appear to be acting as a secondary signalling centre which patterns the hindbrain at this specific axial level. Throughout embryogenesis transient signalling centres exist which pattern the adjacent tissue, examples include Hensens node or the midbrain hindbrain boundary; these transient structures are sources of Fgf in the developing chicken embryo which establish gene expression involved in A-P patterning (Liu et al., 2001; Liu & joyner, 2001).

Indeed positional specification via secreted cues in the A-P axis are critical to the correct development of neural circuits, for example In the spinal cord the alteration of gene expression which governs motor pool formation can be induced by extrinsic factors; expression of GDNF in the plexus of the developing forelimb is required to induce expression of the ETS transcription factor *PEA3* (Haase et al., 2002)*;* loss of *PEA3* expression leads to mis-positioning of spinal motor pools (Livet et al., 2002). Equally limb ablation in chick embryos results in the loss of *Er81* expression; a transcription factor which lies upstream of *cadherin 20* expression, required for the correct segregation of motor pools. Taken together with the effects of Reelin signalling in the ventral spinal cord, which is important in the migration and positioning of LMC neurons, there is a combination of specification events at the level of the limb which act in unison to coordinate the organisation of MNs.

Could Fgf expressed at r5 also be providing such a cue? Evidence presented here suggests that the Fgf signalling pathway is involved in the downstream expression of cadherin genes. Up or down regulation of Fgf signalling results in a failure in the

down regulation of *cadherin 20* expression. The various methods by which Fgf signalling was manipulated during this study allows some insight as to the mechanism by which Fgf signalling may play a role in cadherin expression refinement. Up regulation of the Fgf signalling pathway was achieved using a constitutively active Raf construct, which directly feeds into the MAPK/ERK signalling pathway. Down regulation of Fgf signalling was achieved via FGFR functional knockdown using the dnFGFR1 and a secreted FGFR3 which sequesters Fgf8 in the extracellular matrix. Thus we were able to target Fgf signalling at three separate points, by either blocking Fgf-FGFR binding, inhibiting downstream FGFR signalling at the plasma membrane or by directly altering the MAPK/ERK signalling pathway. That each of these manipulations produced essentially produced identical phenotypes indicates that Fgf8 acting through the FGFR's in MN's may be able to affect cadherin expression via the MAPK/ERK signalling pathway.

This result may be predicted based upon the known dynamics of Fgf signalling; acting as a secreted morphogen the gradient of which is interpreted based upon the French Flag model of morphogen expression (Wolpert, 1969). In fact it has been demonstrated that the interpretation of Fgf morphogen gradient is mediated by endocytic trafficking of the FGFR; trafficking the receptor back to the cell surface as opposed to the lysosome for destruction, leads to an expansion of gradient interpretation (Nowak et al., 2010). As such the extracellular Fgf gradient can be refined via intracellular feedback mechanisms to induce a greater repertoire of cellular responses over small distances. In r5 the motor neurons which will constitute AccAb and FMN undergo a highly stereotyped migration, distance from and exposure to the Fgf source may have a profound effect upon the interpretation of Fgf signalling. Indeed the Fgf signalling pathway has been shown to induce the expression of the ETS transcription factor Pea3 in chicken hindbrain (Weisinger et al., 2010); Pea3 is an important regulator of motor pool positioning in the ventral horn. Whilst knock down of FGFR1 in mutant mice results in down regulation of cadherin 13 and 22 expression at the MHB (Trokovic et al., 2003; Saarimaki-Vire et al., 2007;2011). Unfortunately in this study there have been no identified downstream transcription factors which provide a direct link between Fgf signalling and cadherin expression; investigation in to up or down regulation of known TF targets is required to establish a direct link for Fgf regulation of cadherin expression.

Other potential interactions between cadherins and Fgf signalling appear to be mediated directly by interaction of cadherins and FGFRs at the cell surface. For

example in the up regulation of *N-cadherin* at the cell surface is linked with an increase in the invasive phenotype associated with cancer cell metastasis; the mechanism of this action is believed to be a stabilisation of the FGFR via binging with n-cadherin which mediates increased Fgf signalling duration leading to up reglation of the secreted metaloprotease MMP9 (Suyama et al., 2002). The link between FGFR and cadherin expression in cell motility is interesting when presented in the context of neuronal migration. Perhaps more intriguing is the role that cadherins and Fgfs play in axonal outgrowth. It has been demonstrated for example that *cadherin 11* interacts with FGFR1 to induce neurite outgrowth via the downstream activation of the CAM kinase and PI3K pathways, but not the MAPK/ERK pathway. Cadherin 11 is thought to recruit FGFR1 to the membrane upon making contact with other axons, activating a signal cascade which will ultimately promote axon outgrowth (Boscher & Mege, 2008). Conversely, Soundarajaran et al., 2010 propose that axonal guidance of *Lhx3* positive MMCm spinal motor neurons is dependent upon Fgf signalling downstream of FGFR1 mediated by the MAPK/ERK signalling pathway.

The exact roles of Fgf signalling therefore remain unclear. Certainly based upon the evidence presented here it is possible to propose that Fgf signalling via the MAPK/ERK signalling pathway is important for nucleogenesis to occur; the segregation of AccAb and FMN in r5 is driven by dynamic cadherin expression which may be regulated downstream of Fgf signalling. However, the expression of FGFRs in these MN populations, when viewed in the context of known cadherin-FGFR interactions may suggest that Fgf signalling can play multiple roles in r5 motor nucleus patterning, migration and cranial nerve development.

7.5 Neuronal nuclei and neural circuit development

Neuronal nuclei are a predominant form of neuronal organisation within the CNS, they are an integral part of most neural circuits and act to integrate information before passing it on to higher centres or mediating responses in the periphery. Prime examples of this are found in the cerebellum, where input to the spinal cord from the cerebellar cortex is relayed via the deep cerebellar nuclei (Reviewed in Eccles, 1973), or the nucleus Laminaris which, in birds, integrates sound localisation information from both ears and projects this information to higher brain centres (Reviewed in Hyson, 2006).

Correct targeting of axons to the correct nucleus or peripheral target is therefore, of crucial importance to the development of neural circuitry. However, neuronal nuclei themselves are not passive in this process and the positioning and coalescence of neurons has wide ranging implications for neural circuit formation. I have already discussed the link between central topography of MNs in the spinal cord with reference to axon outgrowth, however another aspect of circuit development is the targeting of peripheral afferent input to the CNS. Recent data suggests that afferent input to spinal motor neurons is pre-programmed, such that in mice where motor pool settling position is scrambled, sensory afferent axons will project to a pre-determined region and form inappropriate connections. Thus there is a breakdown of the central and peripheral topographic mapping. Therefore the independently correct positioning of motor neuron pools is critical for the formation of functional spinal neuronal circuits (Surmeli et al., 2011).

This data perhaps goes against the commonly held view that recognition of cell surface markers is the driving force behind neural circuit formation; however it is likely that a combination of pre-programmed and contact driven behaviour act in combination to drive circuit formation. It has been shown, for example that *Sema3e* and its complementary *PlexinD1* ligand are important for the fine mapping of sensory afferent in specific motor pools (Pecho-Vrieseling et al., 2009). Whilst earlier studies implicate the presence of specific ETS transcription factors in sensory-motor connections as playing an important role in spinal circuit development (Lin et al., 1998).

Moreover there is a large body of data which supports a role for cadherin expression driving specificity in neuronal circuits. For example it has been demonstrated that functional cerebellar circuits and Purkinje cell domains can be delineated by their cadherin expression profiles (Neudert & Redies, 2008). Further to this differential cadherin expression profiles have been demonstrated to be found in the basal ganglia and in layer specific expression patterns in the neocortex (Hertel et al., 2008 ;Hertel & Redies 2011). Cadherins have also been shown to play an important role in the defasciclation of sensory afferent in the spinal cord, where N-cadherin expression provides a guidance cue for sensory axon progression in the spinal cord via homophilic association with N-cadherin positive axons (Redies et al., 1992). These studies may have implications for patterns of connectivity within the hindbrain also, for example in the mapping of axonal input to the AccAb nucleus following nucleus desegregation. Equally important could be the role of Fgf

expressed from the nL/nM complex; expression of Fgf8 could be an important axonal guidance cue for FMN motor axons projecting from large dorso lateral exit points. Interestingly in this context it is important to note that GFP positive axons still project to the region of the presumptive nL following Fgf signalling disruption.

Finally an important developmental consequence of nucleogenesis can be attributed to the effects of electrical activity on motor axon mapping. MNs in the developing spinal cord are connected by gap junction channels which may help to coordinate spontaneous neuronal firing (Brenowitz et al., 1983). Spontaneous rhythmic activity in the chick spinal cord is known to influence motor axon pathfinding decisions. Decreases in electrical episode frequency leads to defects in dorsal ventral pathfinding, whilst increases in frequency lead to a break down in motor pool specific topographic projections (Hanson & Landmesser, 2006; Hanson et al., 2008). The mechanisms which mediate these defects downstream of electrical activity are yet to be elucidated; however it is possible that adhesion during early development of cranial motor nuclei could play a role in the coupling of MNs which may aid in the propagation of rhythmic electrical activity.

8. Bibliography

Abe,K. & Takeichi,M. EPLIN mediates linkage of the cadherin catenin complex to F-actin and stabilizes the circumferential actin belt. *Proc. Natl. Acad. Sci. U. S. A* **105**, 13-19 (2008).

Albazerchi,A. & Stern,C.D. A role for the hypoblast (AVE) in the initiation of neural induction, independent of its ability to position the primitive streak. *Dev. Biol.* **301**, 489-503 (2007).

Agmon-Snir,H., Carr,C.E., & Rinzel,J. The role of dendrites in auditory coincidence detection. *Nature* **393**, 268-272 (1998).

Amaya,E., Musci,T.J., & Kirschner,M.W. Expression of a dominant negative mutant of the FGF receptor disrupts mesoderm formation in Xenopus embryos. *Cell* **66**, 257-270 (1991).

Arber,S. *et al.* Requirement for the homeobox gene Hb9 in the consolidation of motor neuron identity. *Neuron* **23**, 659-674 (1999).

Arber,S., Ladle,D.R., Lin,J.H., Frank,E., & Jessell,T.M. ETS gene Er81 controls the formation of functional connections between group Ia sensory afferents and motor neurons. *Cell* **101**, 485-498 (2000).

Arndt,K. & Redies,C. Restricted expression of R-cadherin by brain nuclei and neural circuits of the developing chicken brain. *J. Comp Neurol.* **373**, 373-399 (1996).

Arenkiel,B.R., Gaufo,G.O., & Capecchi,M.R. Hoxb1 neural crest preferentially form glia of the PNS. *Dev. Dyn.* **227**, 379-386 (2003).

Astick, M.R, The developmental expression of Fgf8, PB-cadherin and T-cadherin in the chick auditory hindbrain. *Undergraduate dissertation*, UCL (2007).

Barnes,S.H., Price,S.R., Wentzel,C., & Guthrie,S.C. Cadherin-7 and cadherin-6B differentially regulate the growth, branching and guidance of cranial motor axons. *Development* **137**, 805-814 (2010).

Bell,E., Wingate,R.J., & Lumsden,A. Homeotic transformation of rhombomere identity after localized Hoxb1 misexpression. *Science* **284**, 2168-2171 (1999).

Bello,S.M., Millo,H., Rajebhosale,M., & Price,S.R. Catenin-dependent cadherin function drives divisional segregation of spinal motor neurons. *J. Neurosci.* **32**, 490-505 (2012).

Bello, S.M. The role of cadherin in the development, migration and pooling of hindbrain motor neurones. *Master's thesis*, UCL (2007).

Birgbauer,E. & Fraser,S.E. Violation of cell lineage restriction compartments in the chick hindbrain. *Development* **120**, 1347-1356 (1994).

Boscher,C. & Mege,R.M. Cadherin-11 interacts with the FGF receptor and induces neurite outgrowth through associated downstream signalling. *Cell Signal.* **20**, 1061-1072 (2008).

Brenowitz,G.L., Collins,W.F., III, & Erulkar,S.D. Dye and electrical coupling between frog motoneurons. *Brain Res.* **274**, 371-375 (1983).

Briscoe,J., Pierani,A., Jessell,T.M., & Ericson,J. A homeodomain protein code specifies progenitor cell identity and neuronal fate in the ventral neural tube. *Cell* **101**, 435-445 (2000).

Briscoe,J. & Ericson,J. The specification of neuronal identity by graded Sonic Hedgehog signalling. *Semin. Cell Dev. Biol.* **10**, 353-362 (1999).

Burger,R.M., Cramer,K.S., Pfeiffer,J.D., & Rubel,E.W. Avian superior olivary nucleus provides divergent inhibitory input to parallel auditory pathways. *J. Comp Neurol.* **481**, 6-18 (2005).

Cajal, S, R. Histology of the nervous system, Volume II. English translation. Oxford University Press, Oxford, UK, 1995 (1909)

Cambronero,F. & Puelles,L. Rostrocaudal nuclear relationships in the avian medulla oblongata: a fate map with quail chick chimeras. *J. Comp Neurol.* **427**, 522-545 (2000).

Canning,C.A., Lee,L., Irving,C., Mason,I., & Jones,C.M. Sustained interactive Wnt and FGF signaling is required to maintain isthmic identity. *Dev. Biol.* **305**, 276-286 (2007).

Cavey,M. & Lecuit,T. Molecular bases of cell-cell junctions stability and dynamics. *Cold Spring Harb. Perspect. Biol.* **1**, a002998 (2009).

Cramer,K.S., Fraser,S.E., & Rubel,E.W. Embryonic origins of auditory brain-stem nuclei in the chick hindbrain. *Dev. Biol.* **224**, 138-151 (2000).

Crick,F. Diffusion in embryogenesis. *Nature* **225**, 420-422 (1970).

Dasen,J.S., Liu,J.P., & Jessell,T.M. Motor neuron columnar fate imposed by sequential phases of Hox-c activity. *Nature* **425**, 926-933 (2003).

Ding,Q. *et al.* Diminished Sonic hedgehog signaling and lack of floor plate differentiation in Gli2 mutant mice. *Development* **125**, 2533-2543 (1998).

Disterhoft,J.F., Quinn,K.J., Weiss,C., & Shipley,M.T. Accessory abducens nucleus and conditioned eye retraction/nictitating membrane extension in rabbit. *J. Neurosci.* **5**, 941-950 (1985).

Dover,K., Solinas,S., D'Angelo,E., & Goldfarb,M. Long-term inactivation particle for voltage-gated sodium channels. *J. Physiol* **588**, 3695-3711 (2010).

Dressler,G.R. & Gruss,P. Anterior boundaries of Hox gene expression in mesoderm-derived structures correlate with the linear gene order along the chromosome. *Differentiation* **41**, 193-201 (1989).

Eccles,J.C. The cerebellum as a computer: patterns in space and time. *J. Physiol* **229**, 1-32 (1973).

Echevarria,D., Belo,J.A., & Martinez,S. Modulation of Fgf8 activity during vertebrate brain development. *Brain Res. Brain Res. Rev.* **49**, 150-157 (2005).

Ericson,J., Thor,S., Edlund,T., Jessell,T.M., & Yamada,T. Early stages of motor neuron differentiation revealed by expression of homeobox gene Islet-1. *Science* **256**, 1555-1560 (1992).

Ericson,J. *et al.* Pax6 controls progenitor cell identity and neuronal fate in response to graded Shh signaling. *Cell* **90**, 169-180 (1997).

Eswarakumar,V.P., Lax,I., & Schlessinger,J. Cellular signaling by fibroblast growth factor receptors. *Cytokine Growth Factor Rev.* **16**, 139-149 (2005).

Feng,G. *et al.* Roles for ephrins in positionally selective synaptogenesis between motor neurons and muscle fibers. *Neuron* **25**, 295-306 (2000).

Fraser,S., Keynes,R., & Lumsden,A. Segmentation in the chick embryo hindbrain is defined by cell lineage restrictions. *Nature* **344**, 431-435 (1990).

Fredette,B., Rutishauser,U., & Landmesser,L. Regulation and activity-dependence of N-cadherin, NCAM isoforms, and polysialic acid on chick myotubes during development. *J. Cell Biol.* **123**, 1867-1888 (1993).

Fredette,B.J. & Ranscht,B. T-cadherin expression delineates specific regions of the developing motor axon-hindlimb projection pathway. *J. Neurosci.* **14**, 7331-7346 (1994).

Fukuchi-Shimogori,T. & Grove,E.A. Neocortex patterning by the secreted signaling molecule FGF8. *Science* **294**, 1071-1074 (2001).

Gao,H. & Lu,Y. Early development of intrinsic and synaptic properties of chicken nucleus laminaris neurons. *Neuroscience* **153**, 131-143 (2008).

Gospodarowicz,D. Localisation of a fibroblast growth factor and its effect alone and with hydrocortisone on 3T3 cell growth. *Nature* **249**, 123-127 (1974).

Gaufo,G.O., Thomas,K.R., & Capecchi,M.R. Hox3 genes coordinate mechanisms of genetic suppression and activation in the generation of branchial and somatic motoneurons. *Development* **130** , 5191-5201 (2003).

Georgia,S., Soliz,R., Li,M., Zhang,P., & Bhushan,A. p57 and Hes1 coordinate cell cycle exit with self-renewal of pancreatic progenitors. *Dev. Biol.* **298**, 22-31 (2006).

Gilland,E. & Baker,R. Evolutionary patterns of cranial nerve efferent nuclei in vertebrates. *Brain Behav. Evol.* **66**, 234-254 (2005).

Glover,J.C., Renaud,J.S., & Rijli,F.M. Retinoic acid and hindbrain patterning. *J. Neurobiol.* **66**, 705-725 (2006).

Goddard,J.M., Rossel,M., Manley,N.R., & Capecchi,M.R. Mice with targeted disruption of Hoxb-1 fail to form the motor nucleus of the VIIth nerve. *Development* **122**, 3217-3228 (1996).

Goldfarb,M. Fibroblast growth factor homologous factors: evolution, structure, and function. *Cytokine Growth Factor Rev.* **16**, 215-220 (2005).

Goldfarb,M. *et al.* Fibroblast growth factor homologous factors control neuronal excitability through modulation of voltage-gated sodium channels. *Neuron* **55**, 449-463 (2007).

Goldfarb,M. Voltage-gated sodium channel-associated proteins and alternative mechanisms of inactivation and block. *Cell Mol. Life Sci.* **69**, 1067-1076 (2012).

Gorlich,A. *et al.* Development of the delay lines in the nucleus laminaris of the chicken embryo revealed by optical imaging. *Neuroscience* **168**, 564-572 (2010).

Grau-Serrat,V., Carr,C.E., & Simon,J.Z. Modeling coincidence detection in nucleus laminaris. *Biol. Cybern.* **89**, 388-396 (2003).

Guthrie,S., Butcher,M., & Lumsden,A. Patterns of cell division and interkinetic nuclear migration in the chick embryo hindbrain. *J. Neurobiol.* **22**, 742-754 (1991).

Guthrie,S. Patterning and axon guidance of cranial motor neurons. *Nat. Rev. Neurosci.* **8**, 859-871 (2007).

Haase,G. *et al.* GDNF acts through PEA3 to regulate cell body positioning and muscle innervation of specific motor neuron pools. *Neuron* **35**, 893-905 (2002).

Hacohen,N., Kramer,S., Sutherland,D., Hiromi,Y., & Krasnow,M.A. sprouty encodes a novel antagonist of FGF signaling that patterns apical branching of the Drosophila airways. *Cell* **92**, 253-263 (1998).

Hamburger, V & Hamilton, H. A series of normal stages in the development of the chick embryo. *J. Morphology*, 88:49-92 (1951).

Hatta,K. & Takeichi,M. Expression of N-cadherin adhesion molecules associated with early morphogenetic events in chick development. *Nature* **320**, 447-449 (1986).

Hatta,K., Takagi,S., Fujisawa,H., & Takeichi,M. Spatial and temporal expression pattern of N-cadherin cell adhesion molecules correlated with morphogenetic processes of chicken embryos. *Dev. Biol.* **120**, 215-227 (1987).

Hendricks,S.J., Rubel,E.W., & Nishi,R. Formation of the avian nucleus magnocellularis from the auditory anlage. *J. Comp Neurol.* **498**, 433-442 (2006).

Hertel,N., Krishna,K., Nuernberger,M., & Redies,C. A cadherin-based code for the divisions of the mouse basal ganglia. *J. Comp Neurol.* **508**, 511-528 (2008).

Hertel,N. & Redies,C. Absence of layer-specific cadherin expression profiles in the neocortex of the reeler mutant mouse. *Cereb. Cortex* **21**, 1105-1117 (2011).

Honig,M.G., Petersen,G.G., Rutishauser,U.S., & Camilli,S.J. In vitro studies of growth cone behavior support a role for fasciculation mediated by cell adhesion molecules in sensory axon guidance during development. *Dev. Biol.* **204**, 317-326 (1998).

Hyson,R.L. The analysis of interaural time differences in the chick brain stem. *Physiol Behav.* **86**, 297-305 (2005).

Inoue,T., Chisaka,O., Matsunami,H., & Takeichi,M. Cadherin-6 expression transiently delineates specific rhombomeres, other neural tube subdivisions, and neural crest subpopulations in mouse embryos. *Dev. Biol.* **183**, 183-194 (1997).

Inoue,Y.U., Asami,J., & Inoue,T. Genetic labeling of mouse rhombomeres by Cadherin-6::EGFP-BAC transgenesis underscores the role of cadherins in hindbrain compartmentalization. *Neurosci. Res.* **63**, 2-9 (2009).

Irving,C. & Mason,I. Signalling by FGF8 from the isthmus patterns anterior hindbrain and establishes the anterior limit of Hox gene expression. *Development* **127**, 177-186 (2000).

Jacob,J. & Guthrie,S. Facial visceral motor neurons display specific rhombomere origin and axon pathfinding behavior in the chick. *J. Neurosci.* **20**, 7664-7671 (2000).

JEFFRESS,L.A. A place theory of sound localization. *J. Comp Physiol Psychol.* **41**, 35-39 (1948).

Jessell,T.M. Neuronal specification in the spinal cord: inductive signals and transcriptional codes. *Nat. Rev. Genet.* **1**, 20-29 (2000).

Liu,A. *et al.* FGF17b and FGF18 have different midbrain regulatory properties from FGF8b or activated FGF receptors. *Development* **130**, 6175-6185 (2003).

Jukkola,T., Lahti,L., Naserke,T., Wurst,W., & Partanen,J. FGF regulated gene-expression and neuronal differentiation in the developing midbrain-hindbrain region. *Dev. Biol.* **297**, 141-157 (2006).

Kao,T.J., Law,C., & Kania,A. Eph and ephrin signaling: lessons learned from spinal motor neurons. *Semin. Cell Dev. Biol.* **23**, 83-91 (2012).

Kania,A. & Jessell,T.M. Topographic motor projections in the limb imposed by LIM homeodomain protein regulation of ephrin-A:EphA interactions. *Neuron* **38**, 581-596 (2003).

Katsamba,P. *et al.* Linking molecular affinity and cellular specificity in cadherin-mediated adhesion. *Proc. Natl. Acad. Sci. U. S. A* **106**, 11594-11599 (2009).

Kawakami,K. & Noda,T. Transposition of the Tol2 element, an Ac-like element from the Japanese medaka fish Oryzias latipes, in mouse embryonic stem cells. *Genetics* **166**, 895-899 (2004).

Kimura,Y., Matsunami,H., & Takeichi,M. Expression of cadherin-11 delineates boundaries, neuromeres, and nuclei in the developing mouse brain. *Dev. Dyn.* **206**, 455-462 (1996).

Kuba,H., Koyano,K., & Ohmori,H. Synaptic depression improves coincidence detection in the nucleus laminaris in brainstem slices of the chick embryo. *Eur. J. Neurosci.* **15**, 984-990 (2002).

Kuba,H., Yamada,R., Fukui,I., & Ohmori,H. Tonotopic specialization of auditory coincidence detection in nucleus laminaris of the chick. *J. Neurosci.* **25**, 1924-1934 (2005).

Kuba,H., Ishii,T.M., & Ohmori,H. Axonal site of spike initiation enhances auditory coincidence detection. *Nature* **444**, 1069-1072 (2006).

Kuratani,S. Development of glossopharyngeal nerve branches in the early chick embryo with special reference to morphology of the Jacobson's anastomosis. *Anat. Embryol. (Berl)* **181**, 253-269 (1990).

Lahti,L., Saarimaki-Vire,J., Rita,H., & Partanen,J. FGF signaling gradient maintains symmetrical proliferative divisions of midbrain neuronal progenitors. *Dev. Biol.* **349**, 270-282 (2011).

Labandeira-Garcia,J.L., Guerra-Seijas,M.J., & Labandeira-Garcia,J.A. The abducens motor and internuclear neurons in the rabbit: retrograde horseradish peroxidase and double fluorescent labeling. *Brain Res.* **497**, 305-314 (1989).

Lance-Jones,C. & Landmesser,L. Pathway selection by chick lumbosacral motoneurons during normal development. *Proc. R. Soc. Lond B Biol. Sci.* **214**, 1-18 (1981).

Landmesser,L. The distribution of motoneurones supplying chick hind limb muscles. *J. Physiol* **284**, 371-389 (1978).

Lemons,D. & McGinnis,W. Genomic evolution of Hox gene clusters. *Science* **313**, 1918-1922 (2006).

Lewis,E.B. A gene complex controlling segmentation in Drosophila. *Nature* **276**, 565-570 (1978).

Lin,J.H. *et al.* Functionally related motor neuron pool and muscle sensory afferent subtypes defined by coordinate ETS gene expression. *Cell* **95**, 393-407 (1998).

Liu,J.P., Laufer,E., & Jessell,T.M. Assigning the positional identity of spinal motor neurons: rostrocaudal patterning of Hox-c expression by FGFs, Gdf11, and retinoids. *Neuron* **32**, 997-1012 (2001).

Livet,J. *et al.* ETS gene Pea3 controls the central position and terminal arborization of specific motor neuron pools. *Neuron* **35**, 877-892 (2002).

Lou,J.Y. *et al.* Fibroblast growth factor 14 is an intracellular modulator of voltage-gated sodium channels. *J. Physiol* **569**, 179-193 (2005).

Lu,Q.R. *et al.* Common developmental requirement for Olig function indicates a motor neuron/oligodendrocyte connection. *Cell* **109**, 75-86 (2002).

Lu,Y. Regulation of glutamatergic and GABAergic neurotransmission in the chick nucleus laminaris: role of N-type calcium channels. *Neuroscience* **164**, 1009-1019 (2009).

Lumsden,A. & Keynes,R. Segmental patterns of neuronal development in the chick hindbrain. *Nature* **337**, 424-428 (1989).

Lumsden,A. Segmentation and compartition in the early avian hindbrain. *Mech. Dev.* **121**, 1081-1088 (2004).

Luo,J., Treubert-Zimmermann,U., & Redies,C. Cadherins guide migrating Purkinje cells to specific parasagittal domains during cerebellar development. *Mol. Cell Neurosci.* **25**, 138-152 (2004).

Luo,J. *et al.* Cadherin-20 expression by motor neurons is regulated by Sonic hedgehog during spinal cord development. *Neuroreport* **20**, 365-370 (2009).

Mahmood,R. *et al.* A role for FGF-8 in the initiation and maintenance of vertebrate limb bud outgrowth. *Curr. Biol.* **5**, 797-806 (1995).

Marthiens,V. *et al.* A novel function for cadherin-11 in the regulation of motor axon elongation and fasciculation. *Mol. Cell Neurosci.* **28**, 715-726 (2005).

McGinnis,W., Garber,R.L., Wirz,J., Kuroiwa,A., & Gehring,W.J. A homologous protein-coding sequence in Drosophila homeotic genes and its conservation in other metazoans. *Cell* **37**, 403-408 (1984).

McGinnis,W., Levine,M.S., Hafen,E., Kuroiwa,A., & Gehring,W.J. A conserved DNA sequence in homoeotic genes of the Drosophila Antennapedia and bithorax complexes. *Nature* **308**, 428-433 (1984).

McKay,I.J., Lewis,J., & Lumsden,A. Organization and development of facial motor neurons in the kreisler mutant mouse. *Eur. J. Neurosci.* **9**, 1499-1506 (1997).

Mears,S.C. & Frank,E. Formation of specific monosynaptic connections between muscle spindle afferents and motoneurons in the mouse. *J. Neurosci.* **17**, 3128-3135 (1997).

Molea,D. & Rubel,E.W. Timing and topography of nucleus magnocellularis innervation by the cochlear ganglion. *J. Comp Neurol.* **466**, 577-591 (2003).

MOSCONA,A. & MOSCONA,H. The dissociation and aggregation of cells from organ rudiments of the early chick embryo. *J. Anat.* **86**, 287-301 (1952).

MOSCONA,M.H. & KARNOFSKY,D.A. Cortisone induced modiffications in the development of the chick embryo. *Endocrinology* **66**, 533-549 (1960).

Munoz-Sanjuan,I., Simandl,B.K., Fallon,J.F., & Nathans,J. Expression of chicken fibroblast growth factor homologous factor (FHF)-1 and of differentially spliced isoforms of FHF-2 during development and involvement of FHF-2 in chicken limb development. *Development* **126**, 409-421 (1999).

Nagafuchi,A., Shirayoshi,Y., Okazaki,K., Yasuda,K., & Takeichi,M. Transformation of cell adhesion properties by exogenously introduced E-cadherin cDNA. *Nature* **329**, 341-343 (1987).

Nagar,B., Overduin,M., Ikura,M., & Rini,J.M. Structural basis of calcium-induced E-cadherin rigidification and dimerization. *Nature* **380**, 360-364 (1996).

Neudert,F. & Redies,C. Neural circuits revealed by axon tracing and mapping cadherin expression in the embryonic chicken cerebellum. *J. Comp Neurol.* **509**, 283-301 (2008).

Niehrs,C. & Meinhardt,H. Modular feedback. *Nature* **417**, 35-36 (2002).

Nishimura,E.K., Yoshida,H., Kunisada,T., & Nishikawa,S.I. Regulation of E- and P-cadherin expression correlated with melanocyte migration and diversification. *Dev. Biol.* **215**, 155-166 (1999).

Nollet,F., Kools,P., & van,R.F. Phylogenetic analysis of the cadherin superfamily allows identification of six major subfamilies besides several solitary members. *J. Mol. Biol.* **299**, 551-572 (2000).

Nose,A., Nagafuchi,A., & Takeichi,M. Expressed recombinant cadherins mediate cell sorting in model systems. *Cell* **54**, 993-1001 (1988).

Nose,A., Tsuji,K., & Takeichi,M. Localization of specificity determining sites in cadherin cell adhesion molecules. *Cell* **61**, 147-155 (1990).

Nowak,M., Machate,A., Yu,S.R., Gupta,M., & Brand,M. Interpretation of the FGF8 morphogen gradient is regulated by endocytic trafficking. *Nat. Cell Biol.* **13**, 153-158 (2011).

Ogou,S.I., Yoshida-Noro,C., & Takeichi,M. Calcium-dependent cell-cell adhesion molecules common to hepatocytes and teratocarcinoma stem cells. *J. Cell Biol.* **97**, 944-948 (1983).

Olsen,S.K. *et al.* Fibroblast growth factor (FGF) homologous factors share structural but not functional homology with FGFs. *J. Biol. Chem.* **278**, 34226-34236 (2003).

Ornitz,D.M. *et al.* Receptor specificity of the fibroblast growth factor family. *J. Biol. Chem.* **271**, 15292-15297 (1996).

Ornitz,D.M. & Itoh,N. Fibroblast growth factors. *Genome Biol.* **2**, REVIEWS3005 (2001).

Ornitz,D.M. & Itoh,N. Fibroblast growth factors. *Genome Biol.* **2**, REVIEWS3005 (2001).

Overholt,E.M., Rubel,E.W., & Hyson,R.L. A circuit for coding interaural time differences in the chick brainstem. *J. Neurosci.* **12**, 1698-1708 (1992).

Pabst,O., Rummelies,J., Winter,B., & Arnold,H.H. Targeted disruption of the homeobox gene Nkx2.9 reveals a role in development of the spinal accessory nerve. *Development* **130**, 1193-1202 (2003).

Palmesino,E. *et al.* Foxp1 and lhx1 coordinate motor neuron migration with axon trajectory choice by gating Reelin signalling. *PLoS. Biol.* **8**, e1000446 (2010).

Parks,T.N. & Rubel,E.W. Organization and development of brain stem auditory nuclei of the chicken: organization of projections from n. magnocellularis to n. laminaris. *J. Comp Neurol.* **164**, 435-448 (1975).

Patel,S.D. *et al.* Type II cadherin ectodomain structures: implications for classical cadherin specificity. *Cell* **124**, 1255-1268 (2006).

Pattyn,A., Vallstedt,A., Dias,J.M., Sander,M., & Ericson,J. Complementary roles for Nkx6 and Nkx2 class proteins in the establishment of motoneuron identity in the hindbrain. *Development* **130**, 4149-4159 (2003).

Persson,M. *et al.* Dorsal-ventral patterning of the spinal cord requires Gli3 transcriptional repressor activity. *Genes Dev.* **16**, 2865-2878 (2002).

Pokutta,S. & Weis,W.I. Structure and mechanism of cadherins and catenins in cell-cell contacts. *Annu. Rev. Cell Dev. Biol.* **23**, 237-261 (2007).

Price,S.R., De Marco Garcia,N.V., Ranscht,B., & Jessell,T.M. Regulation of motor neuron pool sorting by differential expression of type II cadherins. *Cell* **109**, 205-216 (2002).

Ravindranathan,A. *et al.* Contrasting molecular composition and channel properties of AMPA receptors on chick auditory and brainstem motor neurons. *J. Physiol* **523 Pt 3**, 667-684 (2000).

Redies,C., Inuzuka,H., & Takeichi,M. Restricted expression of N- and R-cadherin on neurites of the developing chicken CNS. *J. Neurosci.* **12**, 3525-3534 (1992).

Redies,C. Cadherins in the central nervous system. *Prog. Neurobiol.* **61**, 611-648 (2000).

Redies,C., Neudert,F., & Lin,J. Cadherins in cerebellar development: translation of embryonic patterning into mature functional compartmentalization. *Cerebellum.* **10**, 393-408 (2011).

Romanes, G.J. The development and significance of the cell columns in the ventral horn of the cervical and upper thoracic spinal cord of the rabbit. *J. Anat*. Lond. **76**, 112–130 (1942).

Romanes, G.J. The motor pools of the spinal cord. In Organization of the Spinal Cord, Volume 11, J.C. Eccles, and J.P. Schade,eds. (Amsterdam: Elsevier Publishing), pp. 93–119 (1964).

Saarimaki-Vire,J. *et al.* Fibroblast growth factor receptors cooperate to regulate neural progenitor properties in the developing midbrain and hindbrain. *J. Neurosci.* **27**, 8581-8592 (2007).

Saarimaki-Vire,J., Alitalo,A., & Partanen,J. Analysis of Cdh22 expression and function in the developing mouse brain. *Dev. Dyn.* **240**, 1989-2001 (2011).

Samuels,M.L. & McMahon,M. Inhibition of platelet-derived growth factor- and epidermal growth factor-mediated mitogenesis and signaling in 3T3 cells expressing delta Raf-1:ER, an estradiol-regulated form of Raf-1. *Mol. Cell Biol.* **14**, 7855-7866 (1994).

Saunders,J.C., Coles,R.B., & Gates,G.R. The development of auditory evoked responses in the cochlea and cochlear nuclei of the chick. *Brain Res.* **63**, 59-74 (1973).

Schier,A.F. & Needleman,D. Developmental biology: Rise of the source-sink model. *Nature* **461**, 480-481 (2009).

Schiefferdecker, P. Methode zuer Isolierung von Epithelzel- len. *Z. Wiss. Mikr.* **3,** 483–484 (1886).

Schmitt, F. O. Some protein patterns in cells. *Dev. Biol.* **70,** 195–205.
(Suppl.), 1–20 . (1941).

Schneider-Maunoury,S., Seitanidou,T., Charnay,P., & Lumsden,A. Segmental and neuronal architecture of the hindbrain of Krox-20 mouse mutants. *Development* **124**, 1215-1226 (1997).

Schoorlemmer,J. & Goldfarb,M. Fibroblast growth factor homologous factors are intracellular signaling proteins. *Curr. Biol.* **11**, 793-797 (2001).

Shan,W. *et al.* The minimal essential unit for cadherin-mediated intercellular adhesion comprises extracellular domains 1 and 2. *J. Biol. Chem.* **279**, 55914-55923 (2004).

Shapiro,L. *et al.* Structural basis of cell-cell adhesion by cadherins. *Nature* **374**, 327-337 (1995).

Shapiro,L., Love,J., & Colman,D.R. Adhesion molecules in the nervous system: structural insights into function and diversity. *Annu. Rev. Neurosci.* **30**, 451-474 (2007).

Shi,Q., Chien,Y.H., & Leckband,D. Biophysical properties of cadherin bonds do not predict cell sorting. *J. Biol. Chem.* **283**, 28454-28463 (2008).

Shiga,T. & Oppenheim,R.W. Immunolocalization studies of putative guidance molecules used by axons and growth cones of intersegemental interneurons in the chick embryo spinal cord. *J. Comp Neurol.* **310**, 234-252 (1991).

Shimoyama,Y., Tsujimoto,G., Kitajima,M., & Natori,M. Identification of three human type-II classic cadherins and frequent heterophilic interactions between different subclasses of type-II classic cadherins. *Biochem. J.* **349**, 159-167 (2000).

Shirasaki,R., Lewcock,J.W., Lettieri,K., & Pfaff,S.L. FGF as a target-derived chemoattractant for developing motor axons genetically programmed by the LIM code. *Neuron* **50**, 841-853 (2006).

Simon,H. & Lumsden,A. Rhombomere-specific origin of the contralateral vestibulo-acoustic efferent neurons and their migration across the embryonic midline. *Neuron* **11**, 209-220 (1993).

Smith,D.J. & Rubel,E.W. Organization and development of brain stem auditory nuclei of the chicken: dendritic gradients in nucleus laminaris. *J. Comp Neurol.* **186**, 213-239 (1979).

Smith, R.C.G. Structure and function of the avian neuronal nucleus for sound localisation. *Doctoral Thesis*, UCL (2011).

Smith,Z.D. Organization and development of brain stem auditory nuclei of the chicken: dendritic development in N. laminaris. *J. Comp Neurol.* **203**, 309-333 (1981).

Sockanathan,S. & Jessell,T.M. Motor neuron-derived retinoid signaling specifies the subtype identity of spinal motor neurons. *Cell* **94**, 503-514 (1998).

Soundararajan,P., Fawcett,J.P., & Rafuse,V.F. Guidance of postural motoneurons requires MAPK/ERK signaling downstream of fibroblast growth factor receptor 1. *J. Neurosci.* **30**, 6595-6606 (2010).

Stamataki,D., Ulloa,F., Tsoni,S.V., Mynett,A., & Briscoe,J. A gradient of Gli activity mediates graded Sonic Hedgehog signaling in the neural tube. *Genes Dev.* **19**, 626-641 (2005).

Steinberg,M.S., Armstrong,P.B., & Granger,R.E. On the recovery of adhesiveness by trypsin-dissociated cells. *J. Membr. Biol.* **13**, 97-128 (1973).

Steinberg,M.S. Adhesion in development: an historical overview. *Dev. Biol.* **180**, 377-388 (1996).

Storey,K.G. *et al.* Early posterior neural tissue is induced by FGF in the chick embryo. *Development* **125**, 473-484 (1998).

Studer,M., Lumsden,A., riza-McNaughton,L., Bradley,A., & Krumlauf,R. Altered segmental identity and abnormal migration of motor neurons in mice lacking Hoxb-1. *Nature* **384**, 630-634 (1996).

Suzuki,S.C. & Takeichi,M. Cadherins in neuronal morphogenesis and function. *Dev. Growth Differ.* **50 Suppl 1**, S119-S130 (2008).

Tabdili,H. *et al.* Cadherin Point Mutations Alter Cell Sorting and Modulate GTPase Signaling. *J. Cell Sci.*(2012).

Takeichi,M. Functional correlation between cell adhesive properties and some cell surface proteins. *J. Cell Biol.* **75**, 464-474 (1977).

Takeichi,M., Atsumi,T., Yoshida,C., Uno,K., & Okada,T.S. Selective adhesion of embryonal carcinoma cells and differentiated cells by Ca2+-dependent sites. *Dev. Biol.* **87**, 340-350 (1981).

Taniguchi,H., Kawauchi,D., Nishida,K., & Murakami,F. Classic cadherins regulate tangential migration of precerebellar neurons in the caudal hindbrain. *Development* **133**, 1923-1931 (2006).

Tan,K. & Le Douarin,N.M. Development of the nuclei and cell migration in the medulla oblongata. Application of the quail-chick chimera system. *Anat. Embryol. (Berl)* **183**, 321-343 (1991).

Tanabe,Y., William,C., & Jessell,T.M. Specification of motor neuron identity by the MNR2 homeodomain protein. *Cell* **95**, 67-80 (1998).

Tanabe,K., Takeichi,M., & Nakagawa,S. Identification of a nonchordate-type classic cadherin in vertebrates: chicken Hz-cadherin is expressed in horizontal cells of the neural retina and contains a nonchordate-specific domain complex. *Dev. Dyn.* **229**, 899-906 (2004).

Trokovic,R. *et al.* FGFR1 is independently required in both developing mid- and hindbrain for sustained response to isthmic signals. *EMBO J.* **22**, 1811-1823 (2003).

Tumpel,S., Wiedemann,L.M., & Krumlauf,R. Hox genes and segmentation of the vertebrate hindbrain. *Curr. Top. Dev. Biol.* **88**, 103-137 (2009).

Tsuiji,H., Xu,L., Schwartz,K., & Gumbiner,B.M. Cadherin conformations associated with dimerization and adhesion. *J. Biol. Chem.* **282**, 12871-12882 (2007).

Vaage,S. The segmentation of the primitive neural tube in chick embryos (Gallus domesticus). A morphological, histochemical and autoradiographical investigation. *Ergeb. Anat. Entwicklungsgesch.* **41**, 3-87 (1969).

Volk,T., Cohen,O., & Geiger,B. Formation of heterotypic adherens-type junctions between L-CAM-containing liver cells and A-CAM-containing lens cells. *Cell* **50**, 987-994 (1987).

Vrieseling,E. & Arber,S. Target-induced transcriptional control of dendritic patterning and connectivity in motor neurons by the ETS gene Pea3. *Cell* **127**, 1439-1452 (2006).

Wahl,C.M., Noden,D.M., & Baker,R. Developmental relations between sixth nerve motor neurons and their targets in the chick embryo. *Dev. Dyn.* **201**, 191-202 (1994).

Wang,X., Weng,L.P., & Yu,Q. Specific inhibition of FGF-induced MAPK activation by the receptor-like protein tyrosine phosphatase LAR. *Oncogene* **19**, 2346-2353 (2000).

Weisinger,K., Kayam,G., Missulawin-Drillman,T., & Sela-Donenfeld,D. Analysis of expression and function of FGF-MAPK signaling components in the hindbrain reveals a central role for FGF3 in the regulation of Krox20, mediated by Pea3. *Dev. Biol.* **344**, 881-895 (2010).

Wittmack,E.K. *et al.* Fibroblast growth factor homologous factor 2B: association with Nav1.6 and selective colocalization at nodes of Ranvier of dorsal root axons. *J. Neurosci.* **24**, 6765-6775 (2004).

Wilkinson,D.G., Bhatt,S., Chavrier,P., Bravo,R., & Charnay,P. Segment-specific expression of a zinc-finger gene in the developing nervous system of the mouse. *Nature* **337**, 461-464 (1989).

Wilson,H.V. A NEW METHOD BY WHICH SPONGES MAY BE ARTIFICIALLY REARED. *Science* **25**, 912-915 (1907).

Wilson,S.I., Graziano,E., Harland,R., Jessell,T.M., & Edlund,T. An early requirement for FGF signalling in the acquisition of neural cell fate in the chick embryo. *Curr. Biol.* **10**, 421-429 (2000).

Wittler,L. & Kessel,M. The acquisition of neural fate in the chick. *Mech. Dev.* **121**, 1031-1042 (2004).

Wolpert,L. Positional information and the spatial pattern of cellular differentiation. *J. Theor. Biol.* **25**, 1-47 (1969).

Yoshida-Noro,C., Suzuki,N., & Takeichi,M. Molecular nature of the calcium-dependent cell-cell adhesion system in mouse teratocarcinoma and embryonic cells studied with a monoclonal antibody. *Dev. Biol.* **101**, 19-27 (1984).

Young,S.R. & Rubel,E.W. Frequency-specific projections of individual neurons in chick brainstem auditory nuclei. *J. Neurosci.* **3**, 1373-1378 (1983).

Youngren,O.M. & Phillips,R.E. Location and distribution of tracheosyringeal motorneuron somata in the fowl. *J. Comp Neurol.* **213**, 86-93 (1983).

Yu,K. & Ornitz,D.M. FGF signaling regulates mesenchymal differentiation and skeletal patterning along the limb bud proximodistal axis. *Development* **135**, 483-491 (2008).

Zannino,D.A. & Appel,B. Olig2+ precursors produce abducens motor neurons and oligodendrocytes in the zebrafish hindbrain. *J. Neurosci.* **29**, 2322-2333 (2009).

Zervas,M., Blaess,S., & Joyner,A.L. Classical embryological studies and modern genetic analysis of midbrain and cerebellum development. *Curr. Top. Dev. Biol.* **69**, 101-138 (2005).

Guillemot,F. & Zimmer,C. From cradle to grave: the multiple roles of fibroblast growth factors in neural development. *Neuron* **71**, 574-588 (2011).